พฤติกรรมการรับน้ำหนักในแนวดิ่งและแนวราบของเสาเข็มแบเร็ทรูปตัวทีและเสาเข็มเจาะ

นายชาญชัย ทรัพย์มณีวงศ์

วิทยานิพนธ์นี้เป็นส่วนหนึ่งของการศึกษาตามหลักสูตรปริญญาวิศวกรรมศาสตรดุษฎีบัณฑิต
สาขาวิชาวิศวกรรมโยธา ภาควิชาวิศวกรรมโยธา
คณะวิศวกรรมศาสตร์ จุฬาลงกรณ์มหาวิทยาลัย
ปีการศึกษา 2552

BEHAVIOR OF VERTICAL AND LATERAL LOAD ON T-SHAPE BARRETTE AND BORED PILES

Mr. Chanchai Submaneewong

A Dissertation Submitted in Partial Fulfillment of the Requirements
for the Degree of Doctor of Philosophy Program in Civil Engineering
Department of Civil Engineering
Faculty of Engineering
Chulalongkorn University
Academic Year 2009

Thesis Title	BEHAVIOR OF VERTICAL AND LATERAL LOAD ON T-SHAPE BARRETTE AND BORED PILES
By	Mr. Chanchai Submaneewong
Field of Study	Civil Engineering
Thesis Advisor	Associate Professor Wanchai Teparaksa, D. Eng.

Accepted by the Faculty of Engineering, Chulalongkorn University in Partial Fulfillment of the Requirements for the Doctoral Degree

....Dean of the Faculty of Engineering
(Associate Professor Boonsom Lerdhirunwong, Dr.Ing.)

THESIS COMMITTEE

....Chairman
(Associate Professor Boonsom Lerdhirunwong, Dr. Ing.)

Wanchai Tep..Thesis Advisor
(Associate Professor Wanchai Teparaksa, D. Eng.)

....Examiner
(Associate Professor Tirawat Boonyatee, D. Eng.)

....External Examiner
(Associate Professor Korchoke Chantawarangul, Ph. D.)

Pornpot Tanseng..External Examiner
(Assistant Professor Pornpot Tanseng, Ph. D.)

ชาญชัย ทรัพย์มณีวงศ์ : พฤติกรรมการรับน้ำหนักในแนวดิ่งและแนวราบของเสาเข็มแบเร็ทรูปตัวทีและเสาเข็มเจาะ. (BEHAVIOR OF VERTICAL AND LATERAL LOAD ON T-SHAPE BARRETTE AND BORED PILES) อ. ที่ปรึกษาวิทยานิพนธ์หลัก: รศ. ดร. วันชัย เทพรักษ์, 114 หน้า.

เสาเข็มเจาะขนาดใหญ่ได้นำมาใช้ในระบบฐานรากเสาเข็มรองรับงานอาคารสูงและงานตอม่อสะพานในกรุงเทพ แต่ในกรณีที่ต้องออกแบบเสาเข็มให้มีกำลังรับน้ำหนักบรรทุกสูงโดยต้องก่อสร้างในพื้นที่จำกัด การใช้เสาเข็มแบเร็ทจะเป็นทางเลือกที่เกิดประสิทธิผลมากกว่าการใช้เสาเข็มเจาะ โดยทั่วไปเสาเข็มจะออกแบบไว้รับน้ำหนักบรรทุกในแนวดิ่งแต่ในโครงสร้างบางประเภท ฐานรากเสาเข็มต้องออกแบบให้รับแรงกระทำด้านข้างที่สูงมาก การเลือกใช้เสาเข็มแบเร็ทรูปตัวทีจึงเป็นอีกหนึ่งทางเลือกที่สามารถออกแบบให้รับน้ำหนักบรรทุกทั้งแนวดิ่งและแรงกระทำด้านข้าง เสาเข็มภายใต้น้ำหนักบรรทุกทั้งแนวดิ่งและแรงกระทำด้านข้างจัดเป็นปัญหาที่เกี่ยวข้องกับปฏิกิริยาระหว่างดินและเสาเข็มซึ่งเกี่ยวข้องกับพารามิเตอร์มากมายทั้งคุณสมบัติทางด้านโครงสร้างและคุณสมบัติของดิน การเลือกใช้พารามิเตอร์ต่างๆ สำหรับการวิเคราะห์และออกแบบขนาด, ความยาว และจำนวนเสาเข็มในระบบฐานราก จึงต้องพิจารณากำลังรับน้ำหนักบรรทุก, การทรุดตัวของดินและการเคลื่อนตัวของเสาเข็มที่ยอมรับได้

งานวิจัยนี้ทำการทดสอบเสาเข็มที่มีการติดตั้งเครื่องมือวัดแบบเต็มรูปแบบ สำหรับเสาเข็มแบเร็ทรูปตัวทีและเสาเข็มเจาะที่มีปลายในชั้นทรายแน่นมากกรุงเทพฯ ชั้นที่ 2 ที่ความลึก 55 เมตร ต่ำกว่าระดับผิวดินภายใต้การทดสอบการรับน้ำหนักในแนวดิ่งและแนวราบ การวิเคราะห์พฤติกรรมเสาเข็มใช้โปรแกรมไฟไนต์อิลิเมนท์ (FEM) 3 มิติ, PLAXIS 3D Foundations ผลการวิเคราะห์พบว่าเสาเข็มแบเร็ทรูปตัวทีภายใต้น้ำหนักบรรทุกในแนวดิ่งพบแนวระนาบเฉือนไม่ได้อยู่ตามแนวเส้นรอบรูปของเสาเข็ม สำหรับเสาเข็มภายใต้แรงกระทำด้านข้าง ผลการวิเคราะห์พบว่าสภาพหน้าตัดร้าวของเสาเข็มมีผลต่อกำลังรับแรงด้านข้างของเสาเข็ม การไม่พิจารณาสภาพหน้าตัดร้าว มีแนวโน้มให้ค่าความสามารถในการต้านทานแรงกระทำด้านข้างสูงกว่าค่าออกแบบ สำหรับแนวทางการออกแบบ ผลการวิเคราะห์กลับ (back Analysis) แสดงให้เห็นว่าสติฟเนสของดินสำหรับเสาเข็มแบเร็ทรูปตัวทีภายใต้แรงกระทำด้านข้าง ก่อนเสาเข็มเกิดสภาพหน้าตัดร้าว ควรมีค่าเป็น 3 เท่าของค่าที่ใช้คำนวณการเคลื่อนตัวของเสาเข็มเจาะ และเมื่อเกิดสภาพหน้าตัดร้าวสติฟเนสของเสาเข็มแบเร็ทรูปตัวทีจะลดลงประมาณ 70 % ของค่าสติฟเนสเริ่มต้น

ภาควิชา วิศวกรรมโยธา ลายมือชื่อนิสิต

สาขาวิชา วิศวกรรมโยธา ลายมือชื่อ อ. ที่ปรึกษาวิทยานิพนธ์หลัก

ปีการศึกษา 2552

4871837521: MAJOR CIVIL ENGINEERING
KEYWORDS: BARRETTE / T-SHAPE BARRETTE / BORED PILE / LATERAL LOAD TEST / STATIC LOAD TEST / FEM

CHANCHAI SUBMANEEWONG: BEHAVIOR OF VERTICAL AND LATERAL LOAD ON T-SHAPE BARRETTE AND BORED PILES. THESIS ADVISOR: ASSOCIATE PROFESSOR WANCHAI TEPARAKSA, D. Eng., 114 pp.

The large diameter long bored piles are commonly used as foundation for high-rise buildings and bridges in Bangkok, Thailand. However, in case of high loading capacity requirement in the limited area, the use of barrette pile foundations would make a better alternative to bored piles. Generally, the main load component of pile foundation is vertical loading. For some structures, piled-foundation might be designed to resist the high lateral loading. The T-shape barrette pile is, therefore, proposed to be an alternative deep foundation not only to support vertical loading but also to resist high lateral loading. The pile under vertical and lateral loading is the soil-pile interaction problem which concern to many parameters in both structure and soil properties. Therefore, the selected parameters for analysis and design pile size, pile length and number of piles in footing must be considered with allowable load, allowable settlement and movement of soil and piles.

In this research, The full scale static pile load tests were conducted to verify the vertical and lateral load capacities of T-shape barrette and bored piles with pile tip founded in the second dense silty sand layer about 55 m depth below ground surface. The analyses were performed using PLAXIS 3D Foundations, the 3D Finite Element Method (FEM) Program. The test results show that the shear plane is not positioned along the T-shape barrette shaft perimeter under vertical loading. For piles under lateral loading, apparently, possible concrete cracking in the FEM analysis of the pile significantly affects the calculated results of both T-shape barrette and bored piles. If concrete cracking effect is neglected in the numerical analysis, the results tend to overestimate the pile capacity. For the design approach, the back analysis suggests that input soil stiffness for T-shape barrette should be about 3 times of empirically calculated value for bored pile to predict deflection values before concrete cracking. Besides, that the flexural stiffness of T-shape barrette should be decreased by approximately 70% to obtain the lateral movement after concrete cracking.

Department : Civil Engineering Student's Signature

Field of Study : Civil Engineering Advisor's Signature Wanchai Tep

Academic Year : 2009

ACKNOWLEDGEMENTS

The authors wish to express their appreciation to SEAFCO Public Company Limited who full supported with generous budgets for the load testing programs of this research study. Thanks are also extended to the 90th anniversary of Chulalongkorn university fund (Ratchadaphiseksomphot endowment fund) for a grant provided for the research. Special thanks are given to the staff of SEAFCO PCL, STS Co., Ltd and EDE Co., Ltd for their comprehensive and hard work during testing programs. Finally, A word of thanks is devoted to all professors and the staff of Department of Civil Engineering, Chulalongkorn University who provided coordination during the research.

CONTENTS

CONTENTS (Con't)

CONTENTS (Con't)

Page

LIST OF TABLES

LIST OF FIGURES

LIST OF FIGURES (Con't)

LIST OF FIGURES (Con't)

Page

LIST OF SYMBOLS

3D	Three dimensions or three dimensional
α	Adhesion factor
ρ	Radius of curvature
ε	Measured strain
σ'_{V0}	Effective Overburden Pressure
σ_x	Stress along the x axis
$\varnothing$	Pile curvature
A	Sectional area of pile
A_s, B_s	Slope Coefficients for free head
A_m, B_m	Moment Coefficients for free head
A_p, B_p	Soil Reaction Coefficients for free head
$(AE)_P$	Equivalent Axial Pile Stiffness
B_y	Deflection Coefficients for free head
C_u / S_u	Undrained Shear Strength
C_y	Deflection Coefficients for fixed head
C_m	Moment Coefficients for fixed head
D	Pile Diameter
EI	Pile Stiffness
E_p	Modulus of elasticity of pile
Es	Secant modulus of pile material
H	Applied horizontal load
$I_{\rho H}$	The displacement influence factor for horizontal load only, acting on ground surface
$I_{\rho M}$	The displacement influence factor for moment only, acting on ground surface
I_p	Moment of inertia of pile
K_h	Coefficient of subgrade reaction

LIST OF SYMBOLS (Con’t)

$K_s$tan δ	Friction Factor (ß-Value)
L	Pile length
M	Tangent modulus of composite pile material
M_t	Moment at pile head
Nc	Bearing capacity factor
Nq	Mobilized bearing capacity factor
P	load
P_b	Skin Friction resistance
P_i	Axial Load at i^{th} VWSG level
P_f	End Bearing resistance
P_t	Lateral load at pile head
S_i	Strain at i^{th} VWSG level
W	Weight of pile
x	Depth from ground surface
y	Deflection
z	Depth

CHAPTER I

INTRODUCTION

1.1 BACKGROUND

Recently, with the developments of bored pile construction technology, pile can be designed to carry higher load in comparison with the past. Furthermore, since piling equipments is developed continuously to construct various sizes of pile designers have more choice to arrange different options of pile caps or footing configuration. Generally in geotechnical aspect the footing shall has small number of piles to reduce total stress bulb of external load that helpful for settlement decreasing, pile and footing construction costs. Large diameter bored pile with 1.50, 1.65, 1.80 and 2.00 m diameter and barrette with various shapes such as cruciform, L-shape, V-shape and T-shape are selected for supporting high rise buildings or bridge foundation to solve those reasons.

The main load component for design of pile foundation is in vertical direction. For some structures, horizontal loading direction come from wind load, seismic load or other force causing lateral load on the piles is need to be taken into account in design process. Thus, piled-foundation might be considered the vertical and lateral loads independent of each other. The pile under lateral loading is the soil-pile interaction problem witch concern to many parameters in both structure and soil properties. The analysis and design pile size, pile length and number of piles in footing must be considered with allowable load, allowable settlement or movement of piles.

The lateral resistance of normal barrette pile is very strong in the longer side but very weak in narrow side. The T-shape barrette pile is, therefore, proposed to be the alternative bored pile for carrying not only vertical loading but also high lateral pile resistance. Due to the rectangular geometry in stem and flange component of T-shape barrette, the side friction and lateral resistance may be controlled by pile section which may have different responses to circular bored pile. Based on many methods and criteria, the main parameters from soil and geometry of pile under vertical and lateral loading must be determined from back analysis with actual full scale load testing results compared with previous research. The obtained parameters from this research will be the advantage for design work in the future.

1.2 RESEARCH OBJECTIVES

The principle aims of this research are related to the followings

1. To analysis and investigate parameters from static compression pile load test results on both T-shape barrette and bored pile.
2. To investigate the response of lateral loaded T-shape barrette and bored pile based on the load tests.
3. To compare the performance between T-shape barrette and bored pile in relations with their skin friction and end bearing capacity under vertical load.
4. To study the effects of size and shape factor of T-shape barrette under lateral or vertical loading condition.

1.3 RESEARCH SCOPE

This research involves the data collection directly from the full scale load testing and some data from previous researchers. The pile testing program that consists of 2 loading conditions in static compression load test and static lateral load test are performed on both bored pile and T-shape barrette. All test piles, constructed under the same conditions are installed with the geotechnical instrumentation.

The static compression test are performed on 2.00 m diameter bored pile and 5 m^2 (1.00x3.00 + 1.00x2.00) T-shape barrette with approximately 55 m length in both types of pile. To compare the behavior between both piles under test loading, Vibration wire stain gauge (VWSG) are planned to install in both piles to measure the strain in each layer. The friction and end bearing resistant can be derived from them to compare with numerical method with 3D FEM and empirical method from previous research.

The static lateral load test are performed to compare between 1.65 diameter bored pile and 5 m^2 T-shape barrette with 55 m length. Two sets of both types of pile are planned to install with inclinometer and strain gauges. The test piles will be loaded act together in each other. In this study the analyses are performed using PLAXIS 3D Foundations, the 3D Finite Element Program (FEM) program.

The limitation of this research is study only the behavior of single pile constructed in Bangkok subsoils condition. All test piles in this research are the part of piles in mat foundation for high rise building project located on Sukhumvit soi 20, Bangkok.

1.4 BENEFIT OF THIS RESEARCH

The test results from static compression test for large section instrumented T-shape barrette consist of 2 components as flange and stem member will give the information about the performance of load transfer and trending shear plane of the rectangular cross section compare with the circular cross section in bored pile.

From the lateral load test program, the results will give the relationships between force and pile deflection along pile length corresponding with each loading. The comparison of the behavior between bored pile and T-shape barrette, which have different pile geometry, under lateral loading are able to be evaluated.

CHAPTER II

LITERATURE REVIEW

2.1 STATIC COMPRESSION TEST

In order to appraise the performance of bored pile and T-shape barrette under vertical and lateral loading tests, the load transfer characteristics, the method to evaluate the ultimate capacity and the method to analyze the lateral movement of pile are reviewed.

2.1.1 LOAD TRANSFER MECHANISM

Load distribution along pile shaft can be determined by calculation in conjunction with the readings from the VWSG which be installed at the rebar cage (Figure 2.1) during piling construction stage and the load at each loading increment.

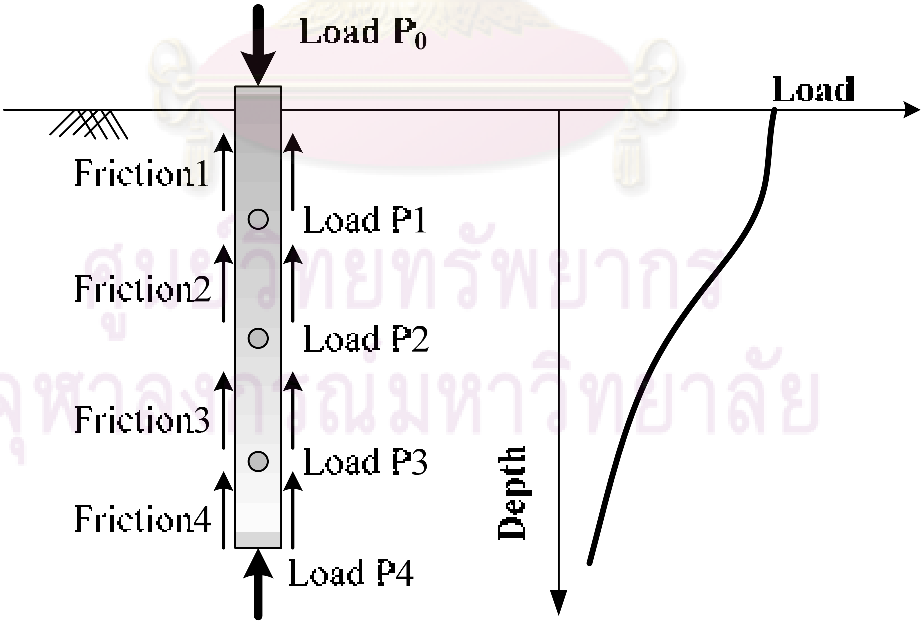

Figure 2.1 Load distribution along pile shaft

The axial load at each strain gauge level can be calculated by the following equation

$$P_i = (AE)_P \text{ x } S_i$$

Where

P_i = Axial Load at ith VWSG level

$(AE)_P$ = Equivalent Axial Pile Stiffness

S_i = Strain at ith VWSG level

Parameter "E" and "A" of pile is difficult to taken real values. Because the modulus of concrete is not know quite accurately, concrete modulus of sample from standard concrete compression test in laboratory may can not use due to difference condition between test pile and sample that testing in laboratory. And the bored pile has possibility to have a defect that makes pile diameter reduces or increase, this can make "EA" value along the pile not necessary the same. However the methods to evaluate "EA" of test pile are shown below.

1. Theory EA

Modulus of concrete can be obtained from standard concrete compression test in laboratory. If not have, an empirical formula such as $Ec = 15210(f'c)^{0.5}$, by Ec (ksc) and f'c (ksc) can be used to calculate the "E" Value.

2. Calibrate Pile Stiffness (EA) from strain gauge near the pile head.

This method calculate from the stress – strain relationship reading from value of strain gauges installed near pile head and value of loading from calibrated hydraulic jack or load cell. The modulus of concrete can be calculate from the stress – strain relationship reading and use it with constant value along the pile shaft.

3. Fellenius's method (1989) Fellenius's approach (1989)

This method assume stress - strain relationship of test pile follow a second-degree line: $y = ax^2 + bx + c$ where y is stress and x is strain.

For a pile taken as a free-standing column (case of no shaft resistance), the tangent modulus of the composite material is a straight line sloping from a larger tangent modulus to a smaller. Every measured strain value can be converted to stress via its corresponding strain-dependent secant modulus.

The equation for the tangent modulus line is:

$$M \times A = \frac{d\sigma}{d\varepsilon} \times A = D\varepsilon + C$$

which can be integrated to:

$$\sigma \times A = 0.5D\varepsilon^2 + C\varepsilon$$

However,

$$\sigma = E_S \times \varepsilon$$

Therefore,

$$P = (E_S \times A)\,\varepsilon = (0.5D\varepsilon + C)\varepsilon$$

Where

M = tangent modulus of composite pile material

Es = secant modulus of composite pile material

D = slope of the tangent modulus line

ε = measured strain

P = load

A = sectional area of pile

C = y-intercept of the tangent modulus line (i.e., initial tangent modulus)

With knowledge of the strain-dependent, composite, secant modulus relation, the measured strain value are converted to the stress in the pile at the gauge location. Then, the load at the gage is obtained by multiplying the stress by the pile cross section area.

2.1.2 DETERMINATION OF PILE CAPACITY BY USING STATIC METHOD

Static method is the calculation method, based on limit equilibrium analysis, to determine pile capacity. The net ultimate pile capacity of a single pile is equals to the sum of the ultimate of end bearing and skin friction resistance, minus weight of the pile as shown below.

$$P_{ult} = P_b + P_f - W$$

where

P_b = Skin friction resistance

= $fs\ A_s$

P_f = End bearing resistance

= $q_b\ A_p$

W = Weight of pile

f_s = αS_u For clay

= $K_s \tan \delta \,.\, \sigma'_{V0}$ For sand

α = Adhesion factor (Figure 2.2)

S_u = Undrained shear strength

$K_s \tan \delta$ = Friction factor (ß-Value) (Figure 2.3)

σ'_{V0} = Effective 0verburden pressure

q_b = $S_u\ Nc + \sigma_{V0}$ For clay

= $\sigma'_{V0}\ Nq$ For sand

A_s = Pile perimeter

A_p = Pile cross section

Nc = Bearing capacity factor

= 9 For pile foundation

Nq = Mobilized bearing capacity factor (Figure 2.4)

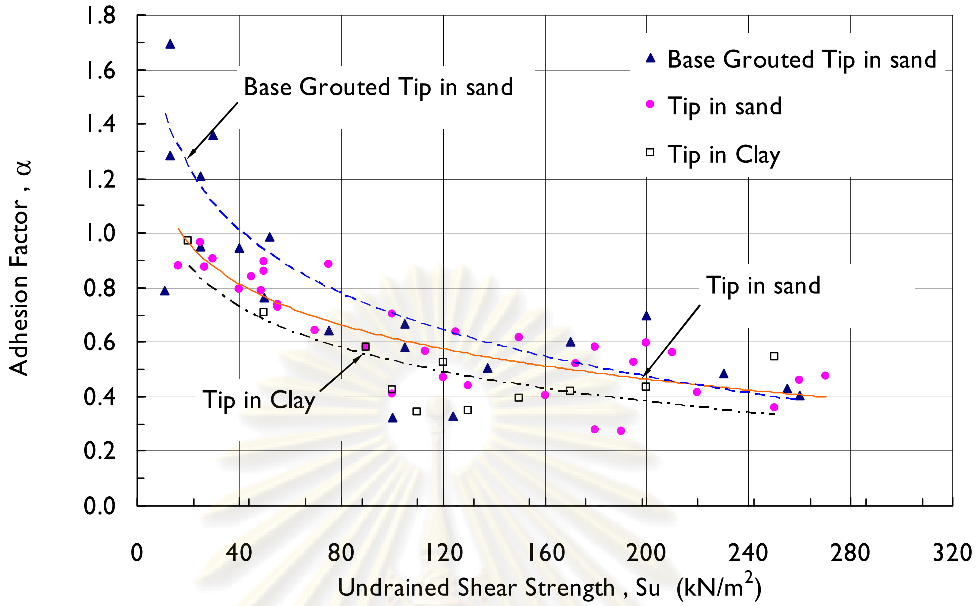

Figure 2.2 Adhesion factor (Submaneewong, 1999)

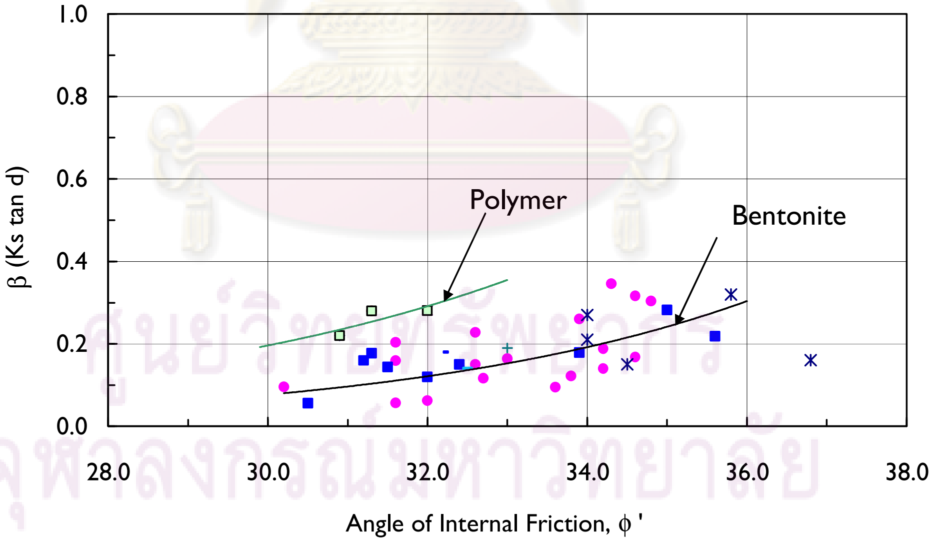

Figure 2.3 Friction factor (β-Value) (Submaneewong, 1999)

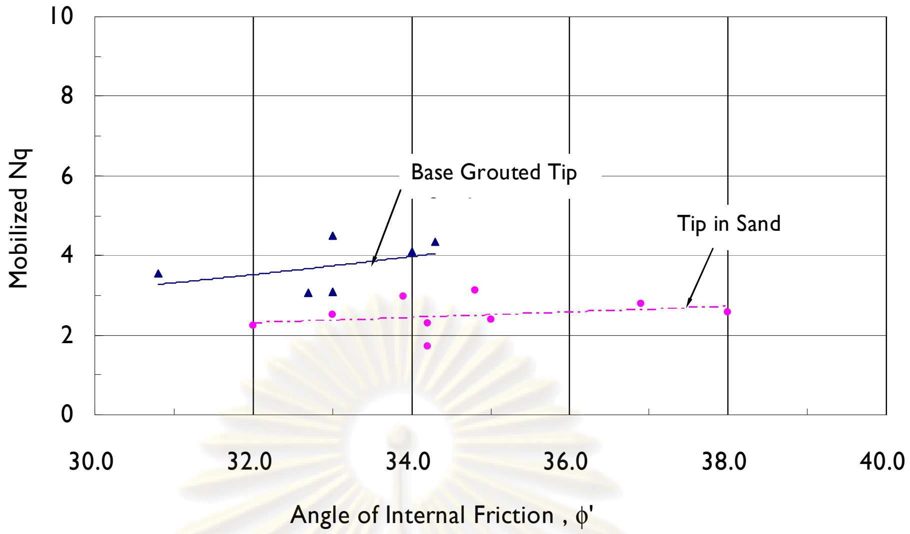

Figure 2.4 Mobilized bearing capacity factor (Submaneewong, 1999)

2.2 LATERAL MOVEMENT ANALYSIS OF SINGLE PILE

2.2.1 BEAM ON ELASTIC FOUNDATION, BEF

Analysis of lateral load pile can use beam on elastic foundation (BEF) method which proposed by Winkler. BEF method assumes that pile-soil interaction is infinite row of isolate spring around the pile. Individual isolate spring can be compressed when subjected to external force. Moreover, the method also assumes that pile is elastic beam, also shown in Figure 2.5.

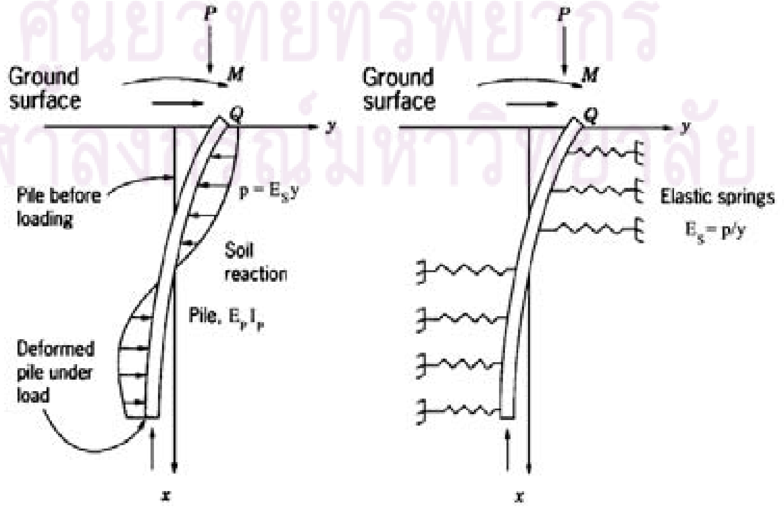

Figure 2.5 Behavior of pile base on Winkler's assumption

Winkler has proposed the following relationship

$$\frac{\mathrm{p}}{\mathrm{y}} = \mathrm{Cons\,tan\,t} = \mathrm{K_h}$$

Where p = Soil pressure $[F/L^2]$
y = Deflection [L]
K_h = Coefficient of subgrade reaction $[F/L^3]$

and elastic curve equation of straight beam for flexible beam is

$$\mathrm{EI}\frac{\mathrm{d}^4\mathrm{y}}{\mathrm{dx}^4} = \mathrm{p}$$

substitute p-value into above equation hence, basic equation for flexible beam analysis is

$$EI\frac{d^4y}{dx^4} = K_h \times y$$

Soil Modulus (E_S) is

$$E_s(x, y) = \frac{p}{y} = K_h \times D$$

Where p = Soil reaction per unit length of pile [F/L]
y = Deflection [L]
x = Depth from ground surface [L]
K_h = Coefficient of subgrade reaction $[F/L^3]$
D = Pile Diameter [L]

Relationship of p and y-value is non-linearity at various depths as shown in Figure 2.6. Then, E_s is a function of depth (x) and deflection distance (y). Hence, relationship between E_S and depth (x) is changed when magnitude of external force changes, as shown in Figure 2.7. However, E_S is normally assumed to function with depth only, in order to avoid the problem of non linear differential equation.

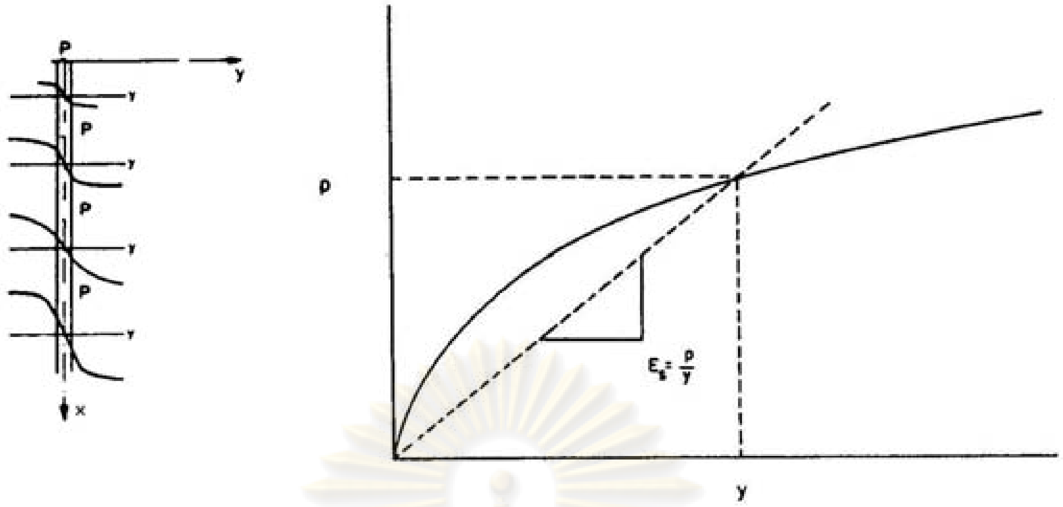

Figure 2.6 Characteristic shape of p-y curve

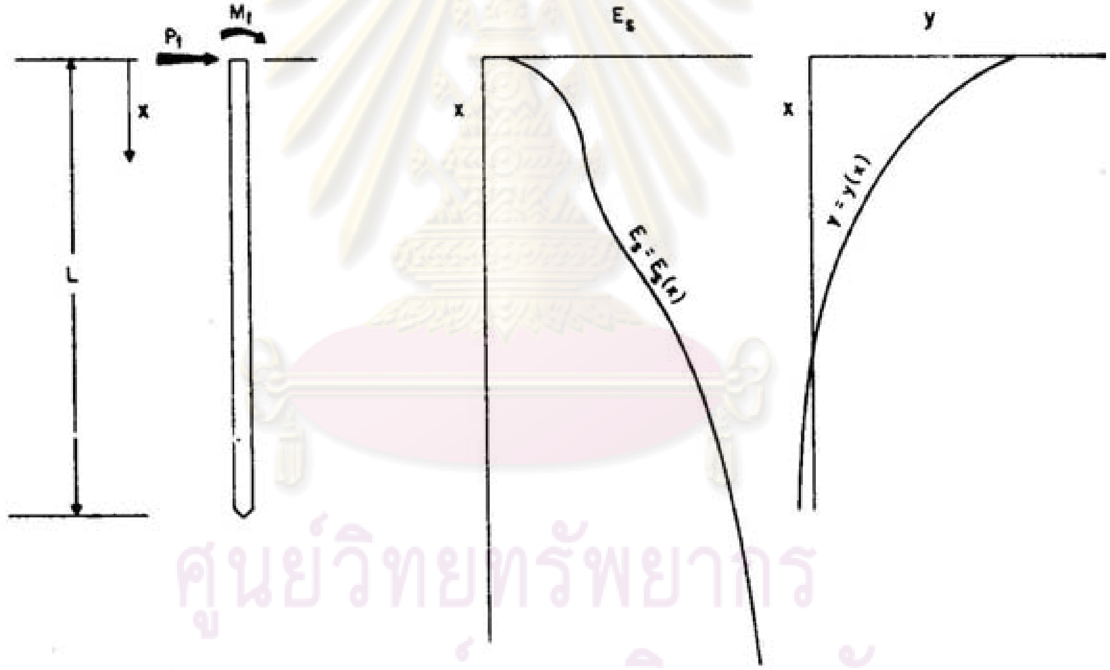

Figure 2.7 Relationship between E_S and depth (x)

When assume that $E_S = f(x)$ then, relationship between E_S and x is the same, although deflection distance or force is changed. Range of E_S-value that is not changes with external force or deflection is the elastic range of soil only. Hence, charts of Matlock and Reese (1960), Davisson and Gill (1963) that refer to $E_S = f(x)$, can only be used when external force is in elastic zone of soil or working load. If external force has exceeded working load then, analysis shall be p-y curve method.

Matlock and Reese (1960) has proposed non dimension chart, when $E_S = kx$ then

$$y = y(x, T, L, E_S, E_pI_p, P_t, M_t)$$

Where

T = Stiffness Factor [L]

$= \sqrt[5]{\frac{E_pI_p}{k}}$ (when $E_S = kx$)

L = Pile length [L]

P_t = Lateral load at pile head [F]

M_t = Moment at pile head [FL]

EI = Pile Stiffness [FL]

k = Constant [F/L^3]

In case that applied force is in the range of soil flexibility or in the range of working load, deflection of pile will be minimum value when compare to pile diameter. Therefore, behavior of pile shall be in flexible range, in order to use super position theory and can calculate force and moment as follow

$$y = y_A + y_B$$

where y_A and y_B are deflection of pile due to force and moment, respectively. Based on non dimension analysis, then

$$\text{Deflection } y = y_A + y_B = \left[\frac{P_tT^3}{E_pI_p}\right] A_y + \left[\frac{M_tT^2}{E_pI_p}\right] B_y$$

$$\text{Slope} = s_A + s_B = \left[\frac{P_tT^2}{E_pI_p}\right] A_s + \left[\frac{M_tT}{E_pI_p}\right] B_s$$

Bending Moment $= M_A + M_B \quad [P_tT]\ A_m + [M_t]\ B_m$

Shearing Force $= V_A + V_B = \quad [P_t]\ A_v + \left[\frac{M_t}{T}\right]\ B_v$

Soil reaction $= p_A + p_B = \quad \left[\frac{P_t}{T}\right]\ A_p + \left[\frac{M_t}{T^2}\right]\ B_p$

and Depth coefficient $Z = x / T$, max depth coefficient $Z_{max} = L / T$

where$_y$, B_y = Deflection Coefficients for free head

A_s, B_s = Slope Coefficients for free head

A_m, B_m = Moment Coefficients for free head

A_p, B_p = Soil Reaction Coefficients for free head

In case of fixed-head pile , slope of pile head is equals to zero. After apply to equation and determine A_s,B_s Chart at x = 0 then, $M_t = -0.93P_tT$

substitute into equation,

Deflection $y = (A_y - 0.93B_y)\frac{P_tT^3}{EI}$

or $= C_y\frac{P_tT^3}{EI}$

and Bending Moment $= C_mP_tT$

where

C_y = Deflection Coefficients for fixed head

C_m = Moment Coefficients for fixed head

Coefficient A_y , B_y , C_y , A_s , B_s , A_m , B_m , A_p , B_p , A_v , B_v when $E_S = kx$ are presented in Figure 2.8 and 2.9.

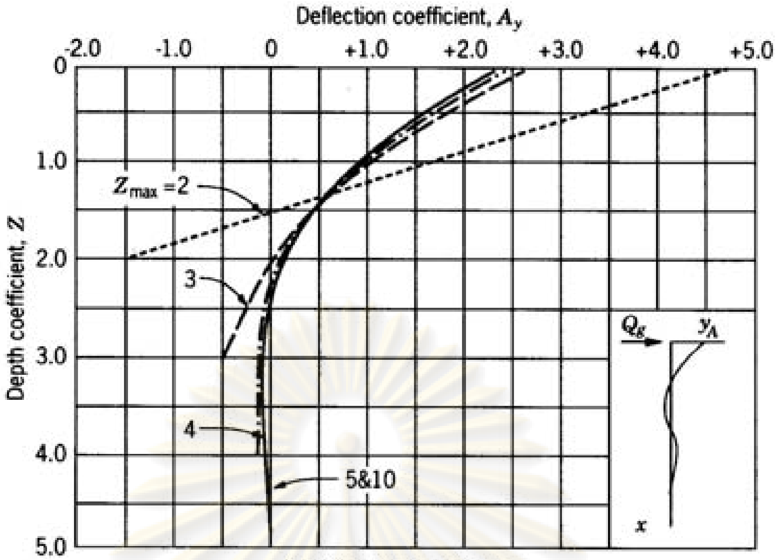

Coefficients for deflection

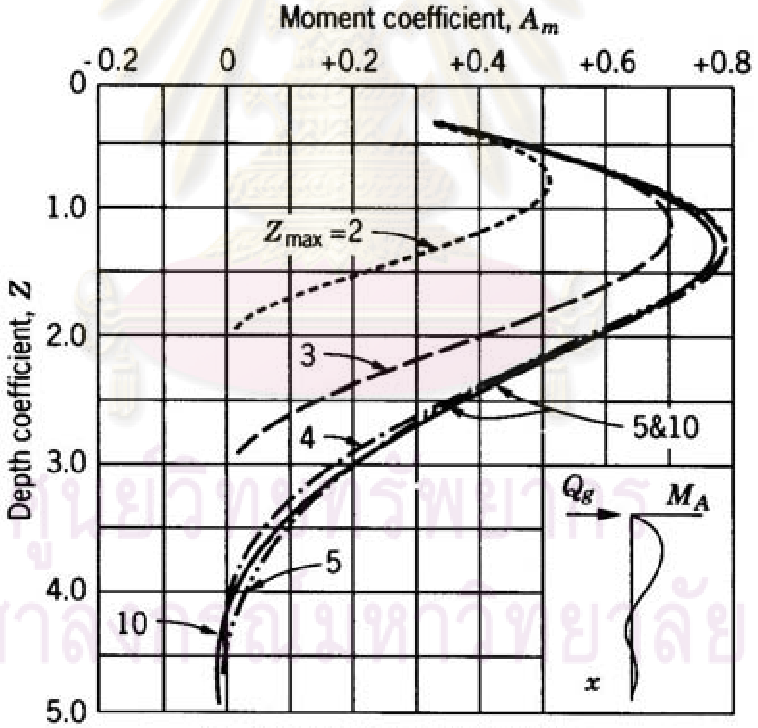

Coefficients for bending moment

Figure 2.8 Coefficients of free-head pile in soil with $E_S = kx$ for pile carrying horizontal load at pile head (Matlock & Reese, 1960)

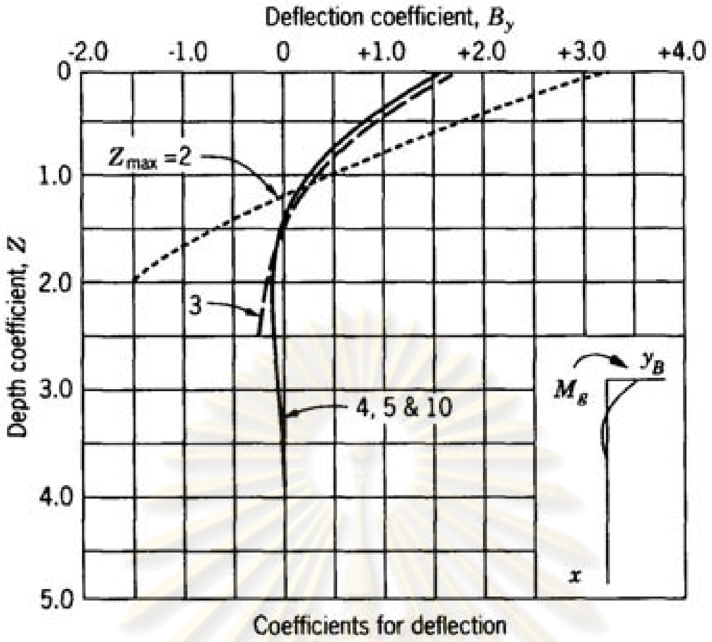

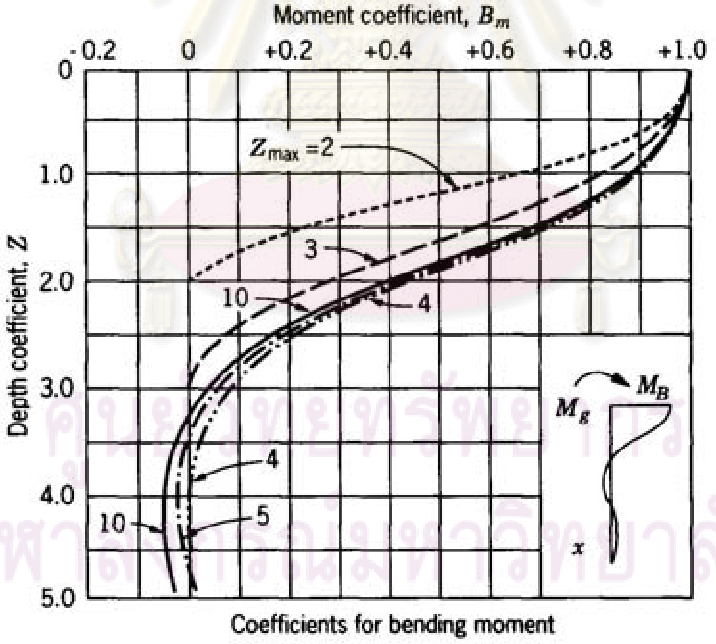

Figure 2.9 Coefficients of free-head pile in soil with $E_S = kx$ for pile carrying moment at pile head (Matlock & Reese, 1960)

2.2.2 ELASTIC APPROACH FOR ANALYSIS OF LATERALLY LOADED PILES

The theory of elasticity is often used to estimate lateral movement of piles and shafts in a variety of geomaterial types. One approach, based on the theory of elasticity, was suggested by Poulos (1971). As presented by Poulos (1971), the lateral behavior of a given pile was generally influenced by the length-to-diameter ratio, L/d, stiffness of the pile, and soil strength and stiffness properties The soil in this case was assumed as an ideal, elastic, homogeneous, isotropic medium, having elastic parameters of Es and νs with depth. The pile was assumed to be a thin rectangular vertical strip of width (d), Length (L), and constant flexibility (E_pI_p). In order to apply the analysis to a circular pile, the width (d) can be taken as the diameter of the pile. To simplify the analysis, horizontal shear stresses, that develop between the soil and the sides of the pile, were not taken into account.

A dimensionless factor KR describing the relative stiffness of the pile/soil material was defined as follows (Poulos, 1971):

$$K_R = \frac{E_P I_P}{E_S L^4}$$

Where, E_p = modulus of elasticity of pile
I_p = moment of inertia of pile
E_S = modulus of elasticity of soil
L = length of pile.

K_R has limiting values of ∞ for an infinitely rigid pile and zero for a pile of infinite length but with no stiffness. The displacement of the pile at the ground surface was presented by using equation below and Figures 2.10 and 2.11 as follows (Poulos, 1971):

$$\rho = I_{\rho H} \frac{H}{E_S L} + I_{\rho M} \frac{M}{E_S L^2}$$

Where,

H = applied horizontal load

M = applied moment

$I_{\rho H}$ = the displacement influence factor for horizontal load only, acting on ground surface (Figure 2.10)

$I_{\rho M}$ = the displacement influence factor for moment only, acting on ground surface (Figure 2.11)

The theory of elasticity approach provides a means to estimate the behavior of pile based on mathematical derivation. However, in reality, soils and weathered rock are highly inelastic materials especially under relatively large deformations. Accordingly, predicted pile deflections commonly match field deflections at low loads (20~30% of total capacity). At higher load levels, the predicted deflections are too small.

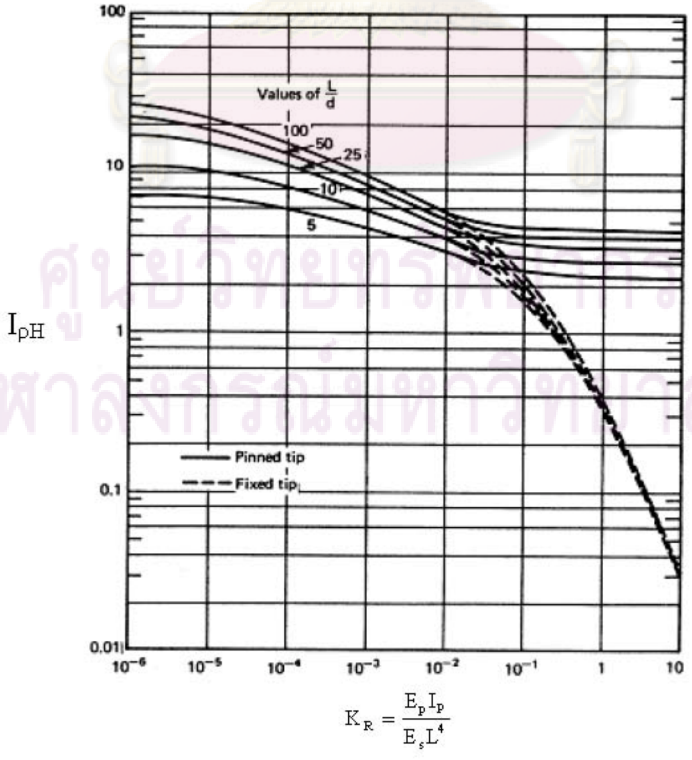

Figure 2.10 Displacement Influence Factor for Horizontal Load (from Poulos, 1971)

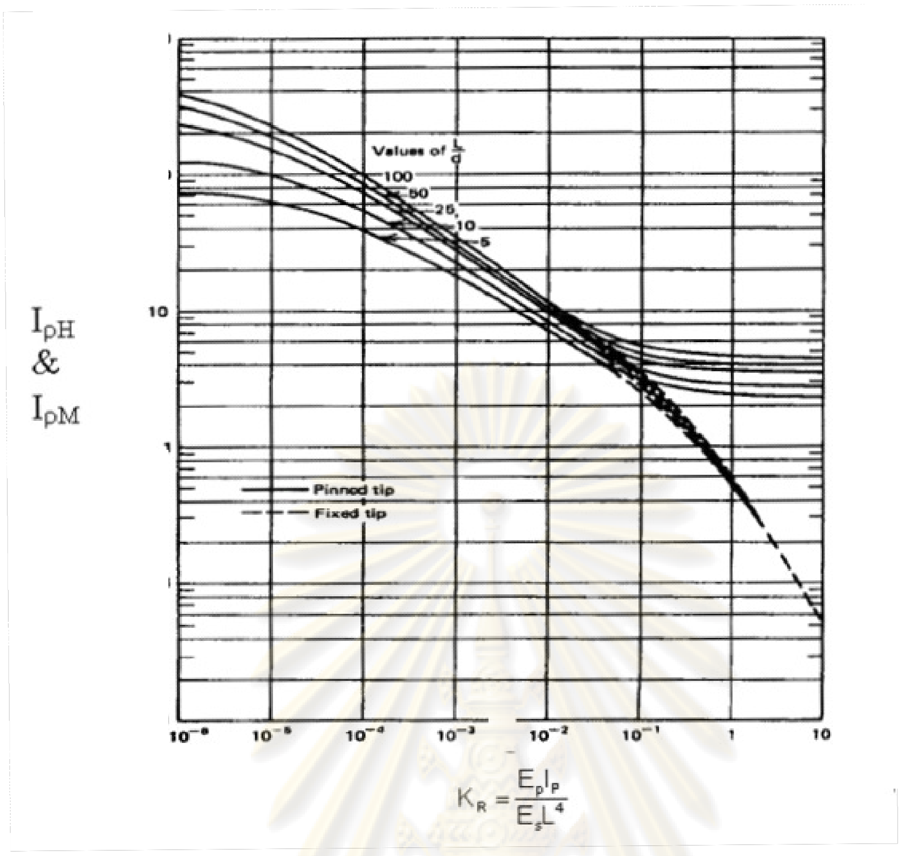

Figure 2.11 Displacement Influence Factor for Moment (from Poulos, 1971)

2.2.3 P-Y CURVE METHOD

p-y curve method is adopted and modified from Winkler principle, by assuming that surrounding ground is infinite rows of non-linear isolate spring and pile is an elastic beam. Behavior of non-linear isolate spring can be presented in p-y curve, also shown in Figure 2.12. , subgrade modulus (E_S) must be the function of x and y in order to simulate the behavior of non-linear isolate spring. To avoid non-linear differential issue, E_S is defined as secant modulus of soil in p-y curve and can be written in form of E_S= f(x) = p / y.

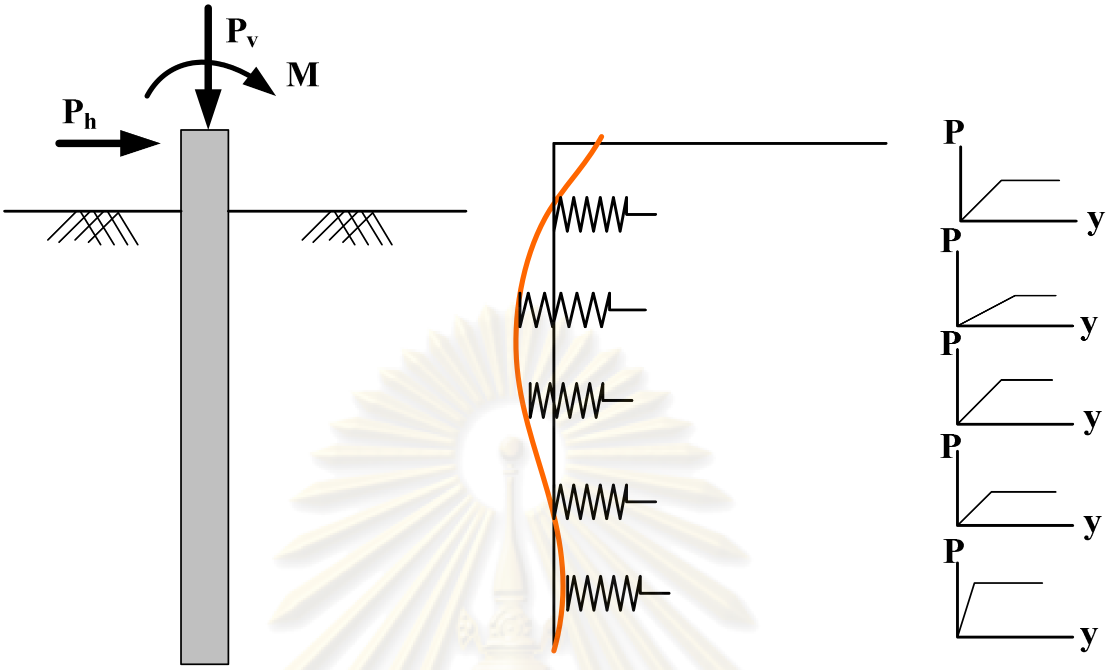

Figure 2.12 Model for pile under the lateral load with p-y curve (Reese, 1997)

The definition of the quantities p and y as used here is necessary because other approaches have been used. The sketch in Figure 2.13 a) shows a uniform distribution of unit stresses normal to the wall of a cylindrical pile. This distribution is correct for the case of a pile that has been installed without bending. If the pile is caused to deflect a distance y (exaggerated in the sketch for clarity), the distribution of unit stresses would be similar to that shown in Figure 2.13 b) The stresses would have decreased on the back side of the pile and increased on the front side. Both normal and a shearing stress component may developed along the perimeter of the cross section. Integration of the unit stresses will result in the quanity p which acts opposite in direction to y. The dimensions of p are load per unit length along the pile. The definitions of p and y that are presented are convenient in the solution of the differential equation and are consistent with the quantities used in the solution of the ordinary beam equation.

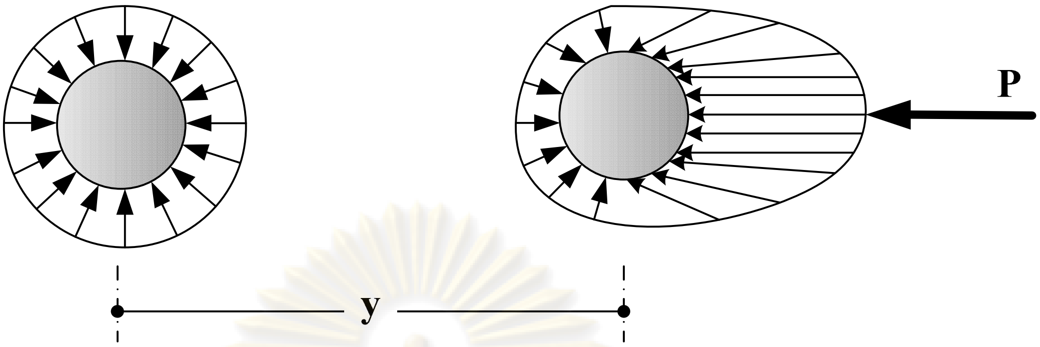

a) Before bending b) After bending

Figure 2.13. Distribution of unit stresses against a pile before and after lateral deflection

In order to solve the problem, the p-y curve have to be created at various depths and then finely adjust Secant Modulus (E_S) of soil in the curve until both deflection distance, based on Beam on elastic foundation, and settlement of soil in the curve are compatible.

P-y curves from measured data can be evaluated using principles of statics. Two sets of equations are used to establish the governing differential equation based on geometry and structural element: the constitutive equation for the pile and the equilibrium equations for the pile element, as shown in Figure 2.14. The constitutive equation for the pile is defined as:

$$M = EI\,\phi = EI\,\frac{d^2 y}{dz^2}$$

Where, M = bending moment at depth, z

E = modulus of elasticity of the pile

I = moment of inertia of the pile around the centroidal axis of the pile section

∅ = pile curvature;

y = pile lateral displacement; and,

z = depth.

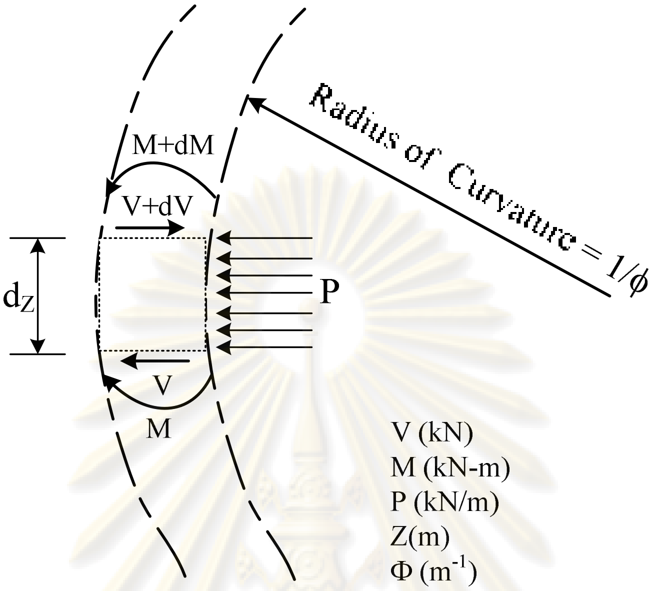

Figure 2.14 Equilibrium of an Element of Pile

Note that the moment of inertia is taken around the centroidal axis of the pile cross section. In the case of concrete piles which may crack, the pile cross section is reduced to account for cracking. In this case it is necessary to first find the neutral axis of the section, under moments and axial loads, in order to evaluate the part of section that remains uncracked. Then the centroidal axis of the uncracked section is found and the a new moment of inertia is calculated around that axis. The horizontal force equilibrium equation for an element of pile is given as (Figure 2.14):

$$dV = Pdz$$

The moment equilibrium equation for the pile element is given as:

$$dM = Vdz$$

Above Equations are combined and lead to the commonly used governing differential equation (Reese and Welch, 1975):

$$EI \frac{d^4 y}{dz^4} + V \frac{d^2 z}{dz^2} - P = 0$$

For pile load tests commonly performed in the field, the major data measured are strains. Stresses acting normal to the cross section of the pile are determined from the normal strain, ε x, which is defined as follows:

$$\varepsilon_x = -\frac{y}{\rho} = -ky$$

Where, y = distance to the neutral axis

ρ = radius of curvature

∅ = curvature of the beam.

Assuming the pile material to be linearly elastic within a given loading range, Hooke's Law for uniaxial stress (σ = Eε) can be substituted to obtain equation

$$\sigma_x = E\varepsilon_x = -\frac{Ey}{\rho} = -Eky$$

Where, σ_x = stress along the x axis

E = Young's Modulus of the material

This equation indicates the normal stresses acting along the cross section vary linearly with the distance (y) from the neutral axis. For a circular cross section, the neutral axis is located along the centerline of the pile. Given that the moment resultant of the normal stresses is acting over the entire cross section, this resultant can be estimated as follows:

$$M_0 = -\int \sigma_x ydA$$

Noting that –Mo is equal to the bending moment, M, and substituting for σ_x, the bending moment can be expressed by equation as:

$$M = -kEI$$

Where, $I = \int y^2 dA$

This equation can be rearranged as follows

$$K = \frac{1}{\rho} = \frac{M}{EI}$$

This equation is known as the moment-curvature equation and demonstrates that the curvature is directly proportional to the bending moment and inversely proportional to EI, where EI is the flexural stiffness of the pile.

During a load test, collected strain-evaluated moment data are used to curve fit the function plotted with depth from the point of load application. Through integration and differentiation, these data can provide soil reaction values with depth. For example, a fourth order regression line is selected to curve fit the data shown in Figure 2.15 and corresponding variable are obtained as follows:

$y = a + bx + cx^2 + dx^3 + ex^4$

Where: a, b, c, d, e = the coefficients of the regression line

x = pile segment length (m).

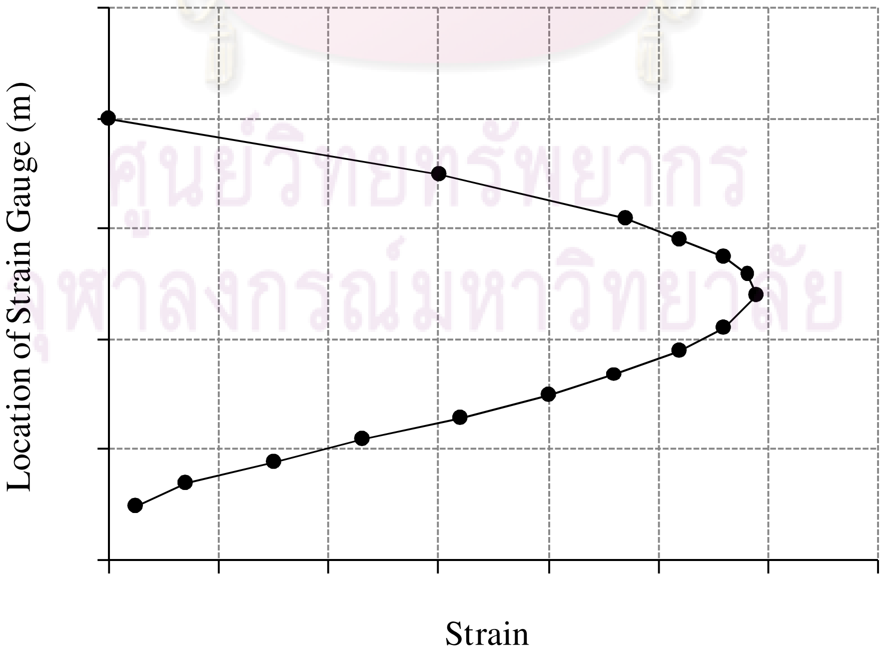

Figure 2.15 Typical Measured Strain from Testing

Once this equation is obtained, it is differentiated, with respect to depth, three times to estimate the resistance of soil P. This equation can be integrated twice to obtain y (m). Alternatively, the lateral deflection can be directly monitored during testing using inclinometer system. These values are then used to create P-y curves with depth.

2.3 SUMMARY OF LITERATURE REVIEW

Plumbridge et al (2000) presented the results of lateral load tested on large diameter bored piles and one lateral load test on barrette carried out for the Kowloon-Canton railway corporation in Hongkong. The test results showed that the traditional assumes horizontal soil stiffness of $E_S = 1xN$ (Mpa) for predicted pile head deflection, where N is the result of the SPT, was conservative.

The offshore lateral load test performed on 1,830 mm diameter pile founded in marl and located in the river in water approximately 15m for the Fuller Warren Bridge project in Jacksonville, Florida was provide useful information presented by Raymond et al (2002). The performance of the laterally loaded test pile was governed by the structural stiffness of the shaft. Lateral displacement of a shaft with a cracked cross section can be mare than twice the displacement computed for an uncracked section.

Zhang (2003) performed the full scale lateral load tests on barrettes in Hongkong. One with a cross section of 2.8 m by 0.86 m and a length of 51 m (DB1) and the other with a cross section 2.7 m by 1.2 m and a length of 30 m (DB2) as shown in figure 2.16. His study aimed to investigate the respond of the two test barrettes by simulate with a numerical procedure using nonlinear p-y curves for soil and nonlinear stress-strain relations for the barrette concrete and reinforcement. His study showed upon cracking of the barrette section, the horizontal displacement and rotation of the barrette increase abruptly under a small lateral load increment and the depth of load transfer in the ground decrease.

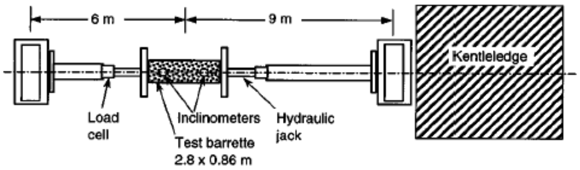

(a) Test barrette DB1

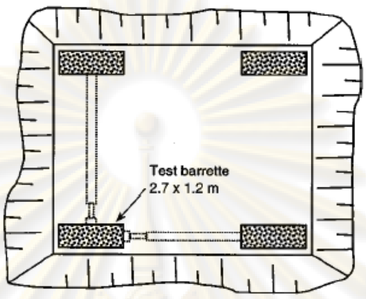

(b) Test barrette DB2

Figure 2.16. Plan view for setup for testing barrette

Hsueh et al (2004) performed load test on pilot bored pile with diameter of 1.5 m and length about 35 m of the high-speed railway (HSR) project located in Taipao, Chiayi County, Taiwan and analyses by adopting the available finite element code , ABAQUS, and considering nonlinearity of structure and material properties of both soil and shaft for a laterally loaded drilled-shaft analysis, they made some conclusions in the following: For the numerical case simulated and examined, the shaft cracked at loading level of 630 kN. The respective deflection is 10.1 mm only, which shows that the elastic performance of shaft can be kept merely within very small displacement range. Neglecting the nonlinear behavior of structure and material will overestimate the lateral shaft capacity. The ground soil uplift in front of the shaft along the loading direction increases with increased loading level. However, the maximum amount of ground soil uplift is not located at the closed soil/shaft interface, it occurs at the adjacent place in front of the shaft, probably caused by the friction between the shaft and the soil.

Jasim M Abbas (2008) presented the results of the 3D finite element analysis on the behavior of single pile under lateral loadings. The effect of pile shape for both circular and square cross-section on pile response was investigated. In addition, an effect of slenderness ratio L/B is also be carried out in his analysis. Linear elastic model of pile was used for modelling the piles. Mohr-Coulomb model was used to simulate the surrounded soil. The pile – soil interaction composed of 16-node interface elements. A good correlation between the experiments and the analysis was observed in validation example. He found that the pile response is affected by the amount of loading, the pile cross – sectional shape and pile slenderness ratio. The lateral resisting of pile increase in proportioned to the square shape of the pile. In both pile shape, a short pile (L/B = 8.3) gave a small amount of lateral tip deflection than the long piles with a slenderness ratio more than 8.3 for the same amount of loading. Also, the negative base deflection is high for short pile and reduces to zero for long piles.

Intraratchaiyakit (2001) collected the lateral pile load test data for bored piles at four locations in Bangkok, and back analyses to obtaining soil parameters comes from eight single vertical piles. His analyses were done from computer programs, which include his program, developed from the theory of beam on elastic foundation. Com624P, developed based on p-y curve concept (Reese 1977), His program was used for the back analyses for obtaining the normalized soil parameters for the design, based on the behavior of mostly 1.5 m diameter bored piles having the 1.5 to 2.0 percents of reinforced steel. The program Com624P was used for single pile analysis for comparing result of his program. The results of the back analyses show that the yield point of the load deformation plot was resulted from the tension crack occurred in the reinforced concrete pile, obtained from using several E_S versus depth and also with S_u relations. His Analyzed results show all the back analyses using these functions are good and the differences of results are small for practical purpose, for the single pile behavior.

CHAPTER III

RESERCH PROJECT DESCRIPTION

3.1 RESEARCH PROJECT AREA

The research project area is located on Sukhumvit Soi 20, Bangkok as shown in Figure 3.1. This project was planned to be constructed with four 51 to 53 storey towers (Figure 3.2). All of test piles in this research were the part of pile arranged in mat foundation at Tower No. 4. Foundation bored pile of 1.00, 1.35, 1.65, 2.00 m in diameter embedded in sand layer at depth of 55 m were designed to support the building . The test pile location in this research for static compression test and lateral test is shown in Figure 3.3 and 3.4.

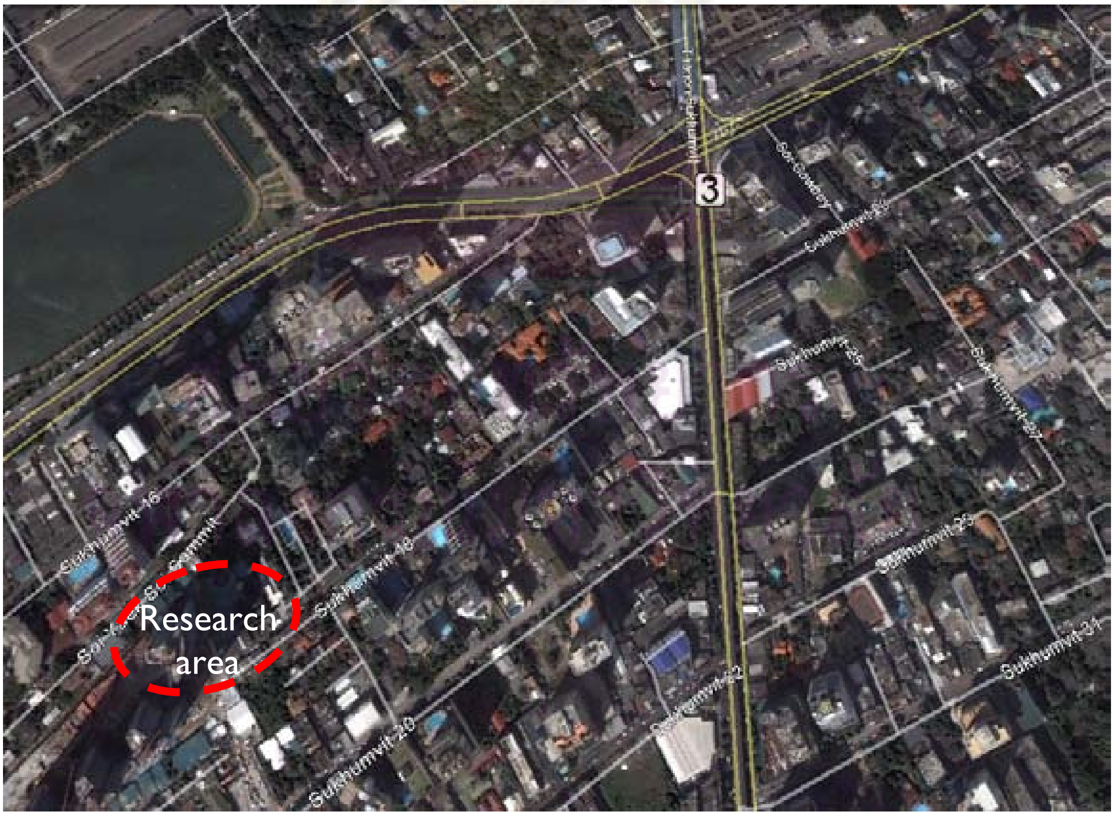

Figure 3.1 Research project area

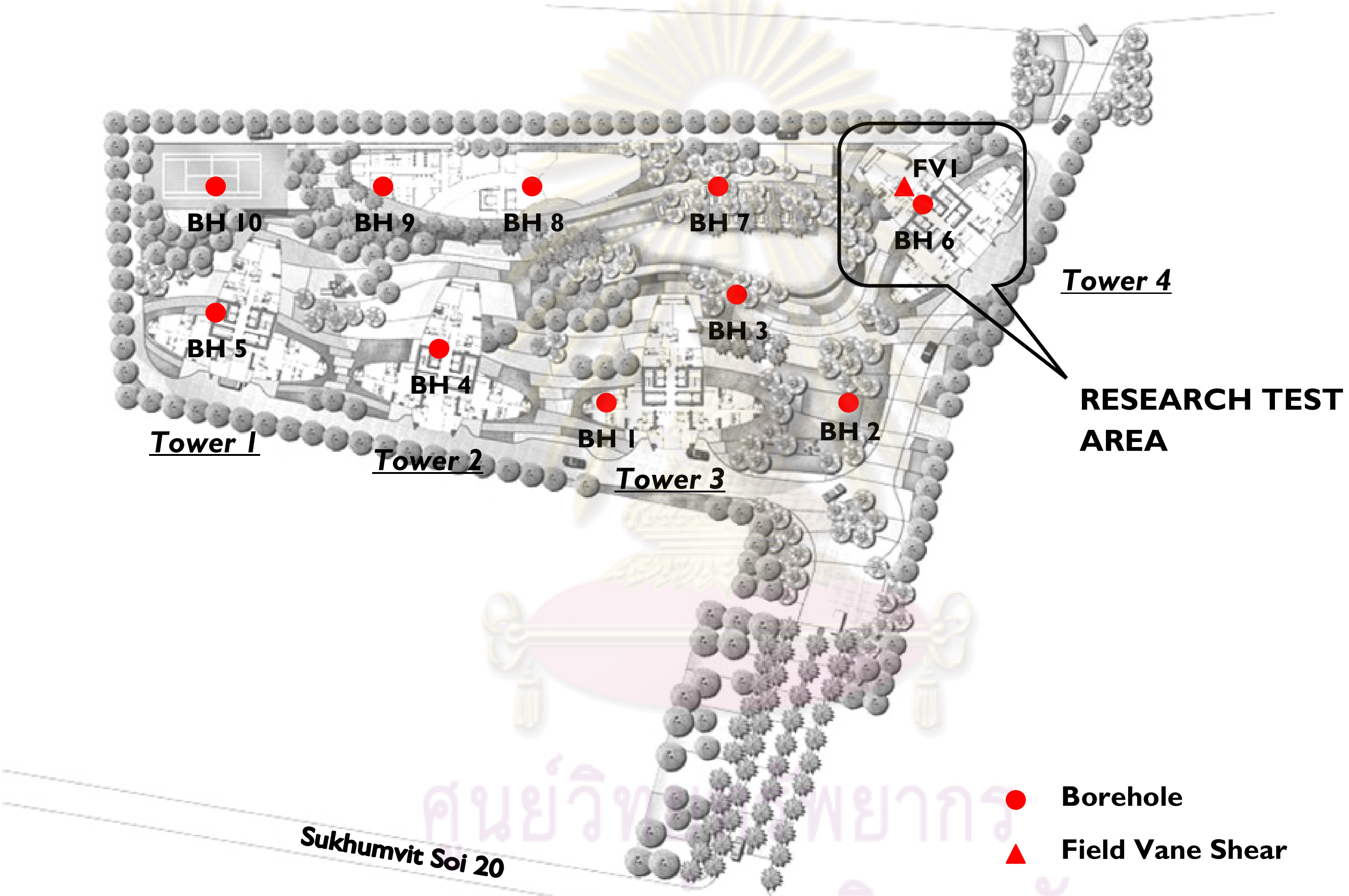

Figure 3.2 Research test area

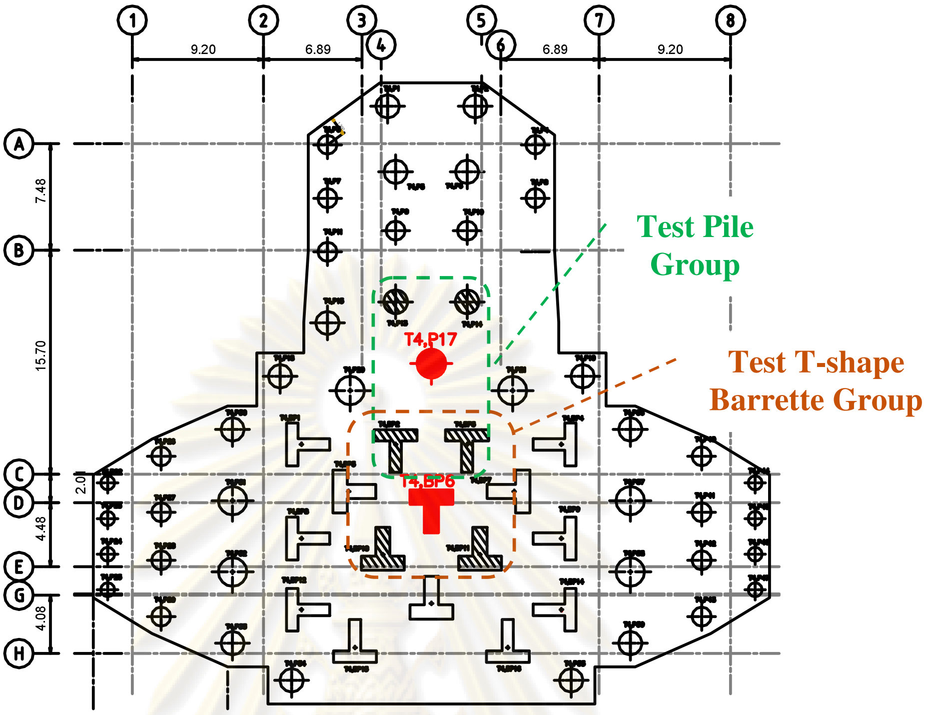

Figure 3.3 Test piles for static compression test

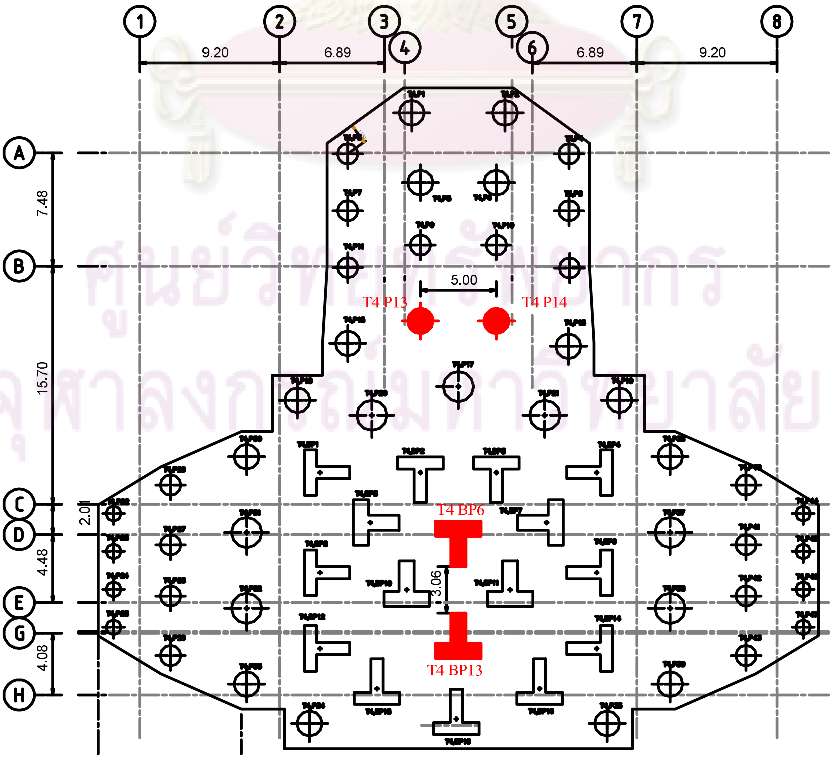

Figure 3.4 Test piles for static lateral test

3.2 GEOLOGY AND SUBSOIL CONDITIONS

3.2.1 GEOLOGY OF BANGKOK SOIL

The Bangkok subsoil is relatively uniform throughout the whole metropolitan area (Phienwej, 1996 and 1997; Shibuya and Tamrakar, 2003). This subsoil consists of two kinds of deposits: First, the terrestrial or quaternary deposits originated from the sedimentation at the delta of the ancient river in the Chao Phraya and second, the marine deposits occuring due to the changes in sea levels during quaternary period. Bangkok is located in the low lying Chao Phraya plain which is about 20 km north of the Gulf of Thailand (Figure 3.5).

The plain becomes a slope towards Tanawsri Moutain range on the west along Thai-Myanmar border and it is developed into Khorat Plateau on the east. The Chao Phraya River and its tributaries such as Tajeen are the major drainage system for the surrounding highlands. Therefore, the Chao Phraya basin is filled with sedimentary soil deposits, which from alternative layers of sand, gravel and clay. The marine clay of Bangkok plain, which is the uppermost claylayer, extends from 200 to 250 km in the East-West direction and 250 to 300 km in the North-South direction. The formation of this layer is known as Bangkok clay and it is believed to be approximately 4000 yeas ago. The deposits, which are confined within the radius of 60 to 80 km from Bangkok, had taken placed during the Pleistocene and Holocene period (Shibuya and Tamrakar, 2003).

The general Bangkok subsoil profiles for the top 70 m thickness reported by Teparaksa (1999) based on the Mass Rapid Transit Authority of Thailand (MRTA) subway project is presented in Figure 3.6. During this MRTA subway project, which is the first subway project to be built in Bangkok, the subsoil layers along the route were investigated by means of the first six self-boring pressuremeter tests ever carried out in Thailand and more than 200 boreholes were made. The subsoils consist of 13-16 m thick soft marine clay at the upper layer. This clay is sensitive, anisotropic and creep (time dependent stress-strain-strength behavior) susceptible. These characteristics have made the design and construction of deep basements, filled embankments and tunneling in soft clay difficult. The first stiff to very stiff silty clay layer is encountered below soft clay and medium clay varying from 21 to 28 m depth. This first stiff silty clay has low sensitivity and high stiffness, which is appropriate to be bearing layer for underground structures. The first dense silty sand layer located below stiff silty clay layer at 21-28 m depth contributes to variations in skin friction and mobilization of end bearing resistance of pile foundations. The similar variations are also contributed by the second dense and coarse silty sand found at about 45-55 m depth (Figure 3.6).

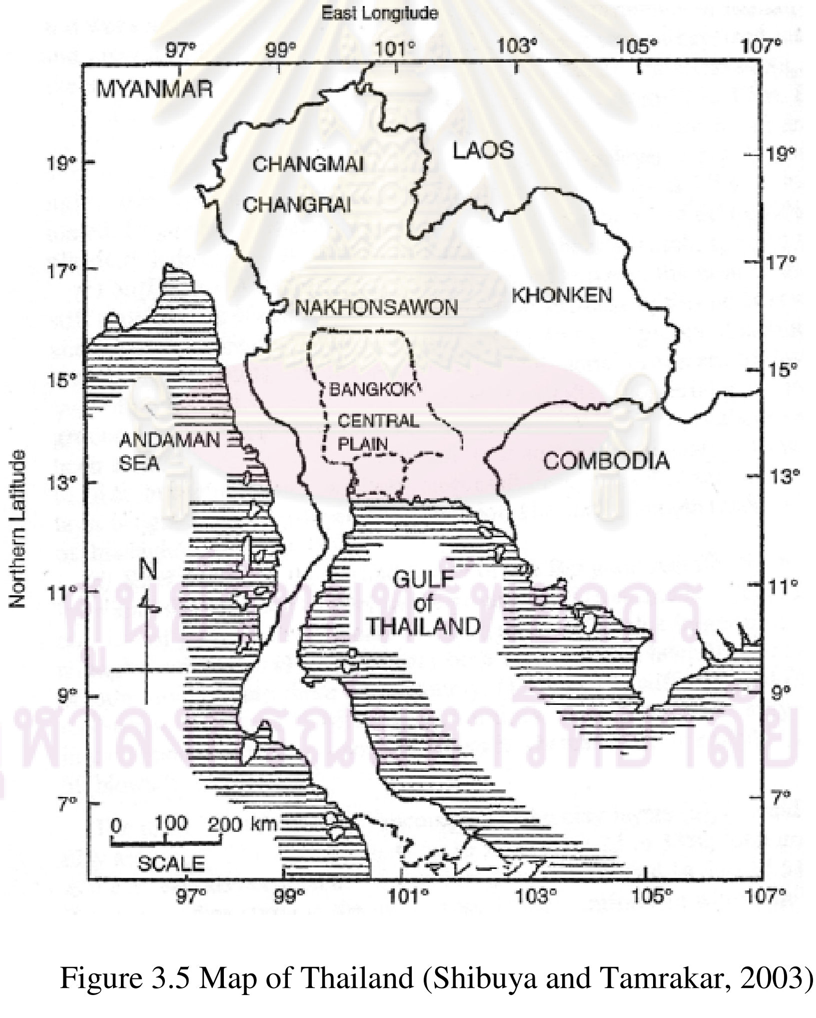

Figure 3.5 Map of Thailand (Shibuya and Tamrakar, 2003)

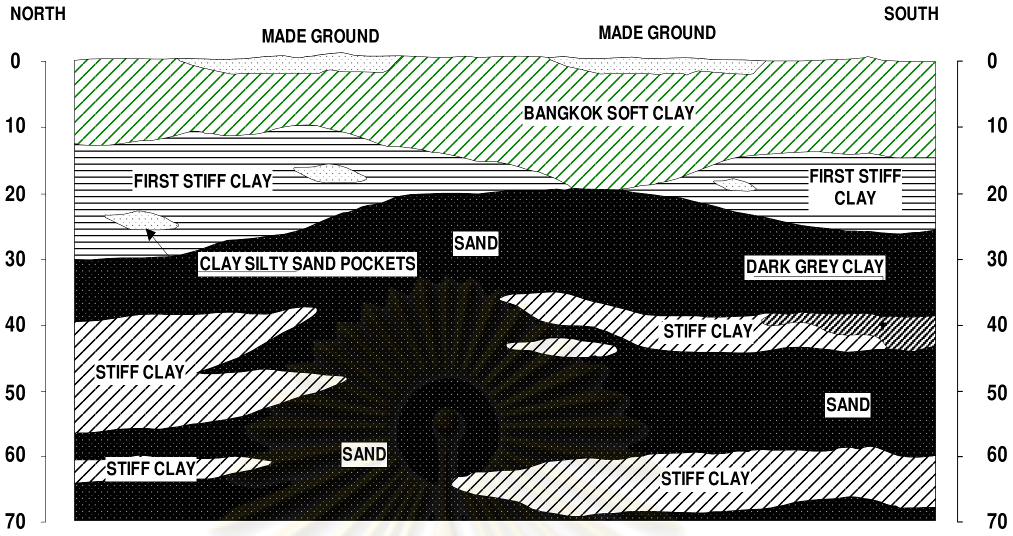

Figure 3.6 General subsoil profile (Teparaksa, 1999)

3.2.2 UNDERGROUND WATER OF BANGKOK

The piezometric profile has been known for Bangkok is hydrostatic starting from 1 to 2 m below ground level to a depth about 7 up to 10 m (Teparaksa, 1999; Teparaksa and Heidengren, 1999; Shibuya and Tamrakar, 2003). However, beneath this depth (about 10 m), due to deep well pumping from the aquifers, a successive reduction of water pressure appeared within the lower part of soft clay and the first stiff clay layers and the zero water pressure could be seen again at the depth about 23 m below ground surface as shown in Figure 3.7 (Teparaksa and Heidengren, 1999; Teparaksa, 1999; Yeow et al., 2004). The piezometer profile beyond this depth becomes a hydrostatic profile for a second time. Teparaksa and Heidengren (1999) and Teparaksa (1999) stated that “the low piezometric level contributes to the increase in effective stress, causing ground subsidence in this city. However, the benefit of this low piezometric level is easy to construct bored piles having pile tip in the first stiff clay using dry process and dry excavation for basement construction up to the silty clay level without any dewatering or pumping system”.

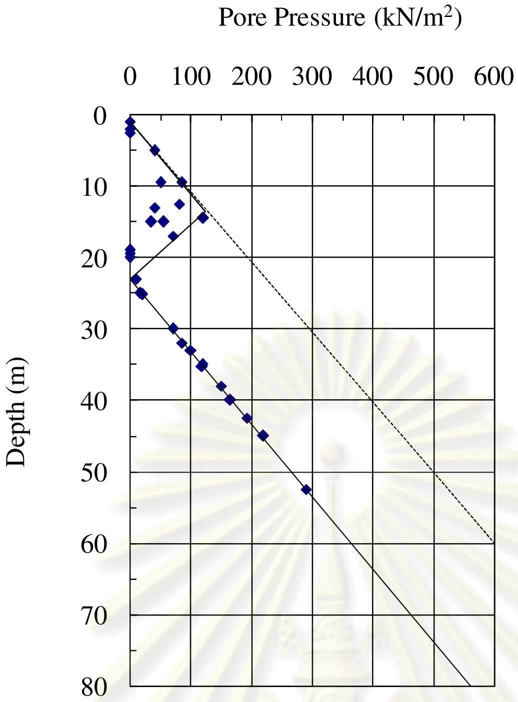

Figure 3.7 Piezometric level of Bangkok subsoils (Teparaksa, 1999)

3.2.3 SUBSOIL CONDITIONS AT THE PROJECT SITE

Soil investigation for this project was planned to perform with 10 borings to the depth of 80 m, namely BH1 to BH-10 as shown in Figure 3.2. The test area for bored pile and T-shape barrette are located at the tower No. 4 with the same soil condition . Figure 19 illustrates the specified soil profile at the test area from borehole BH-6. Very soft to medium clay layer, approximately 15 m thick lies beneath a two meter thick weathered crust. A stiff to very stiff clay layer occurred directly underneath medium stiff clay and its depth goes up to 20.5 m. Below the stiff to very stiff clay layer, thin layer of 3m thick medium dense sand layer can be found. Thick layer of very stiff to hard clay underlies medium dense sand layer and it is found to be about 25 m thick. Another sand layer which is the embedded depth of pile occurs at depths between 48 m and 72 m. Within the second sand layer, a thin layer of hard clay is found. Undrained shear strength obtained from both unconfined compressive test and field vane shear test and SPT-N value were plotted as shown in Figure 3.8.

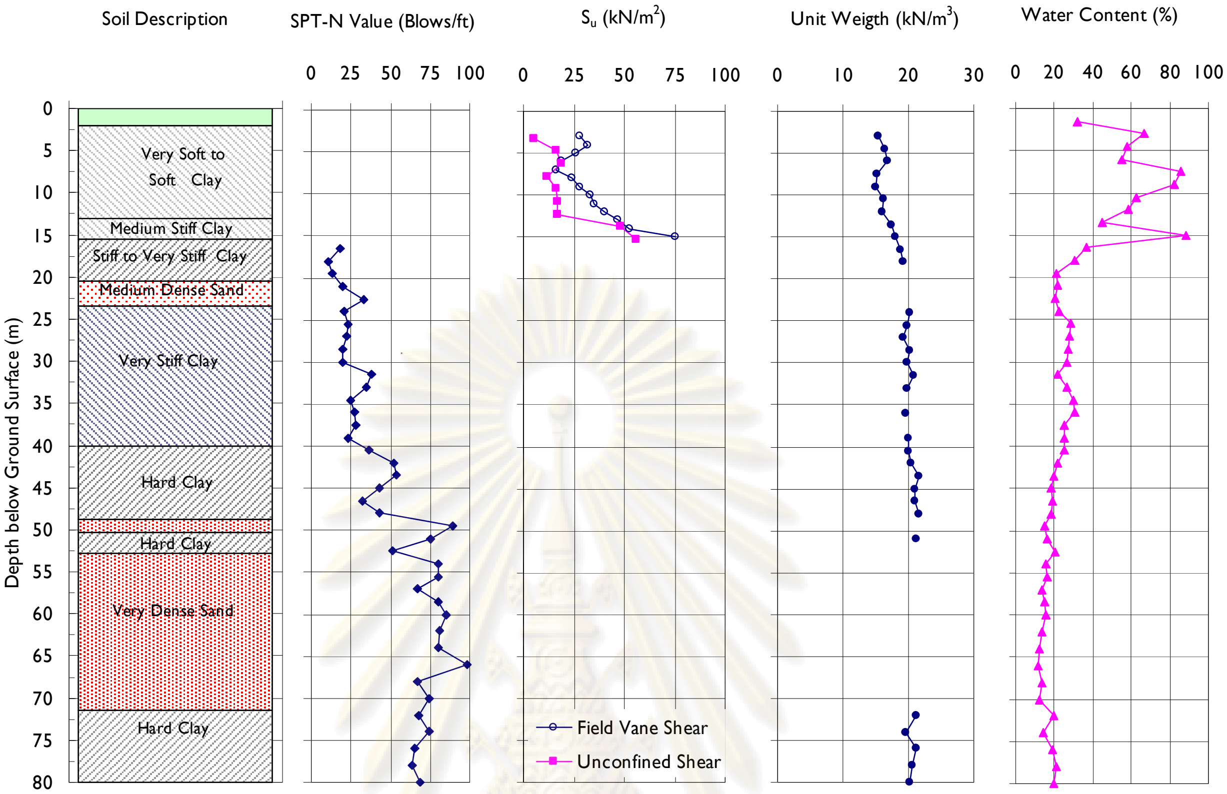

Figure 3.8 Subsoil condition from boring BH-6 at the test area

3.3 TEST PILE CONSTRUCTION METHOD

3.3.1 BORED PILE

Rotary drilling was employed for bored pile excavation. Temporary casing of 15 m length was used as a support in soft clay layer to assure the stability of the borehole. Firstly, auger was used to drill within the temporary casing, followed by rotary bucket with polymer based slurry down to final depth of excavation. Before lowering the reinforcement cage special cleaning bucket was used to scrap of the borehole walls and the base. Reinforcement cages were then lowered inside the borehole while attaching the instrumentation simultaneously at specified locations. Soon after lowering the rebar cage tremie concreting was commenced. Construction sequence for bored piling work is shown in Figure 3.9

a) Install casing

b) drilling by auger & bucket

c) Install rebar cage

d) concreting

Figure 3.9 Construction sequence for bored piling work

3.3.2 T-SHAPE BARRETTE

The construction of T-shape barrette is identical to that of combination of 2 single rectangular diaphragm wall panels. Hydraulic grab, 1.0x3.0 m. was used to excavate the required dimension of T-shape excavation under bentonite slurry. The sercive crane was used for excavation and lifting reinforcement cages as well as construction plant and facilities. A T-shape guide wall with inside clear dimensions slightly larger than the nominal size of the barrette was used to guide the grab during initial bites. Circulation of slurry was continuously done to keep the bentonite slurry agitated, to minimize the building up of filter cake on trench wall surfaces. Properties of bentonite slurry were maintained within the specified ranges in wide use.

Sediment or loose materials at the bottom of the trench were removed and any built-up filter cakes were scraped off by the grab before reinforcement cage installation. The reinforcement cage of T-shape barrette was fabricated in two complete sections. For the purpose of lifting and handling the cage, temporary stiffeners, lacing and tie bars were necessary. These temporary bars were removed section by section while the cage was lowered into the trench. After excavation, the trench profile was checked with Koden drilling monitoring equipment. Tremie concreting method by using 2 sets of tremie pipes was used for casting the T-shape barrettes for both flange and stem. Since the cutoff level of T-shape barrettes was generally at ground level, ready-mixed concrete was poured until all slurry and slime in the trench was completely displaced and fresh concrete could be seen.

Construction sequences are shown schematically in Figure 3.10. The construction sequence of T-shape barrette at the project site is shown in Figure 3.11.

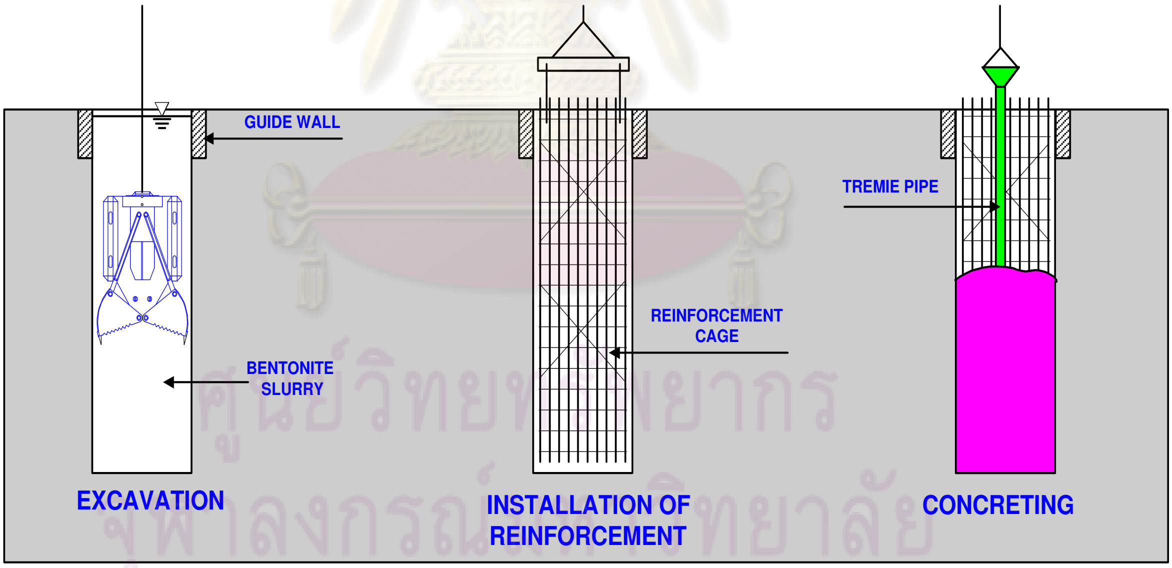

Figure 3.10 Barrette construction sequences (schematic)

a) Install guide wall b) Excavate soil

c) Install rebar cage d) concreting by

Figure 3.11 Construction sequence for T-shape barrette

3.3.3 QUALITY CONTROLS

All drill hole and trenches were checked for verticality and dimensions by using drilling monitoring / Koden test (Figure 3.12) prior to reinforcement cage installation to avoid any obstruction associated with trench inclination. In particular, all sides of the trench were checked. If necessary, verticality of trench was improved by careful chiselling with the grab. As the subsoil conditions varied from one location to another, they were observed during trenching process and verified with the soil conditions assumed in design, especially in the lower section of the barrette. Slurry quality was regularly tested and maintained within the specified ranges. Since test pile and T-shape barrettes were highly reinforced, in order to achieve a good flow of concrete, the concrete mix was checked for appropriateness of slump and cohesiveness prior to casting.

Figure 3.12 Trench profile recorded with drilling monitoring/Koden equipment

Sonic integrity/seismic test was carried out on all test pile about 5 days after casting for checking pile integrity as shown in Figure 3.13 and 3.14.

Figure 3.13 Pile integrity recorded with Sonic integrity/seismic test

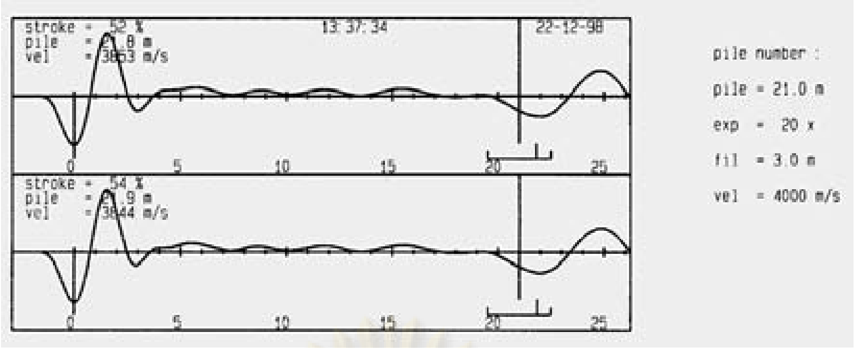

Figure 3.14 Example of seismic test results

CHAPTER IV

RESERCH METHODOLOGY

4.1 TEST PILE CONSTRUCTION

The construction procedure for test piles in this research are reviewed in topic 3.3. The description and records of the test pile construction in this research are presented in Table 4.1 and 4.2. Additional procedure to measure the as-built profile of the drilling/excavating trench were performed by drilling monitoring (Figure 4.1). The drilling monitoring test results are shown in Figure 4.2 and 4.3.

Table 4.1 The description and records of the test pile for static compression test

Parameter	Test Pile for Static Compression Test	
Pile No.	T4 P17	T4 BP 6
Pile Type	Bored pile	T-shape barrette
Pile Size (m)	∅ 2.00	(1x3)+(1x2)
Pile tip (m)	-55.98	-55.70
Slurry Type	Polymer based	Bentonite
Viscosity (sec)	50	36
Density (g/cc)	1.03	1.05
Sand Content (%)	0.25	2.5
pH Value	9	9
Concrete fc' (ksc)	280	280
Rebar fy (ksc)	4000	5000
1st Rebar Case	32 DB 25 - 10m	10 DB 25 + 15 DB25 - 6m
2nd Rebar Cage	32 DB 25 - 10m	22 DB 25 + 30 DB25 - 10m
3rd Rebar Cage	32 DB 25 - 10m	22 DB 25 + 30 DB25 - 10m
4th Rebar Cage	25 DB 20 - 10m	22 DB 25 + 30 DB25 - 10m
5th Rebar Cage	25 DB 20 - 10m	10 DB 25 + 15 DB25 - 10m
6th Rebar Cage	25 DB 20 - 12m	22 DB 25 + 30 DB25 - 16m
Construction time (Hrs)	15:10	32:30


Figure 4.1 Drilling monitoring test

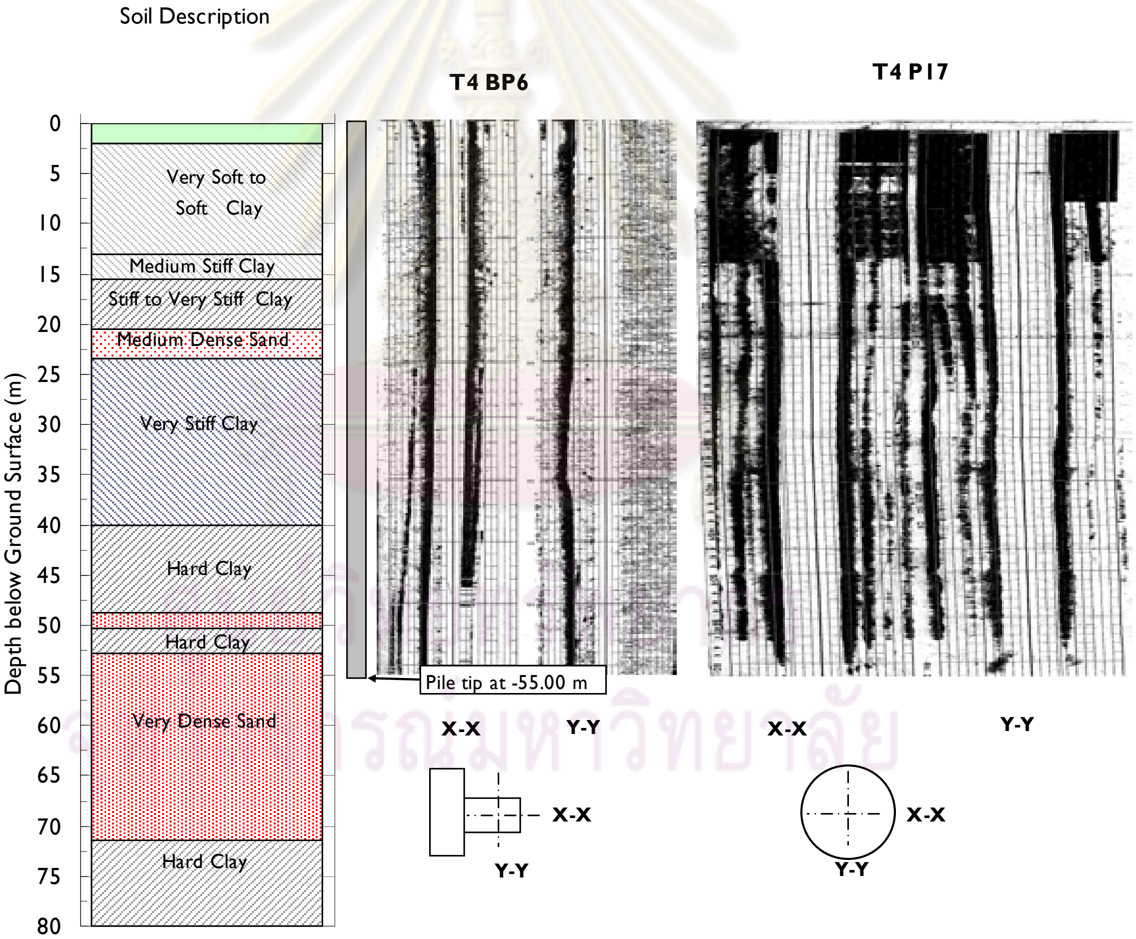

Figure 4.2 Drilling monitoring test results for static compression test piles

Table 4.2 The description and records of the test pile for static lateral test

Parameter	Test Pile			
Pile No.	T4 P13	T4 P14	T4 BP 6	T4 BP 13
Pile Type	Bored pile	Bored pile	T-shape barrette	T-shape barrette
Pile Size (m)	∅ 1.65	∅ 1.65	(1x3)+(1x2)	(1x3)+(1x2)
Pile tip (m)	-55.52	-55.70	-55.70	-55.20
Slurry Type	Polymer based	Polymer based	Bentonite	Bentonite
Viscosity (sec)	47	49	36	35
Density (g/cc)	1.03	1.03	1.05	1.05
Sand Content (%)	0.25	0.25	2.0	2.5
pH Value	9	9	9	9
Concrete fc' (ksc)	280	280	280	280
Rebar fy (ksc)	5000	5000	5000	5000
1st Rebar Cage (12m)	44 DB 32	44 DB 32	20 DB 32 + 22 DB25	20 DB 32 + 22 DB25
2nd Rebar Cage (12m)	44 DB 32	44 DB 32	20 DB 32 + 46 DB25	20 DB 32 + 46 DB25
3rd Rebar Cage (12m)	38 DB 32	38 DB 32	52 DB25	52 DB25
4th Rebar Cage (12m)	32 DB 32	32 DB 32	25 DB25	25 DB25
5th Rebar Cage (12m)	26 DB 32	26 DB 32	25 DB25	25 DB25
6th Rebar Cage (10m)	18 DB 32	18 DB 32	25 DB25	25 DB25
Construction time (Hrs)	18:10	18:30	32:30	46:55

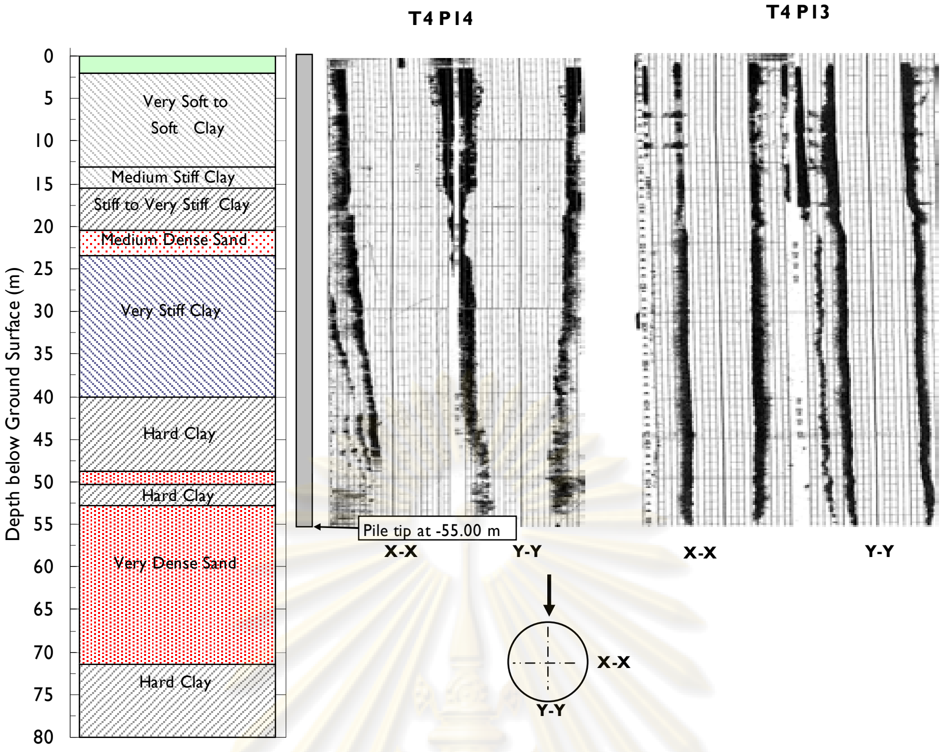

a) Bored pile 1.65m in diameter

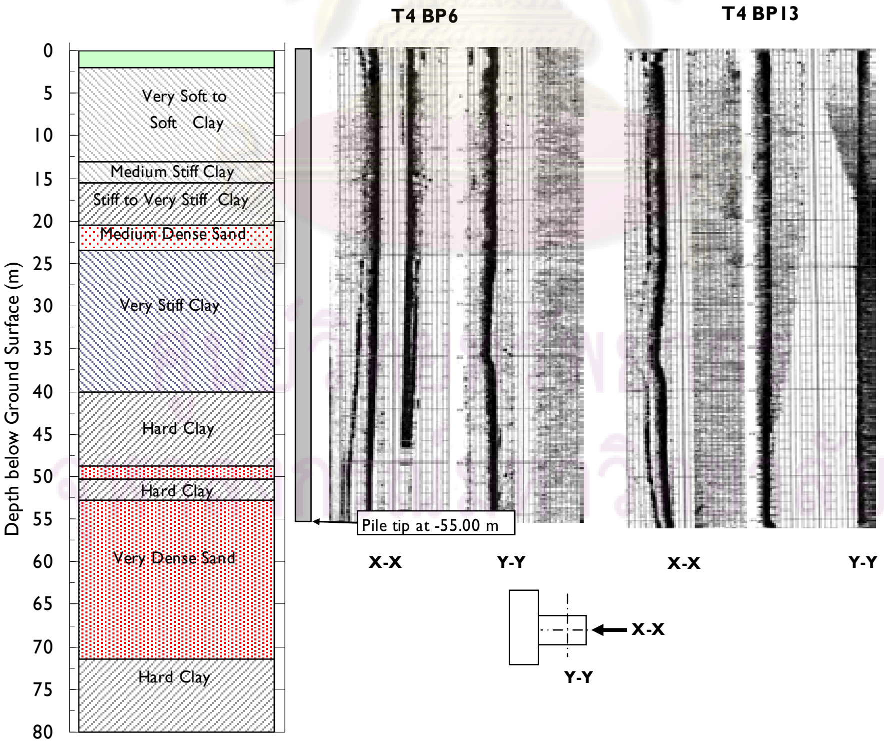

b) T-shape barrette

Figure 4.3 Drilling monitoring test results for static lateral test piles

4.2 GEOTECHNICAL INSTRUMENTATION

4.2.1 INSTRUMENTATION FOR STATIC COMPRESSION TEST

Direct measurement from four dial gauges placed in diametrically opposite positions having equidistance from the test pile axis was used as a main monitoring system of test pile head movement. Precise leveling and piano wire were also utilized as backup for pile head movement measurement. Additional two dial gauges were also used to monitor the lateral movement of the pile. SINCO load cells of 500 ton capacity each were installed on top of the hydraulic jacks to evaluate the actual applied load. Vibrating wire strain gauges (VWSG) were fixed at specified 7 levels along the pile. At each level, two sets of VWSG were installed for the bored pile whereas six sets of VWSG were installed for the barrette. Details of instrumentation are presented in Table 4.3 and Figure 4.4.

Table 4.3 Details of test piles for static compression test

Test pile	Maximum test load (kN)	Instrumentation
Bored Pile ∅ 2.00 m -55.0 m tip 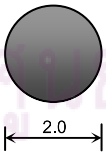	35200	VWSG 7 levels (2 Nos / level) (Figure 4.4)
T-Shape Barrette $(1x3) + (1x2)\ m^2$ - 55.0 m tip 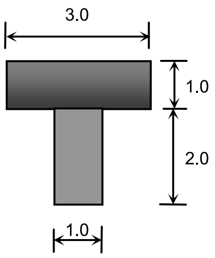	52000	VWSG 7 levels (6 Nos / level) (Figure 4.4)

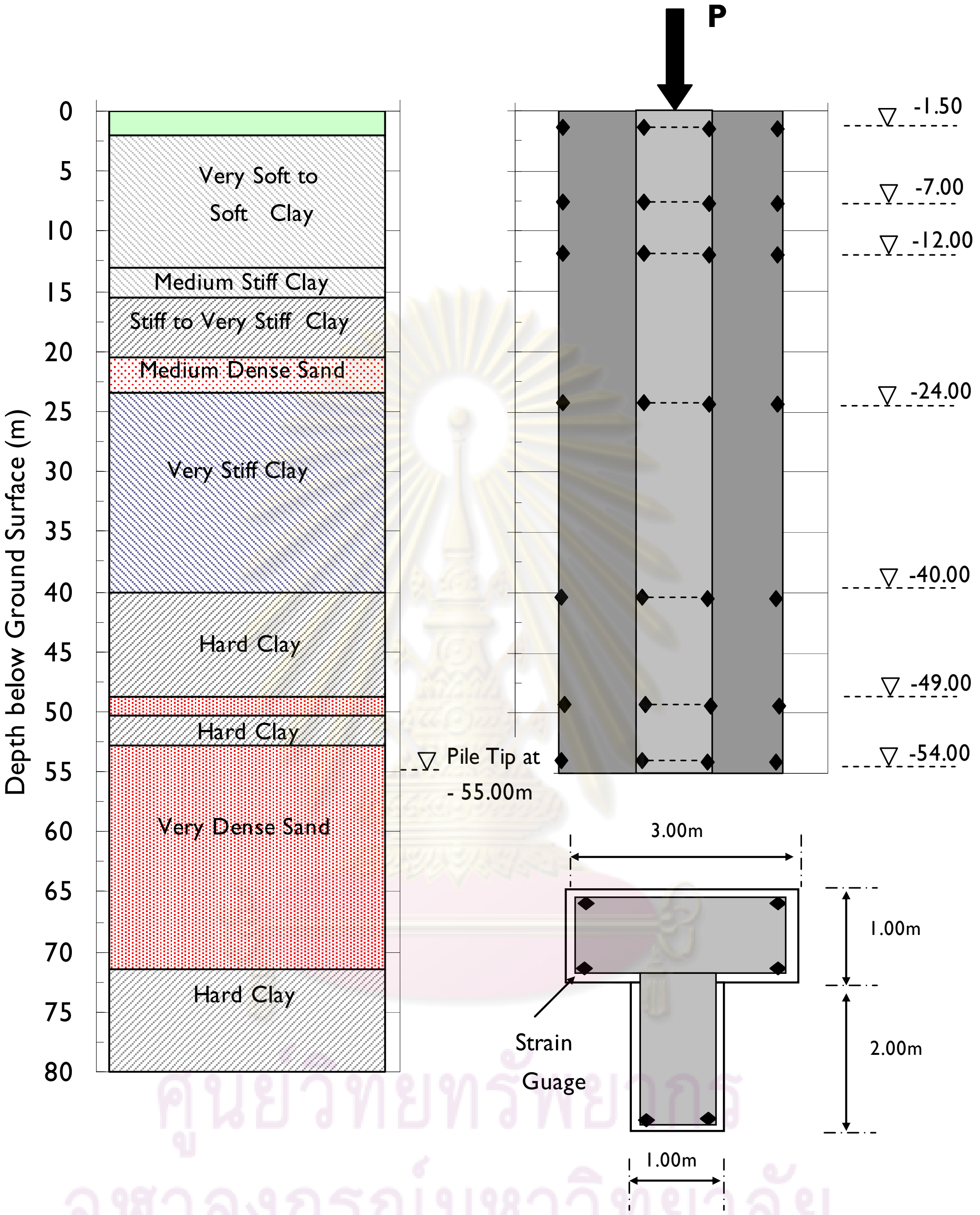

a) T-Shape Barrette

Figure 4.4 VWSG Location for static compression test

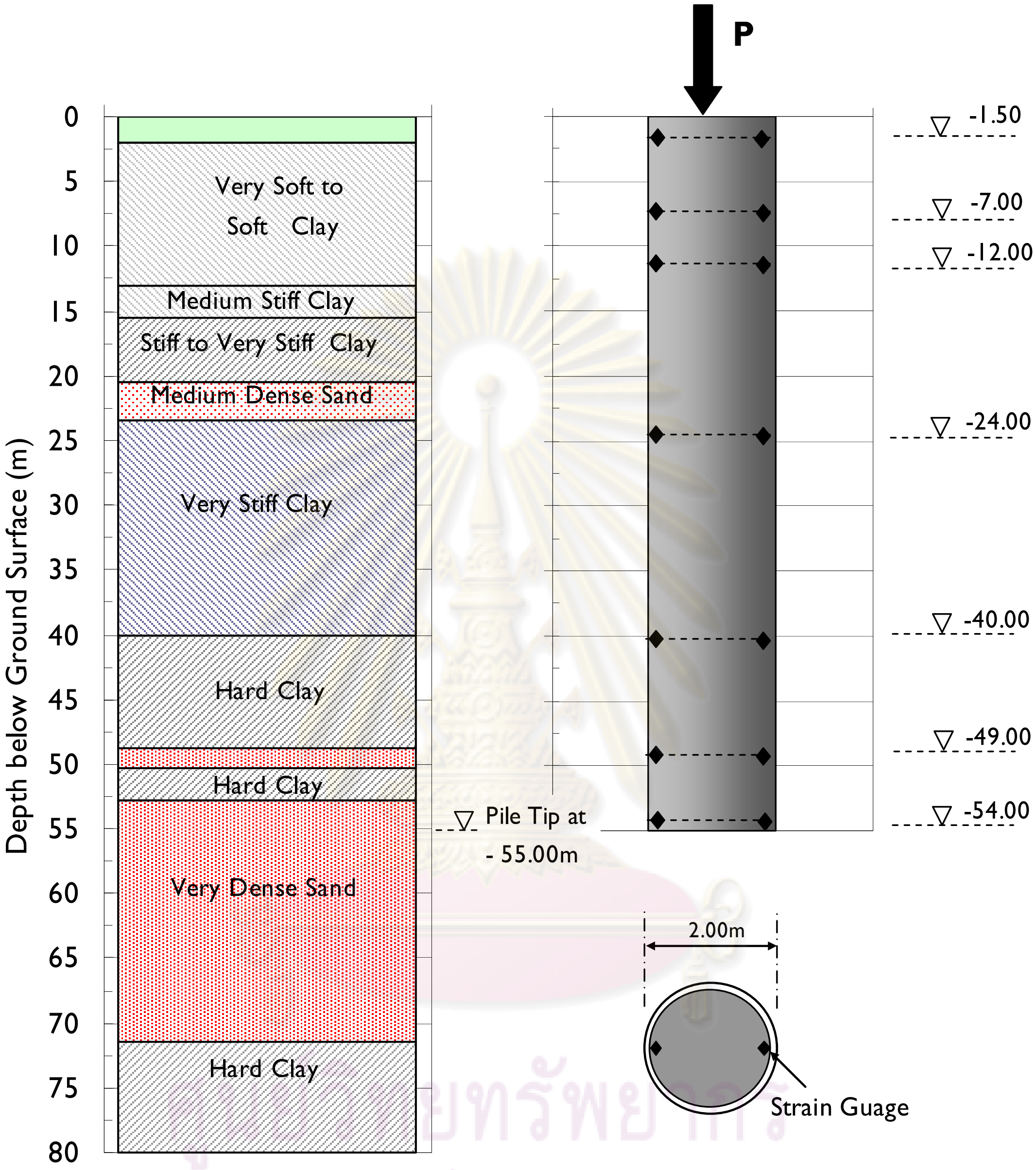

b) Bored Pile

Figure 4.4 (Con't) VWSG Location for static compression test

4.2.2 INSTRUMENTATION FOR STATIC LATERAL LOAD TEST

Lateral displacement of the pile head is measured from two dial gauges one placed in alignment with loading axis and another one place at 0.50m higher. Displacement along the length of the pile is measured by inclinometer tube that be provided in both test pile with 40 m in length to make sure that the rotation point of the pile under lateral load is within the inclinometer length.

SINCO load cells of 5000 kN capacity were installed at each of test pile which between the test pile and hydraulic jack to evaluate the actual applied load.

Vibrating wire strain gauges (VWSG) were fixed at specified 5 levels along the pile for stain measurements of reinforcement during applied each load increment. At each level, 2 sets of VWSG were installed for the bored pile whereas 6 sets of VWSG were installed for T-shape barrette.

Details of instrumentation are shown in Table 4.4 and Figure 4.5 and 4.6.

Table 4.4 Details of test piles for static compression Lateral Load Test

Test pile	Max. lateral test	Instrumentation	
	Load (kN)	Inclinometer	Strain Gauge
Bored Pile ∅ 1.65 m -55.0 m tip 2 Nos.	1200	40 m length	VWSG 5 levels (2 Nos / level)
T-Shape Barrette (1x3) + (1x2) m^2 - 55.0 m tip 2 Nos.	4000	40 m length	VWSG 5 levels (2 Nos / level)

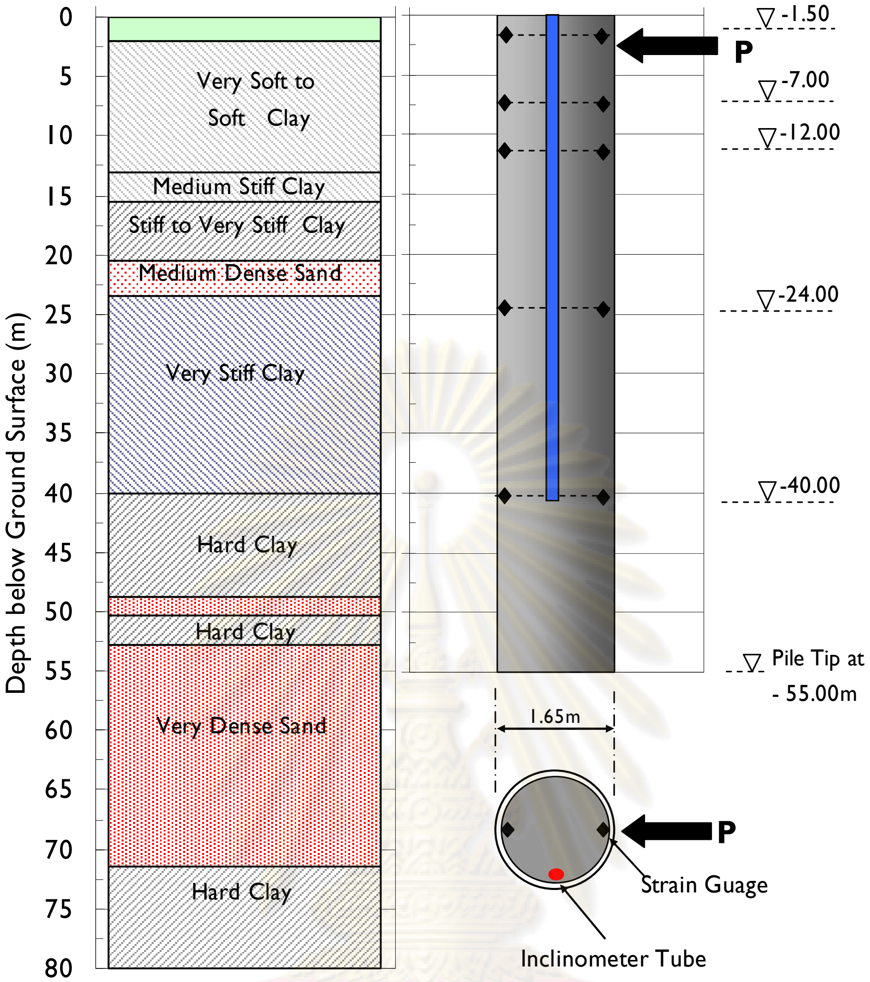

a) Instrument diagram for lateral load test

b) Geotechnical Instruments during installation

Figure 4.5 Geotechnical instrumentation for bored pile

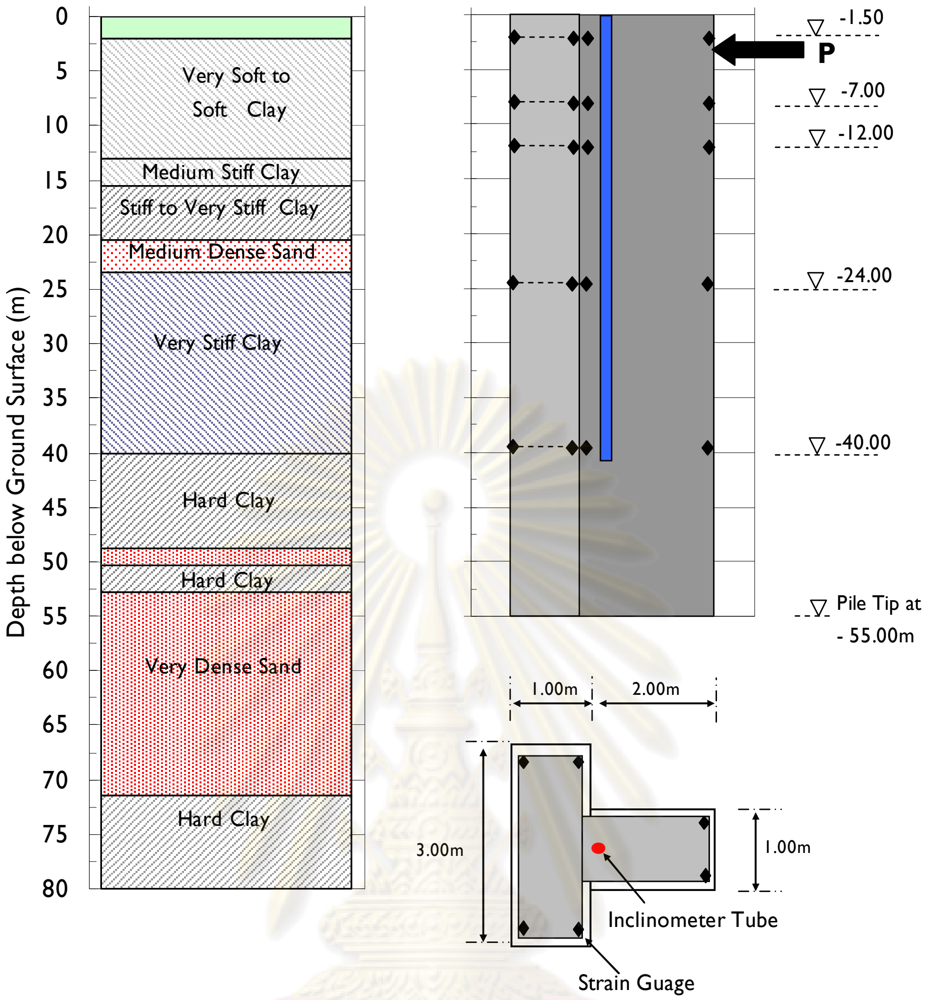

a) Instrument diagram for lateral load test

b) Geotechnical Instruments during installation

Figure 4.6 Geotechnical instrumentation for T-shape barrette

4.3 TESTING PROGRAM

4.3.1 SEISMIC TEST RESULTS

Sonic integrity/seismic test was carried out on test T-shape barrette and bored pile about 14 days after casting for checking pile integrity. The test indicated that integrity of all test pile were sound. Figure 4.7 and 4.8 shows a signal acquired by sonic integrity test on both test pile.

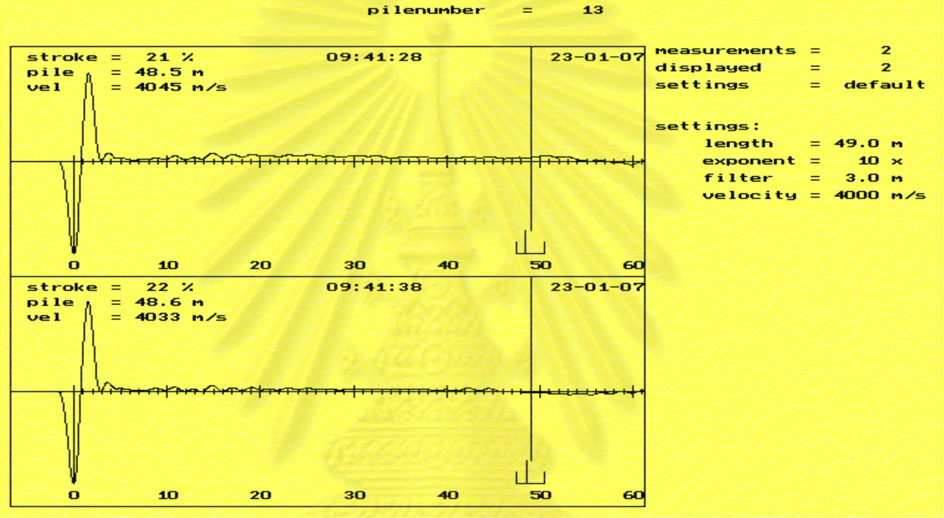

pilenumber = 13

stroke = 21 %
pile = 48.5 m
vel = 4045 m/s
09:41:28
23-01-07

stroke = 22 %
pile = 48.6 m
vel = 4033 m/s
09:41:38
23-01-07

measurements = 2
displayed = 2
settings = default

settings:
length = 49.0 m
exponent = 10 x
filter = 3.0 m
velocity = 4000 m/s

a) Test bore pile No. T4P13

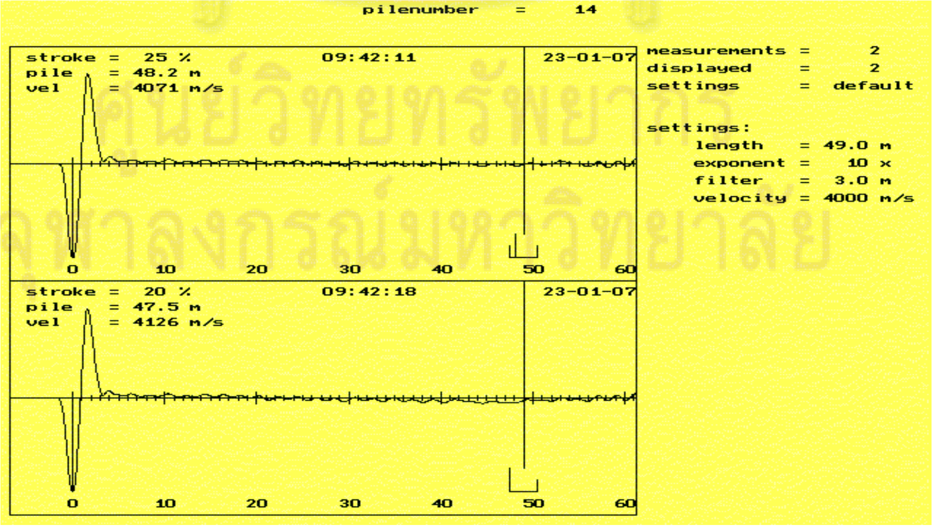

pilenumber = 14

stroke = 25 %
pile = 48.2 m
vel = 4071 m/s
09:42:11
23-01-07

stroke = 20 %
pile = 47.5 m
vel = 4126 m/s
09:42:18
23-01-07

measurements = 2
displayed = 2
settings = default

settings:
length = 49.0 m
exponent = 10 x
filter = 3.0 m
velocity = 4000 m/s

b) Test bore pile No. T4P14

Figure 4.7 Seismic test result for test bored pile

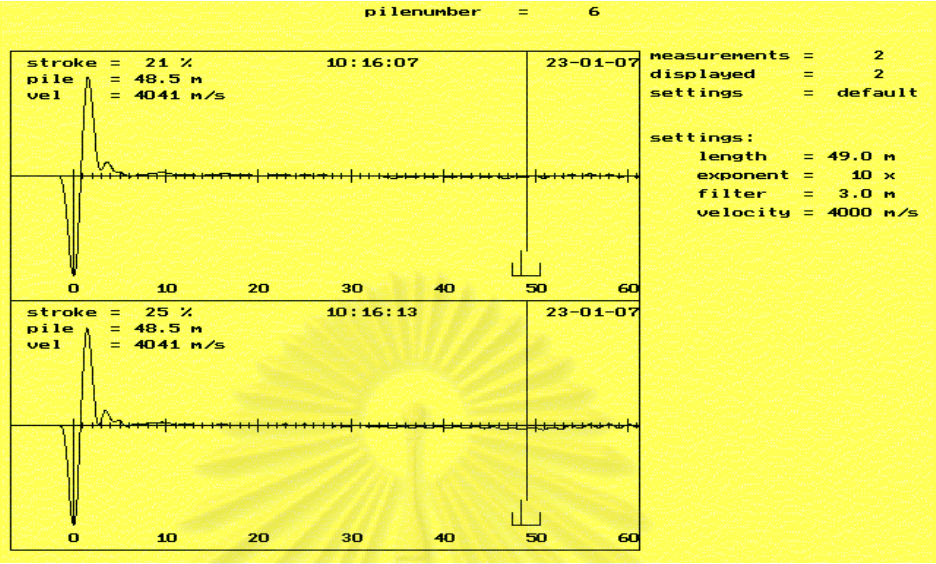

```
pilenumber    =     6

stroke =   21 %        10:16:07        23-01-07    measurements =      2
pile   =  48.5 m                                   displayed    =      2
vel    =  4041 m/s                                 settings     =  default

                                                   settings:
                                                        length   = 49.0 m
                                                        exponent =   10 x
                                                        filter   =  3.0 m
                                                        velocity = 4000 m/s

stroke =   25 %        10:16:13        23-01-07
pile   =  48.5 m
vel    =  4041 m/s
```

a) Test T-shape barrette No. T4BP6

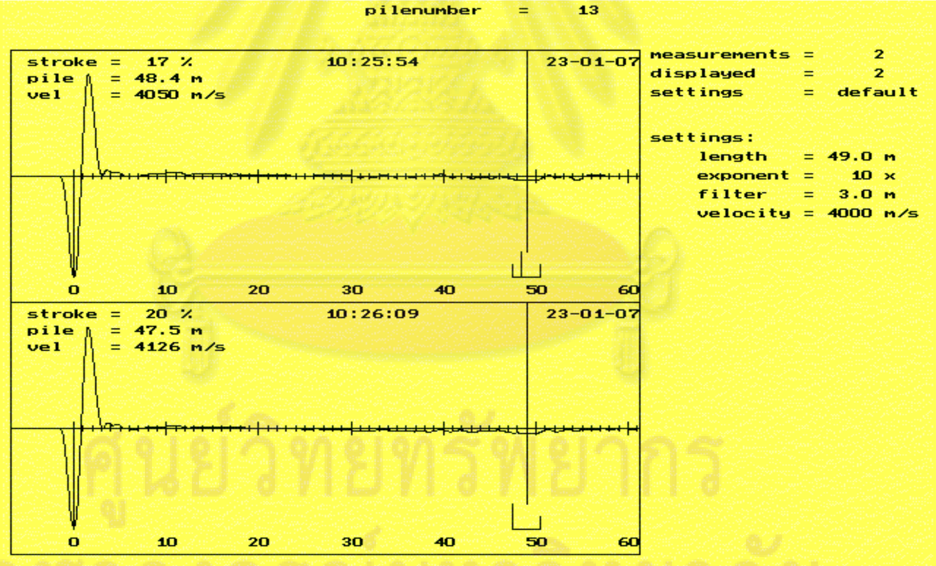

```
pilenumber    =    13

stroke =   17 %        10:25:54        23-01-07    measurements =      2
pile   =  48.4 m                                   displayed    =      2
vel    =  4050 m/s                                 settings     =  default

                                                   settings:
                                                        length   = 49.0 m
                                                        exponent =   10 x
                                                        filter   =  3.0 m
                                                        velocity = 4000 m/s

stroke =   20 %        10:26:09        23-01-07
pile   =  47.5 m
vel    =  4126 m/s
```

b) Test T-shape barrette No. T4BP13

Figure 4.8 Seismic test results for test T-shape barrette

4.3.2 STATIC COMPRESSION TEST

Two bored piles with 1.65m diameter and two T-shape barrettes were used as anchoring system for test bored pile with 2.00m diameter. Two numbers of built-up steel girders supported on each side by two cross beams were used as main beams to achieve the maximum capacity of 35200 kN. Main beams were supported against the cross beams. Cross beams in each side were anchored against surrounding anchored pile using anchor blocks at the top. Specially fabricated rigid transfer girders were used to distribute the tension force coming from the tie-bars to dowel bars above the anchor heads. Ten numbers of hydraulic jacks each having 5000 kN capacity were placed between the test barrette cap and the main beams of the reaction frame.

Test pile layout of T-shape barrette was similar to those of static bored pile load tests .For T-shape barrette test, four T-shape barrettes were used as anchoring system. Maximum test load 52000 kN was carried out from fourteen numbers of hydraulic jacks. General view of both load test set up is presented in Figure 4.9 and 4.10.

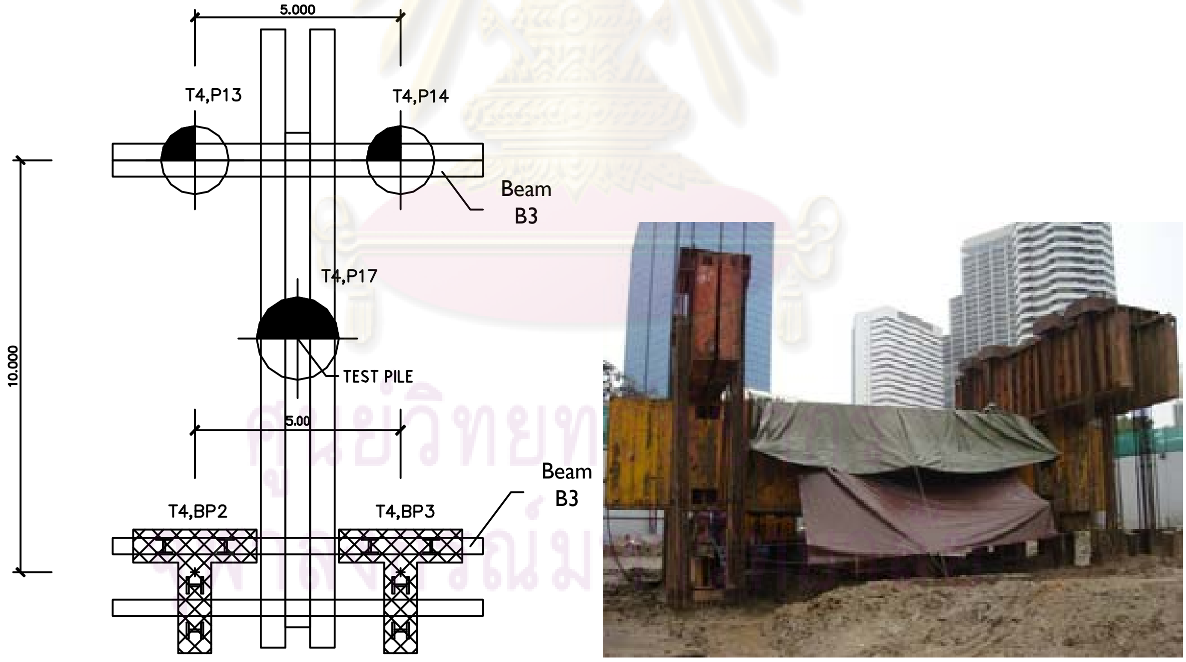

Figure 4.9 Static compression load test layout for bored pile

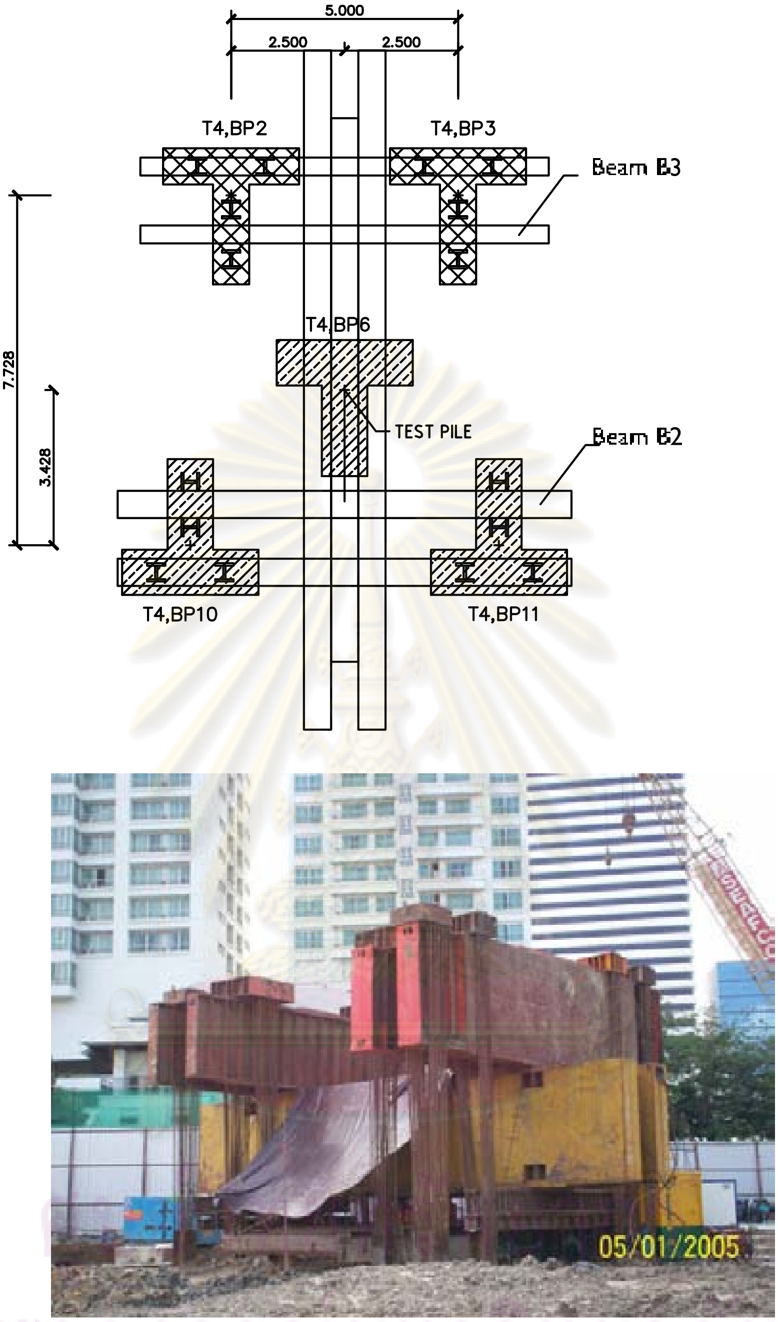

Figure 4.10 Static compression load test layout for T-shape barrette

4.3.3 STATIC LATERAL LOAD TEST

Static lateral testing programs are proposed to perform static loading test on bored pile 1.65 m. diameter and 55.0 m. in length compare with T-shape barrette 5 m^2 sectional area and 55.0 m length. Each test setup consists of two piles which are either jacked apart or pulled together using a hydraulic loading system. Test T-shape barrette and bores piles layout plans for the static lateral load test are shown in Figure 4.11 and 4.12.

The test was performed in general accordance with the procedures of the ASTM standard method. Load was applied to the test piles in increments, with each increment maintained for about 30 minutes to obtain the inclinometer readings. The test was terminated at a maximum test load of 1200 kN and 4000 kN for bored pile and T-shape barrette, respectively as shown in Table 4.4.

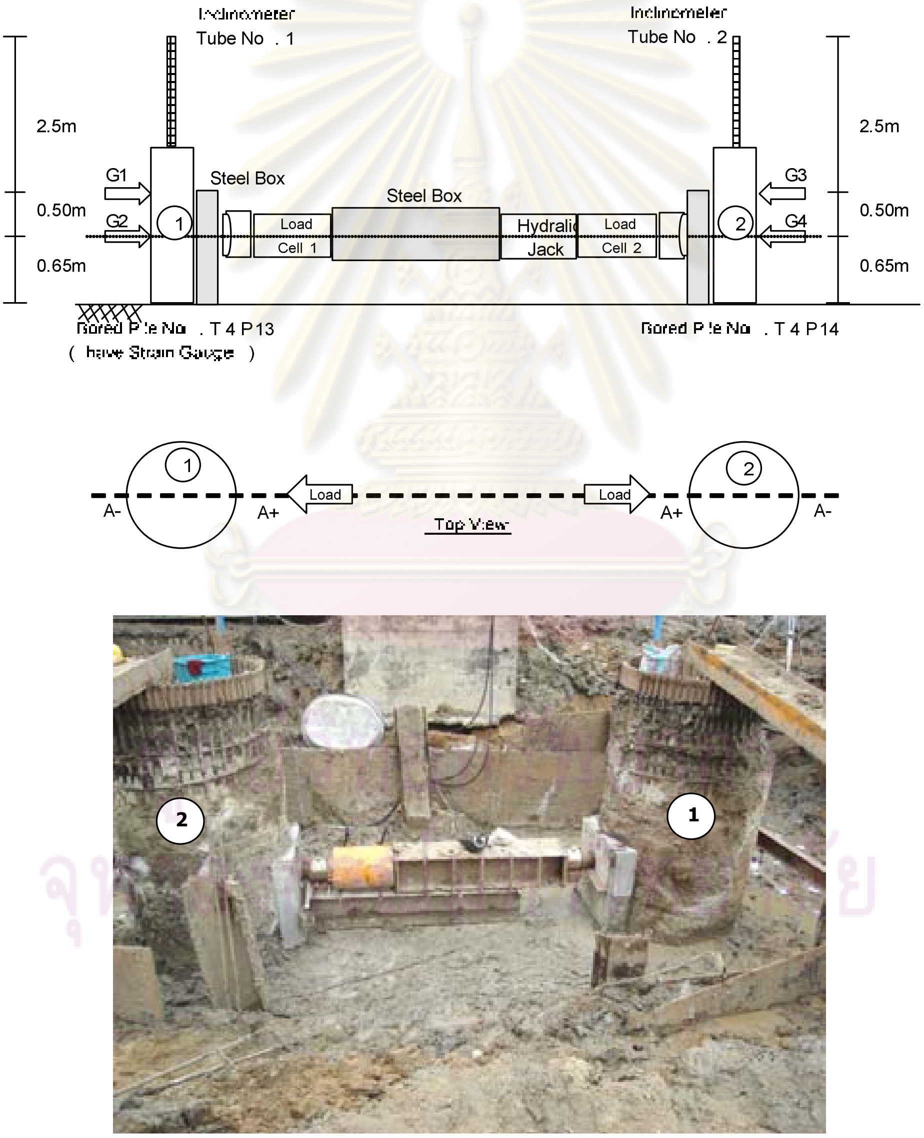

Figure 4.11 Layout for static lateral load test on bored pile with loading frame

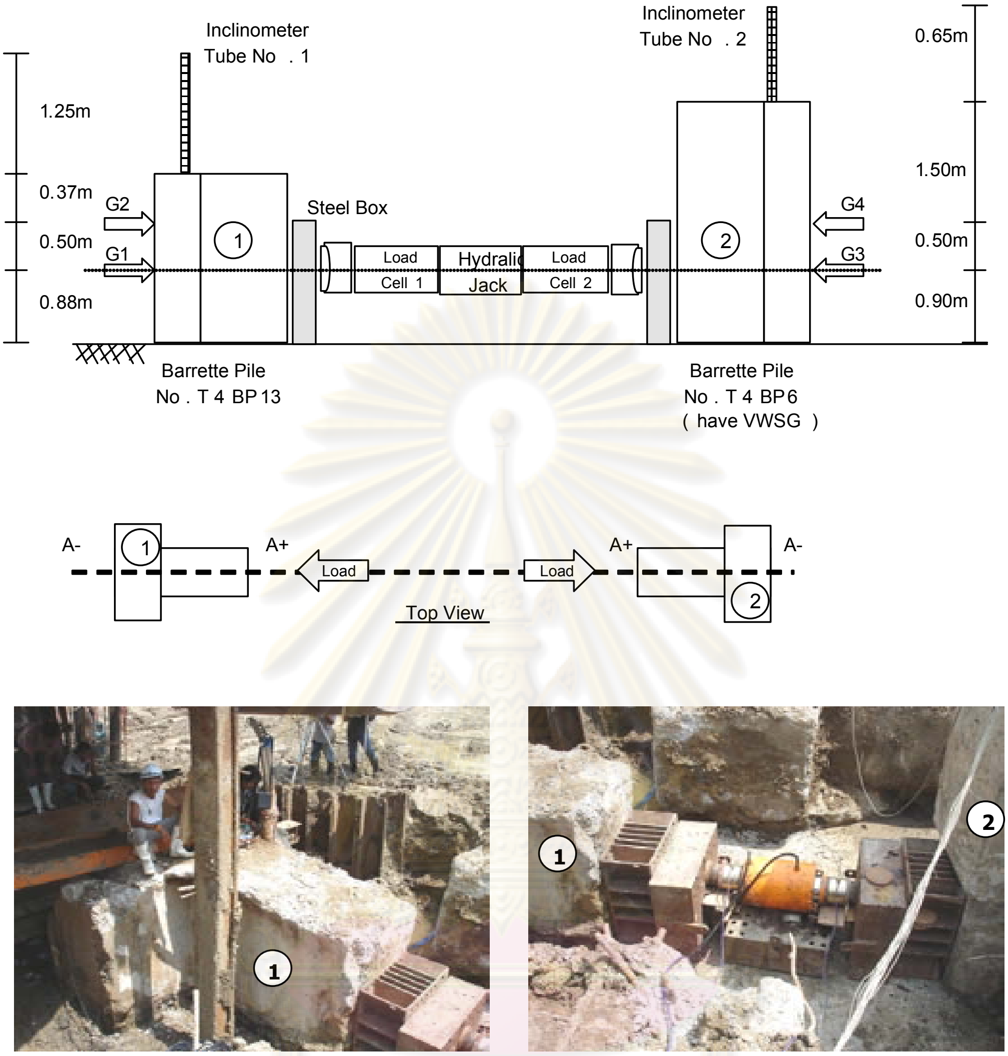

Figure 4.12 Layout for Static lateral load test on T-shape barrette with loading frame

In order to measure horizontal and vertical soil movement at the back of test bore pile and T-shape barrette during applied lateral load, series of surface markers were placed in grid as shown in Figure 4.13.

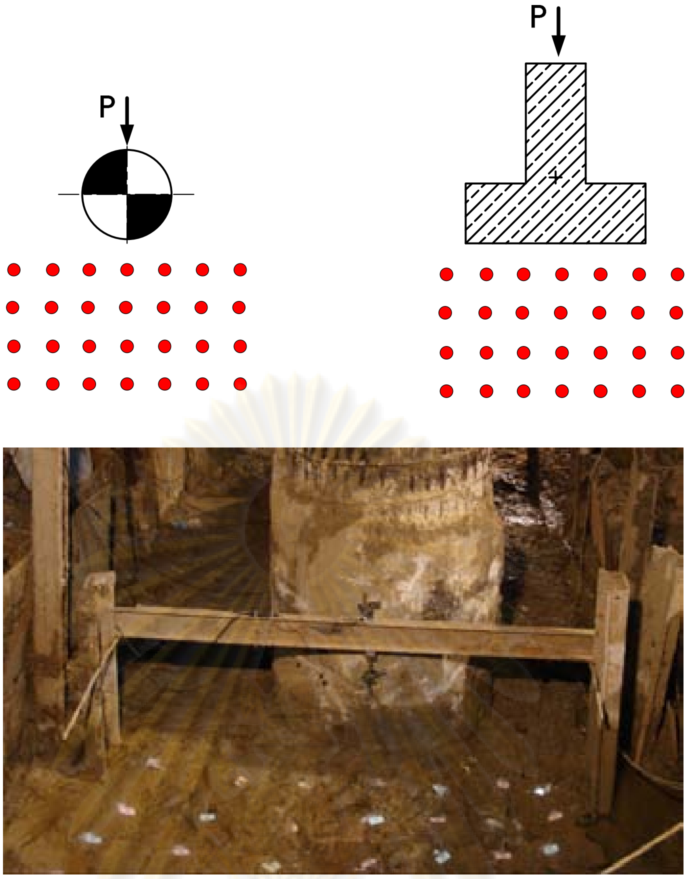

Figure 4.13 Grid pattern of surface-markers for measuring horizontal and vertical soil movement

4.4 NUMERICAL MODELING

In order to gain insight into the behavior of the test piles, Compression and lateral load test analyses were performed using PLAXIS 3D Foundations, the 3Dimentional Finite Element Program. The pile and the soil were modeled by 15-node wedge elements that contains 6 stress points (Figure 4.14). A relative fine mesh was defined near the pile-soil interface while a coarser mesh was used further from the pile. The lateral boundary of the model was determined on the basic of trial calculations which the boundaries extended until stresses and deformations have sufficiently stabilized. It was extended to 55m. on back side in loading direction. The bottom boundary was set at the depth of 80m. below pile tip level. The 3D finite element model with generated meshes mentioned above for T-shape barrette and bored pile are shown in Figure 4.15 and 4.16, respectively.

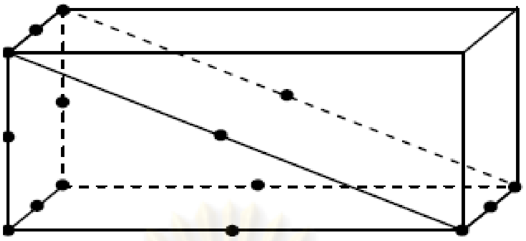

Figure 4.14 The 15-node wedge elements for modeling of pile and soil

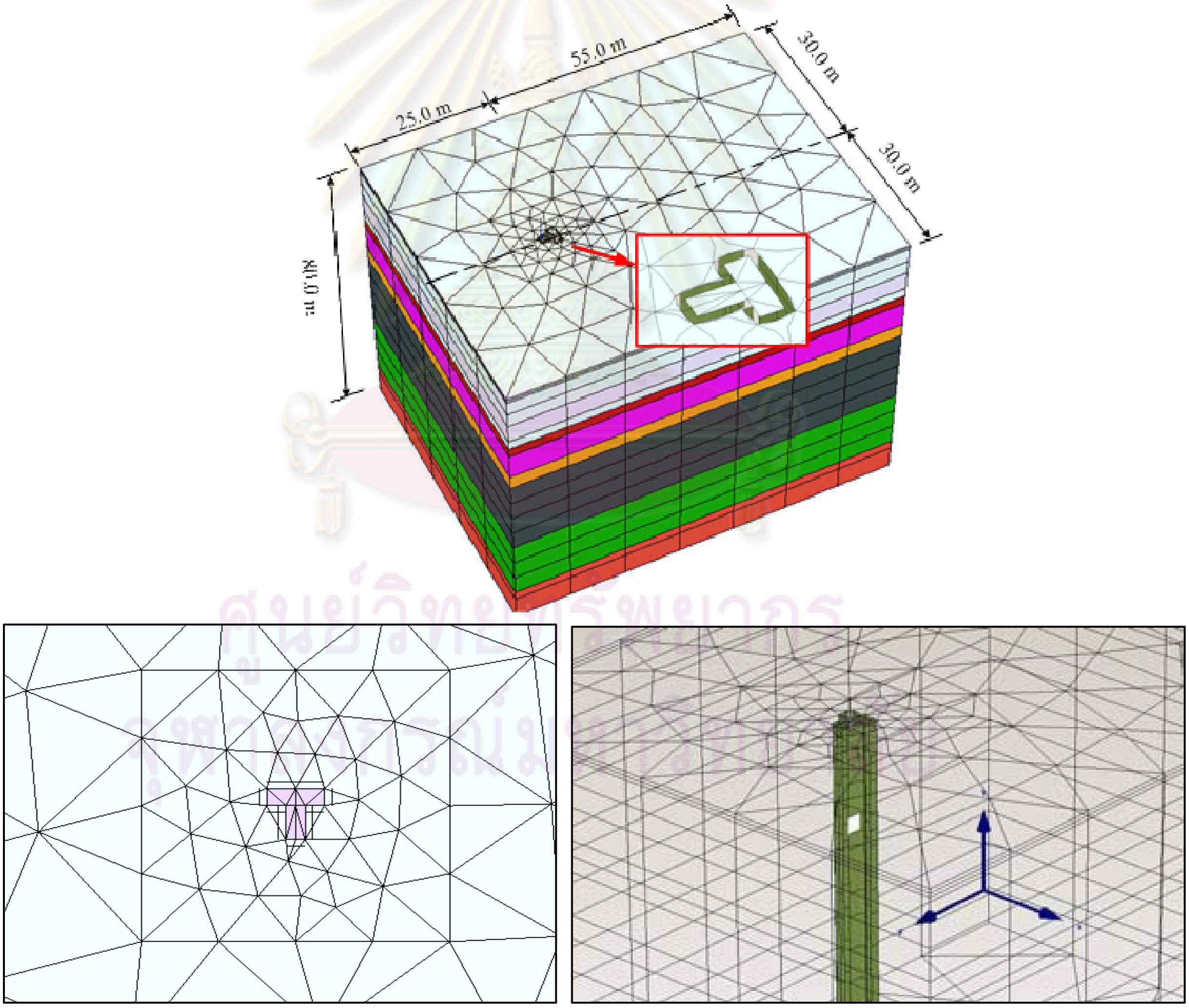

Figure 4.15 3D finite element model for T-shape barrette

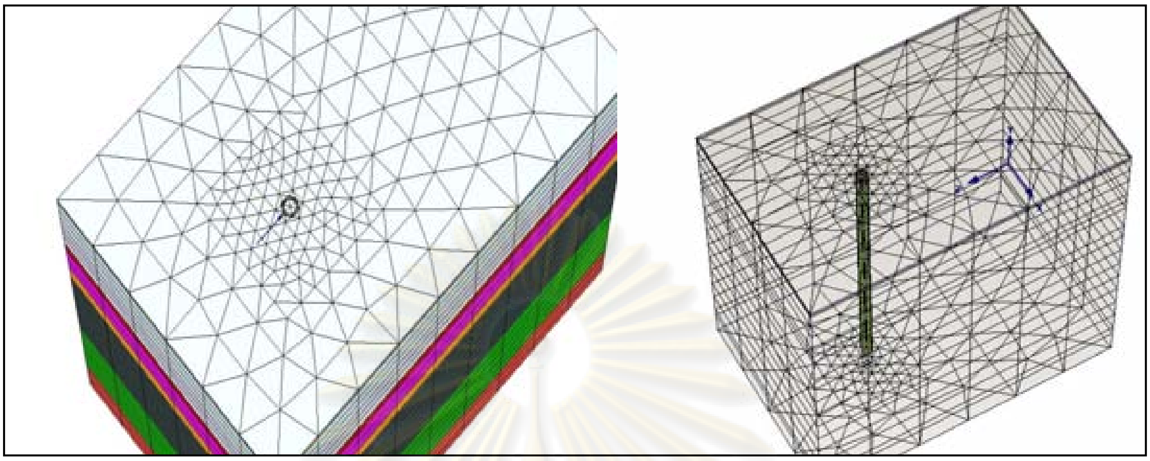

Figure 4.16 3D finite element model for bored pile

4.4.1 MODELING OF PILE

Reinforced concrete piles exhibit nonlinear behavior under load. Based on the ACI code 2005, Reese and Van Impe (2001), and Ooi and Ramsey (2003), the effective elastic modulus of a reinforced concrete pile can be expressed as

$$E_{\bar{p}} = \left[1 + (n-1)\frac{A_s}{A_c}\right] E_c$$

Where n is the ratio of E_s/E_c, E_s is elastic modulus of steel and E_c is elastic modulus of concrete.

Cracking of concrete will reduce the moment of inertia of the pile. Applying the effective moment of inertia concept in ACI (1995), when the moment less than cracking moment ($M < M_{cr}$), the effective moment of inertia is $I_e = I_p$ or when the moment is more than cracking moment and less than ultimate moment ($M_{cr} < M < M_u$), the effective moment of inertia is expressed as

$$I_e = \left(\frac{M_{cr}}{M_a}\right)^3 I_g + \left[1 - \left(\frac{M_{cr}}{M_a}\right)^3\right] I_{cr}$$

Where M_a is maximum moment along the pile, I_g is moment of inertia of gross concrete section about central axis and I_{cr} is moment of inertia of cracked transformed concrete section.

For the numerical simulation in this study, Solid elements are used for modeling the pile. Separate analyses were performed using the gross flexural stiffness value along the pile length to model the pile before concrete cracked. For cracked section, the reduced flexural stiffness was used to model at the region of maximum curvature of test pile. Material properties used in the analysis are given in Table 2.

Table 4.5 Material parameters for in numerical analysis

Pile Type	Pile Size	Pile Tip (m)	Concrete fc' (kN/m^2)	Possion's ratio	E kN/m^2
Bored pile	∅ 1.65 m	-55.52	320	0.15	$2.8x10^6$
T-shape barrette	(1x3)+(1x2) m^2	-55.70	320	0.15	$2.8x10^6$

4.4.2 ELASTIC-PERFECTLY PLASTIC MOHR-COULOMB SOIL MODEL

The Mohr-Coulomb model is used to describe the soil behavior. In the Mohr-Coulomb model used herein, it is assumed that failure occurs when the shear stress on any point in a material reaches a value that depends linearly on the normal stress in the same plane. The Mohr-Coulomb model is based on plotting Mohr's circle for states of stress at failure in the plane of the maximum and minimum principal stresses. The failure line is the best straight line that touches these Mohr's circles as shown in Figure 4.17. The definition of soil behavior in PLAXIS includes the elastic properties, unit weight, angle of friction and cohesive yield stress vs. plastic strain. Soil parameters used for defining the Mohr-Coulomb model in PLAXIS program and their assigned values for this particular bored pile simulation in total stress analysis are shown in Table 4.6

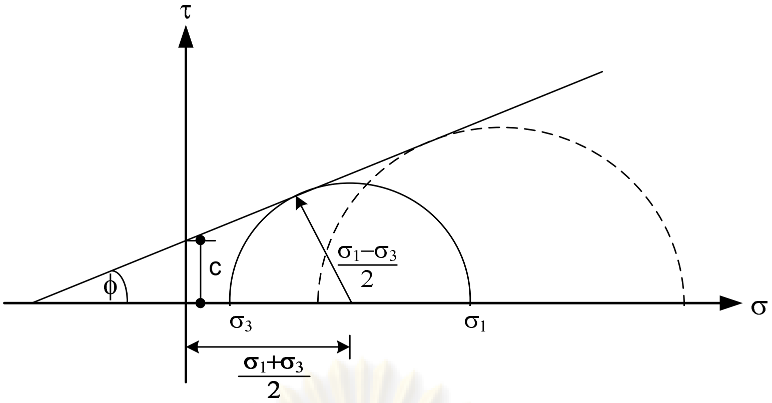

Figure 4.17 Mohr Coulomb's failure surface (Coulomb, 1776)

The failure envelop is expressed as

$$\tau = c + \sigma \tan\phi$$

Where τ is the shear strength, σ is the normal stress and ϕ is the angle of internal friction.

Based on the Mohr circle, we can obtain

$$\tau = \frac{(\sigma_1 - \sigma_3)}{2}\cos\phi$$

$$\sigma = \frac{(\sigma_1 - \sigma_3)}{2} + \frac{(\sigma_1 - \sigma_3)}{2}\sin\phi$$

Substituting for τ and σ, multiplying both sides by cos ϕ, and reducing, the Mohr-Coulomb model can be written as

$$\frac{(\sigma_1 - \sigma_3)}{2} + \frac{(\sigma_1 - \sigma_3)}{2}\sin\phi + c\cos\phi = 0$$

where σ_1 is the maximum principal stress, and σ_3 is the minor principal stress.

Table 4.6 Soil parameters for defining the Mohr-Coulomb model in numerical analysis of bored pile

Layer	Soil	From	to	γ kN/m^3	Su kN/m^2	E kN/m^2	Ko
1	Crust	0.0	1.0	18.00	35	20000	0.70
2	Very soft clay	1.0	6.0	16.00	18	9700	0.60
3	Soft clay	6.0	13.0	16.50	22	12000	0.60
4	Medium stiff clay	13.0	15.0	18.00	35	19000	0.65
5	Stiff clay	15.0	20.5	17.50	100	110000	0.70
6	Medium dense sand	20.5	23.5	18.00	-	50000	0.80
7	Very stiff clay	23.5	40.0	18.00	110	120000	0.80
8	Hard clay	40.0	53.0	19.00	200	190000	0.80
9	Very dense sand	53.0	70.0	19.50	-	120000	0.80

4.4.3 MODELING OF PILE-SOIL INTERFACE

Modeling of the pile-soil interface is critical under strong loads that cause separation between the pile and the soil. PLAXIS provides a number of an elastic-plastic models for the modeling of soil-structure interaction. The coulomb criterion is used to distinguish between elastic behavior and plastic interface behavior when permanent slip may occur. The main interface parameter is the strength reduction factor.

The shear stress σ is given by:

$$|\tau| < c_i + \sigma_n \tan\phi_i$$

Where

$$|\tau| = \sqrt{\tau_{s1}{}^2 + \tau_{s2}{}^2}$$

Where $\tau_{s1}$and τ_{s2} are shear stresses in the two shear direction, σ_n is the effective normal stress ϕ_i and c_i are the friction and cohesion of the interface. The interface properties are calculated from soil properties in the associated data set and the strength reduction factor by:

$$c_i = R \times c_{soil}$$

$$\tan\phi_i = R \times \tan\phi_{soil} \leq \tan\phi_{soil}$$

In general, for soil-pile structure interaction the value of reduction factor, R should be less than 1, which mean the interface is weaker and more flexible than the surrounding soil. The classical isotropic Coulomb friction model, which defines a reduction factor/friction coefficient relating shear stress to the contact pressure, was used. A value of reduction factor about 0.4 - 0.9 depending on shear strength of soil was assumed for the reduction factor, as used by Bentley and Naggar (2000).

CHAPTER V

TEST RESULTS AND ANALYSES

5.1 STATIC COMPRESSION LOAD TEST

5.1.1 TEST RESULTS

The test results for static compression test on T-shape barrette and bored pile are shown in Figure 5.1 and 5.2. At the maximum test load, the rate of settlement for both pile were more than 0.25 mm./hr. They can be reported that both piles tended to fail. The failure load defined by Butler & Hoy (1977) is about 48000 kN for T-shape barrette and 30000 kN for bored pile. Almost load is carried by friction along the pile. The end bearing load at the failure load for T-shape barrette and bored pile is 3100 kN and 1100 kN about 5% of failure load.

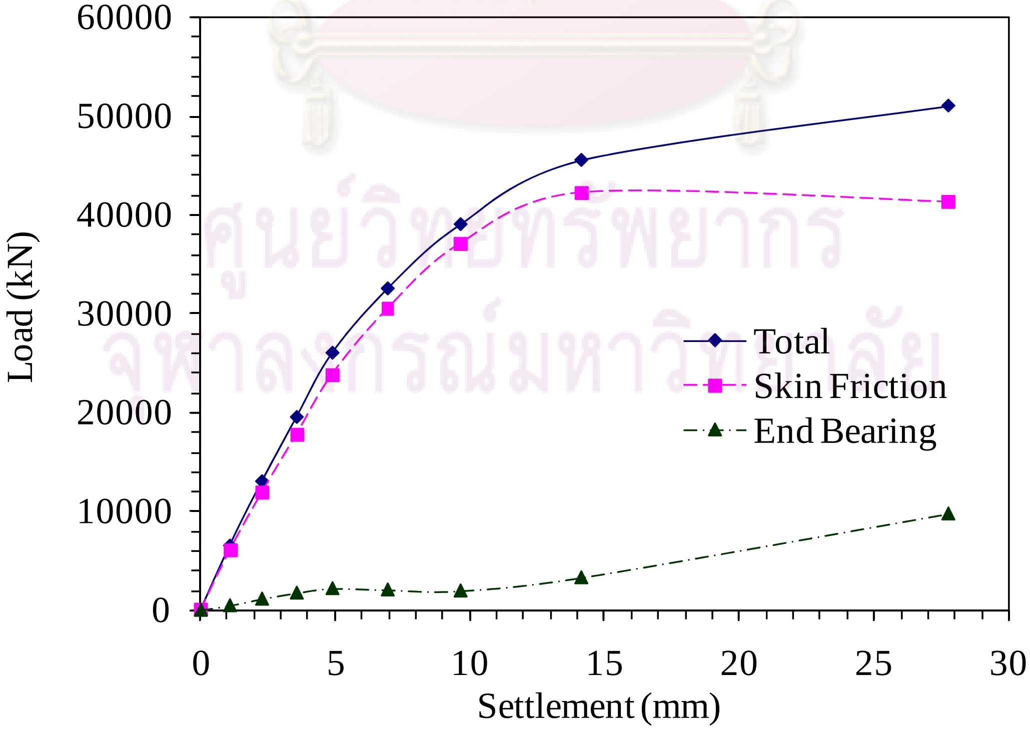

Figure 5.1 Load-settlement curve for T-shape barrette

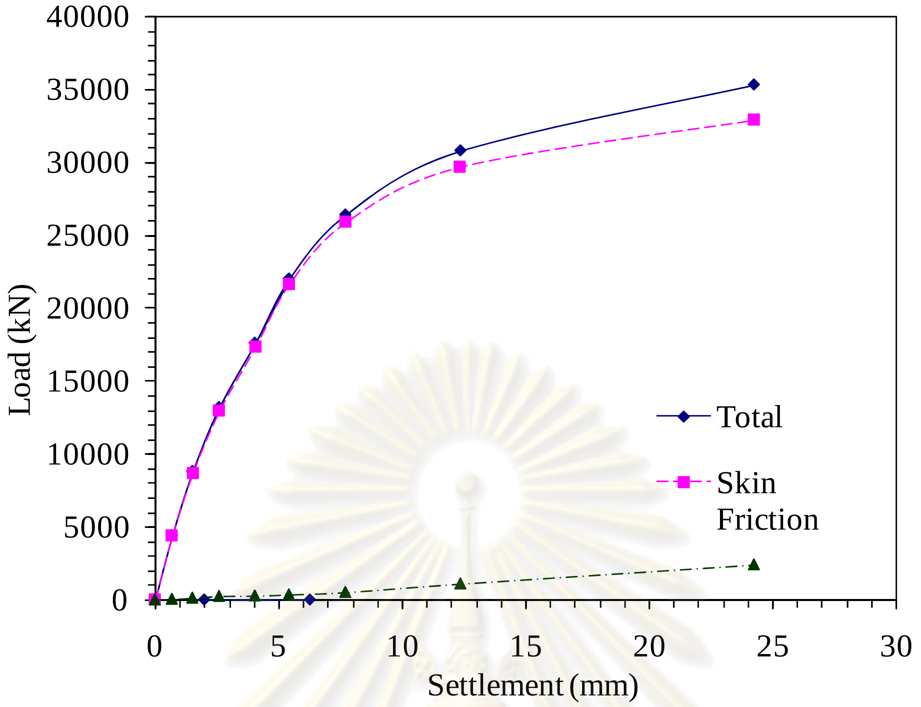

Figure 5.2 Load-settlement curve for Bored pile

5.1.2 NUMERICAL SIMULATION AND ANALYSIS FOR VERTICAL LOAD

Figure 5.3 and 5.4 give the results of the three dimensions and top view of the finite element meshes considered in the numerical simulation and analysis, including 6,120 elements and 17,347 nodes for T-shape barrette. Total Stress analysis with the undrained parameter is the process used to simulate the model in 3D FEM analysis due to the short term condition of test period. Table 5.1 presented the soil parameter used to simulate in 3D FEM analysis.

From the compression load test results of T-shape barrette as shown in Figure 5.1, the results showed that the load up to about 48000 kN was almost supported by friction. Based on the FEM analysis as shown in Figure 5.3, the result show that the shear plane of T-shape barrette under the compression load is not at the shaft perimeter. The inner soil develop sufficient frictional resistance to prevent further soil intrusion, causing the pile to become "plugged". Thus, the shear plane of T-shape barrette consist of 2 parts. Almost shear plane is boundary interface between pile shaft and soil around the shaft. Another plane is in the soil mass. To calculate the shaft perimeter of T-shape barrette with considering soil plug, the results give the unit friction in similar as bored pile which all shear plane is located at shaft perimeter. Figure 5.5 show the unit skin friction calculated from load given by strain measurement compare with bored pile in each soil layer with using 20% reduction in perimeter of T-shape barrette due to effect of soil plug. For the mobilized end bearing of T-shape barrette, the increasing of sectional area about 80% give the unit end bearing similar to the bored pile as shown in Figure 5.6

Figure 5.7 show the predicted load-settlement curve for T-shape barrette from 3D FEM compare with measurement.

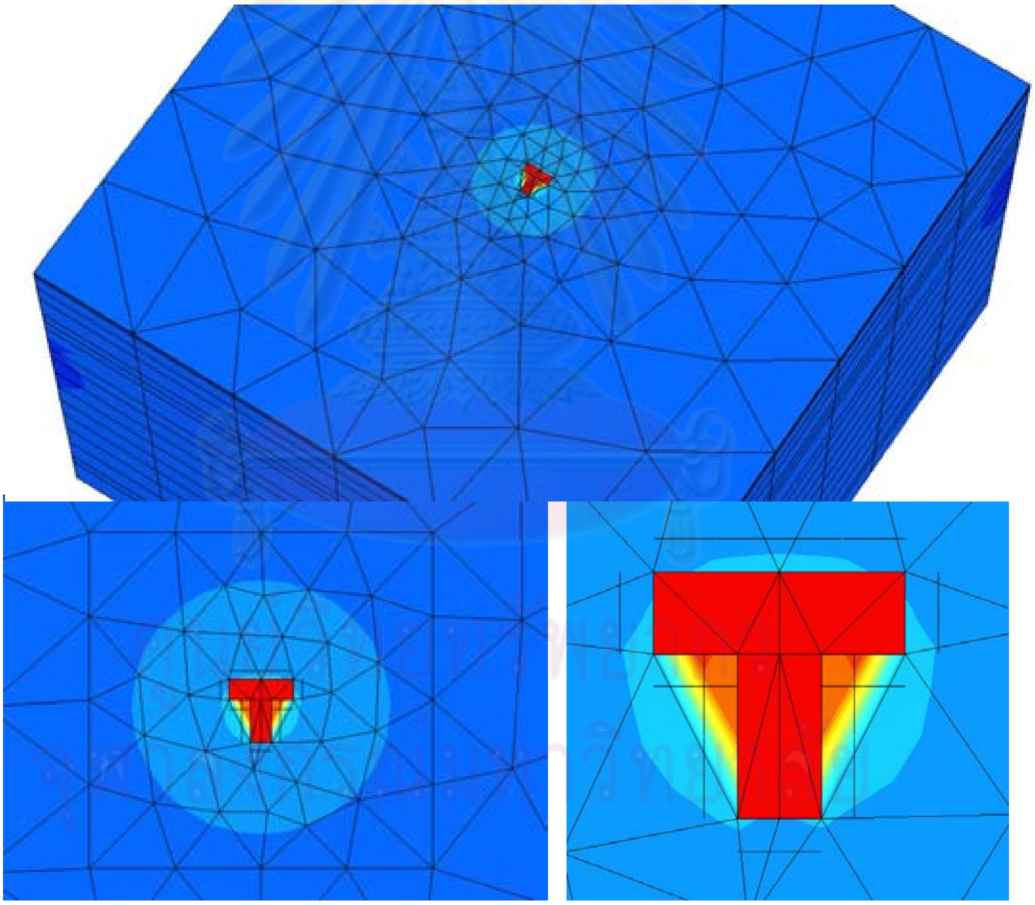

Figure 5.3 Shear plane for T-shape barrette under vertical load

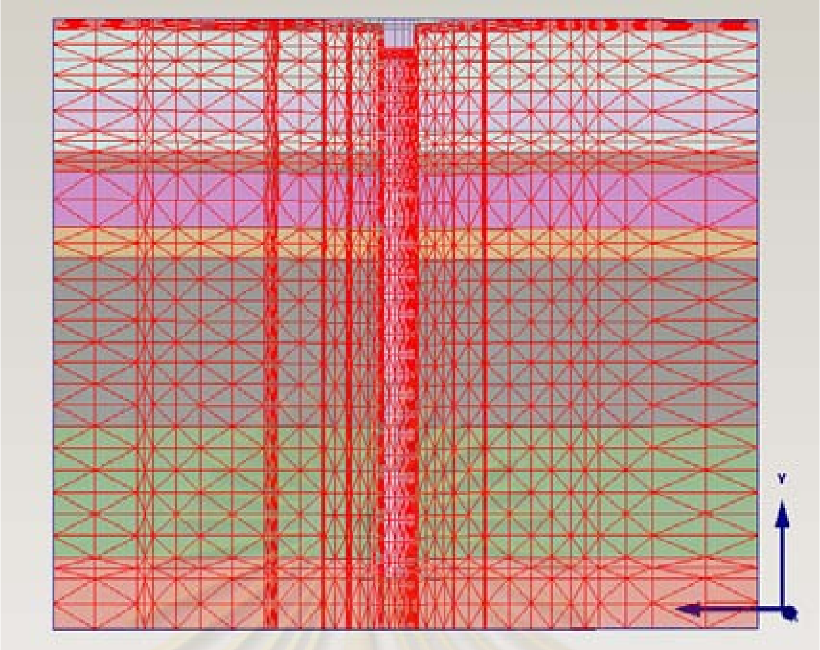

Figure 5.4 Vertical movement of T-shape barrette under the compression load

Table 5.1 Soil parameters simulate in numerical analysis of T-shape barrette

Layer	Soil	From	to	γ kN/m^3	Su kN/m^2	E kN/m^2	Ko
1	Crust	0.0	1.0	18.00	35	109500	0.70
2	Very soft clay	1.0	6.0	16.00	18	63000	0.60
3	Soft clay	6.0	13.0	16.50	22	79000	0.60
4	Medium stiff clay	13.0	15.0	18.00	35	109500	0.65
5	Stiff clay	15.0	20.5	17.50	100	580000	0.70
6	Medium dense sand	20.5	23.5	18.00	-	1050000	0.80
7	Very stiff clay	23.5	40.0	18.00	110	608000	0.80
8	Hard clay	40.0	53.0	19.00	200	1060000	0.80
9	Very dense sand	53.0	70.0	19.50	-	1190000	0.80

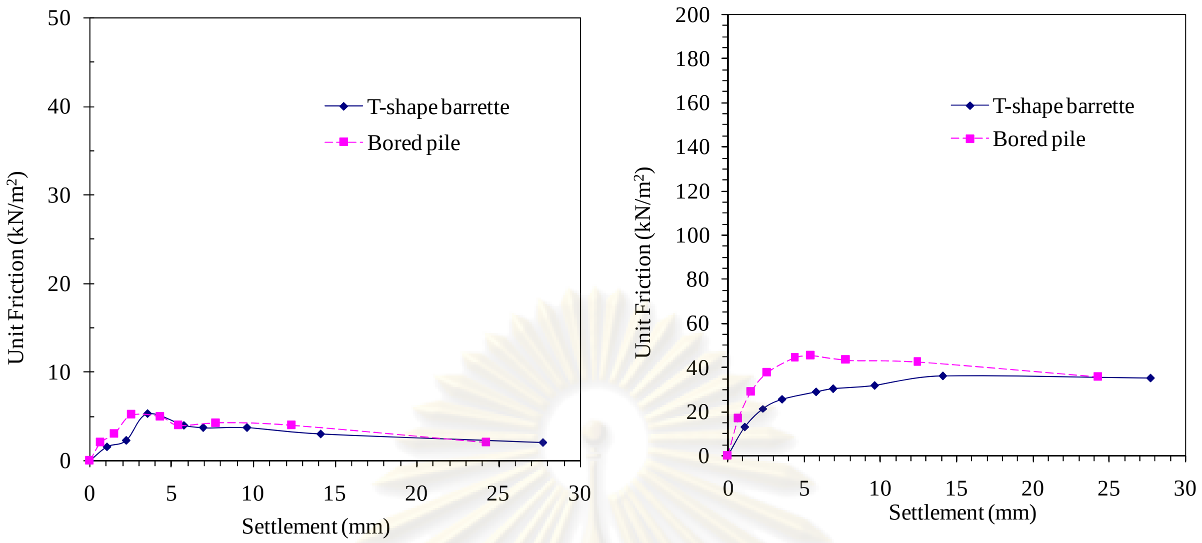

a) Soft clay)

(VWSG at -7.4&-1.5m)

b) Stiff clay

(VWSG at -24.4&-7.4m)

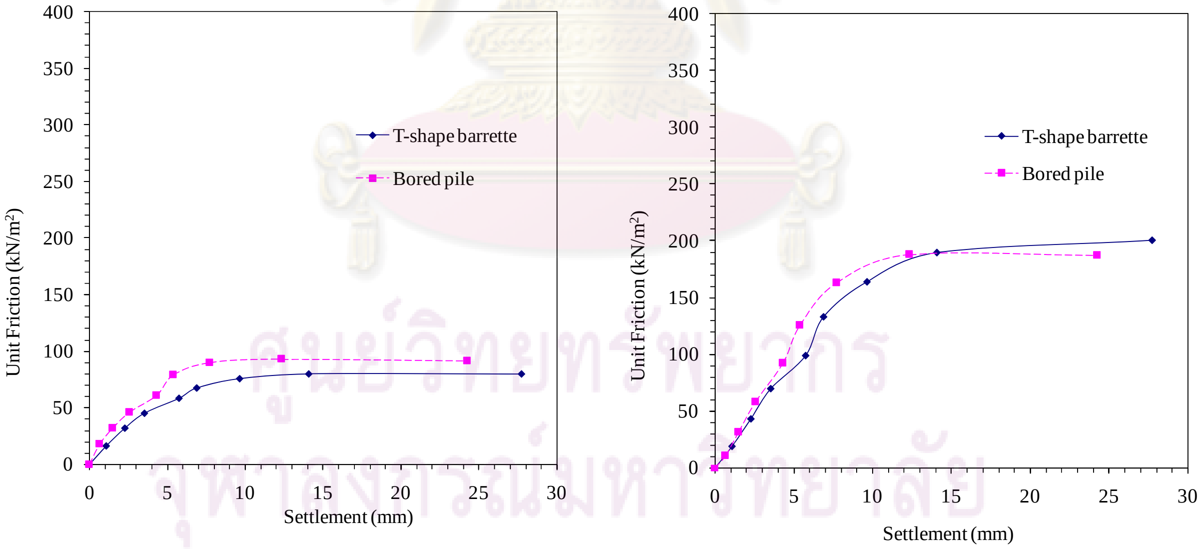

c) Very stiff clay

(VWSG at -40.4&-24.4m)

d) Hard clay

(VWSG at -52.4&-40.4m)

Figure 5.5 Unit skin friction- settlement curve

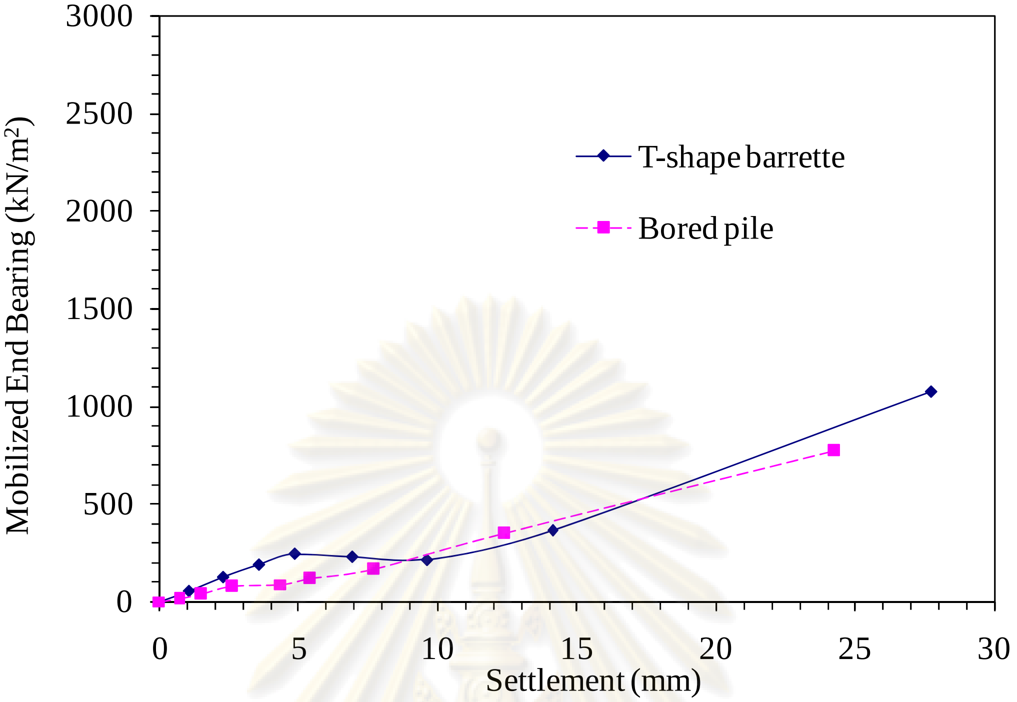

Figure 5.6 Mobilized end bearing- settlement curve

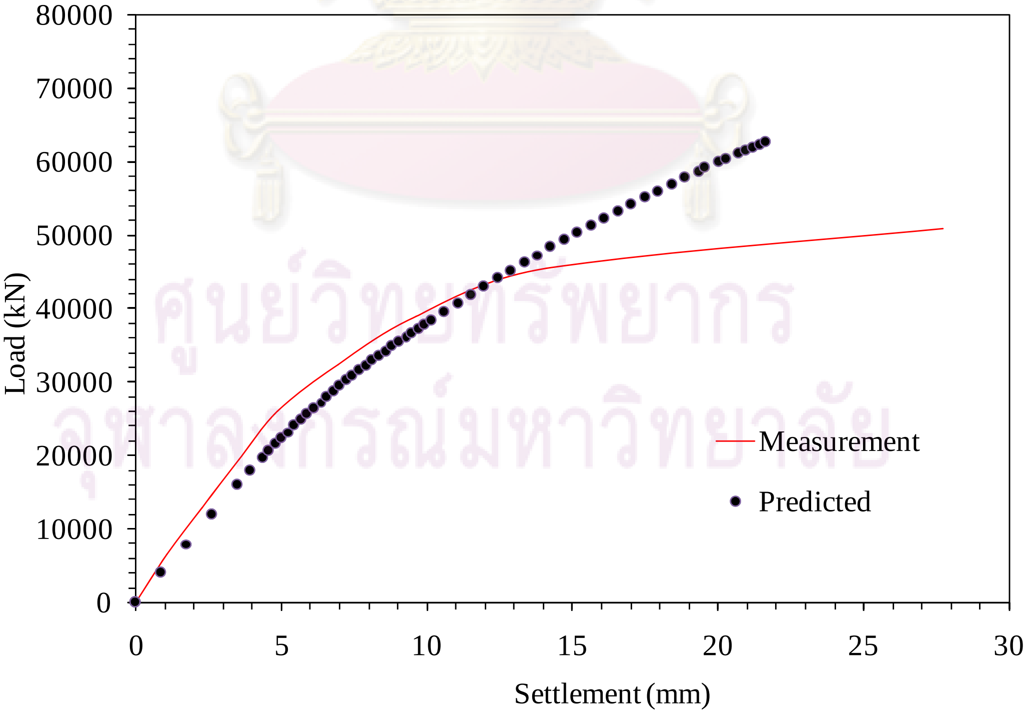

Figure 5.7 Predicted load-settlement curve for T-shape barrette

5.2 STATIC LATERAL LOAD TEST

5.2.1 TEST RESULTS

Lateral load with magnitude of 3901 kN and 1139 kN were applied for T-shape barrette and bored pile, respectively. Deflection profiles obtained from the inclinometer data at test bored pile and test T-shape barrette are shown in Figure 5.8 and 5.9. Plots of pile head movement from dial gages (at about -2.0 m below pile top) versus applied load from load cell are presented in Figure 5.10. Similar deflection pattern can be observed for both T-shape barrette and bored pile. It can be observed that the location of rotation point (neutral point) at higher load is deeper than lower load which indicates that the both T-shape barrette and bored pile behaves as a flexible pile despite its large cross section. The pile movement measured from dial garages installed at the pile top shape of both T-shape barrette and bored pile showed that both members were behaving as long pile as defined by Tomlinson (1995).

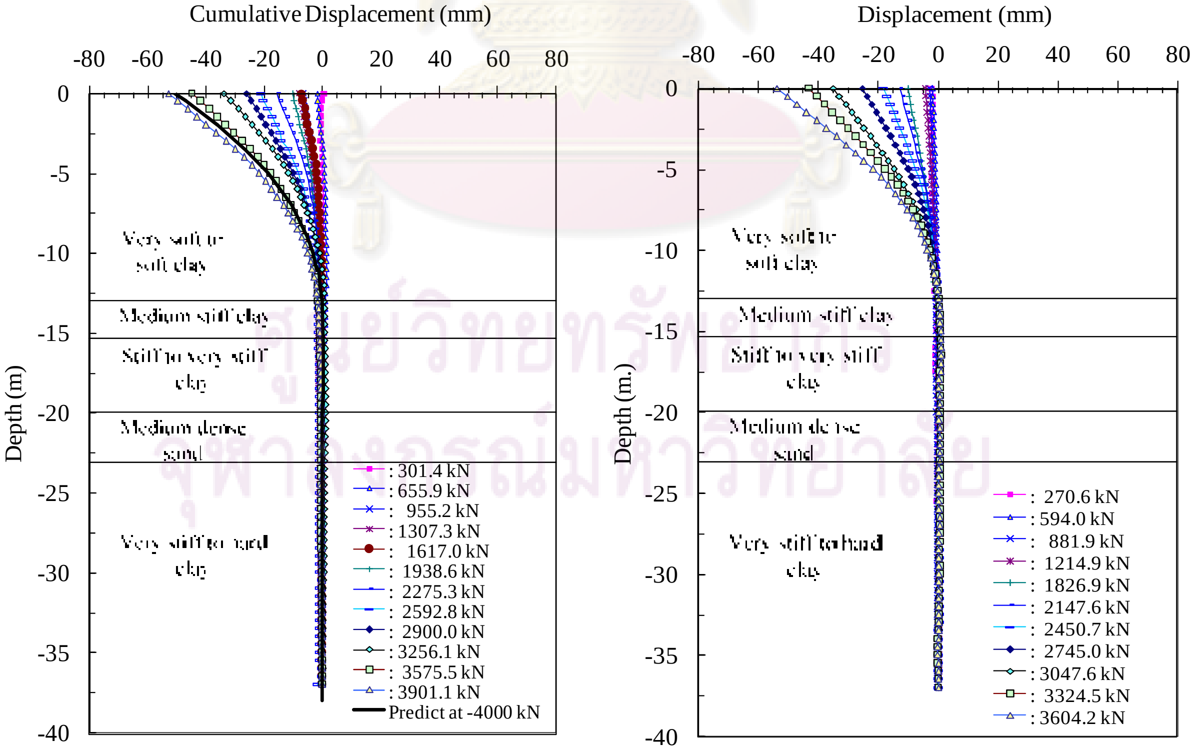

a) T-shape barrette, T4BP13 b) T-shape barrette, T4BP6

Fig. 5.8 Lateral defection profiles for test T-shape barrette

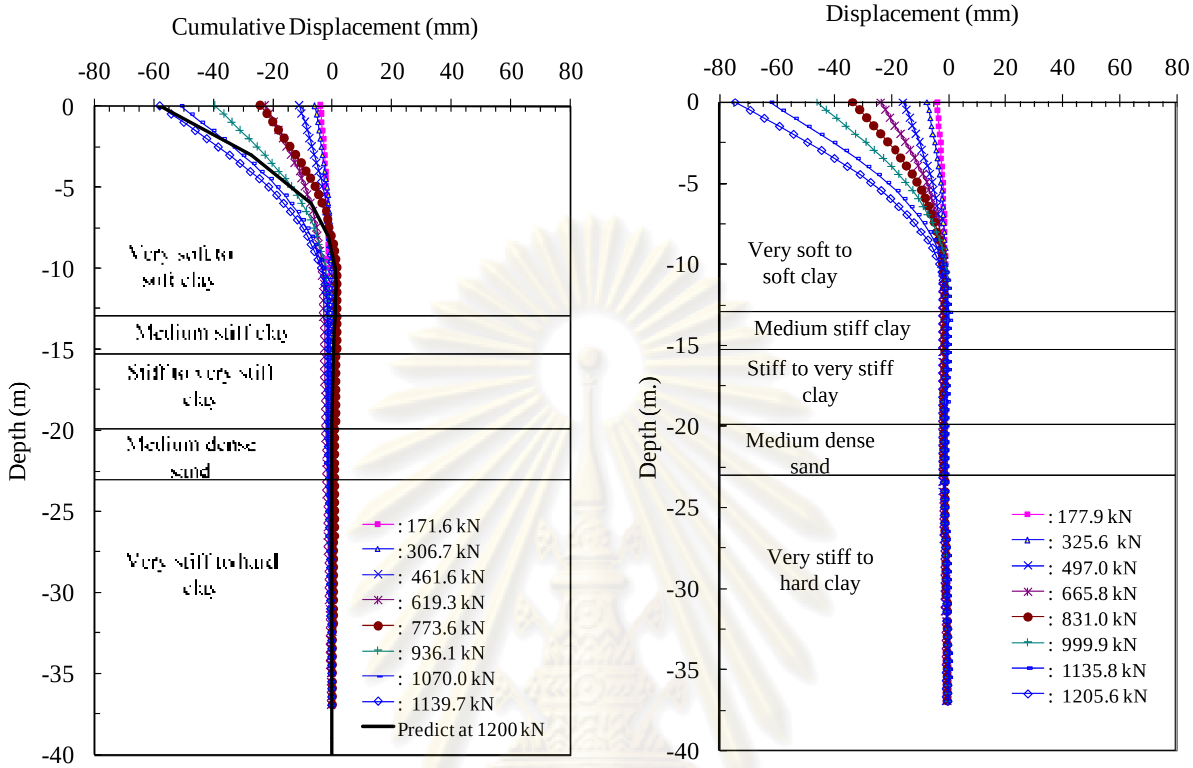

a) Bored Pile, T4P13   b) Bored Pile, T4P14

Fig. 5.9 Lateral defection profiles for test bored pile

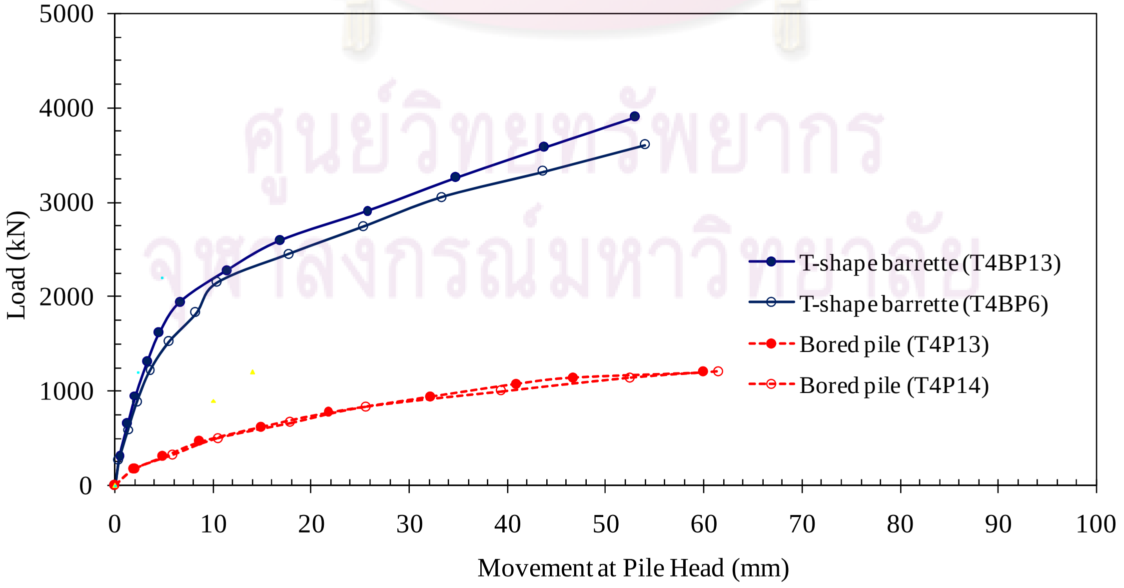

Fig. 5.10 Movement at pile head under lateral load

5.2.2 NUMERICAL SIMULATION AND ANALYSIS FOR LATERAL LOAD

The 3D finite element model for piles under the lateral load include 3,492 elements and 10,337 nodes for T-shape barrette and 3,708 elements and 10,585 nodes for bored pile, are shown in Figure 5.11.

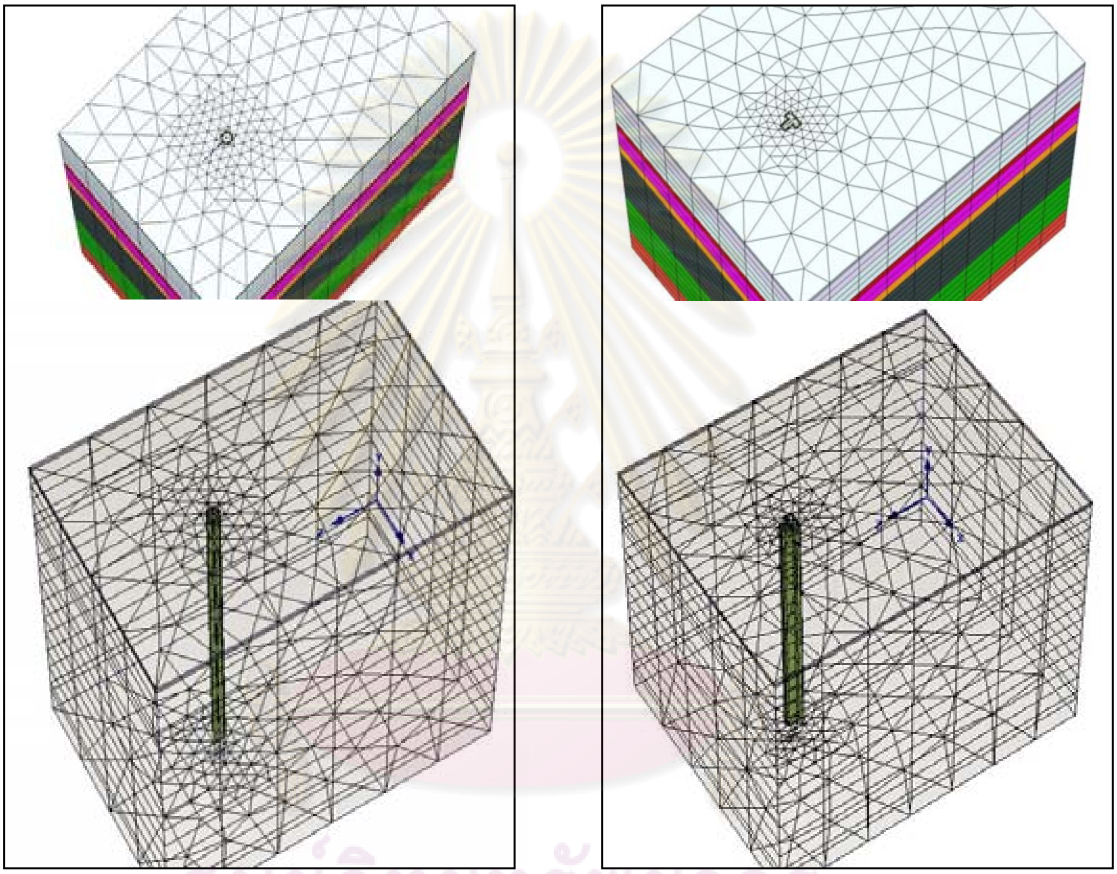

a.) Bored Pile b.) T-shape barrette

Figure 5.11 3D finite element model

Based on the numerical simulation and analysis, the FEM predicted pile head load vs. movement is compared with measured value as shown together in Figure 5.12. The following topics will deal with the analysis results.

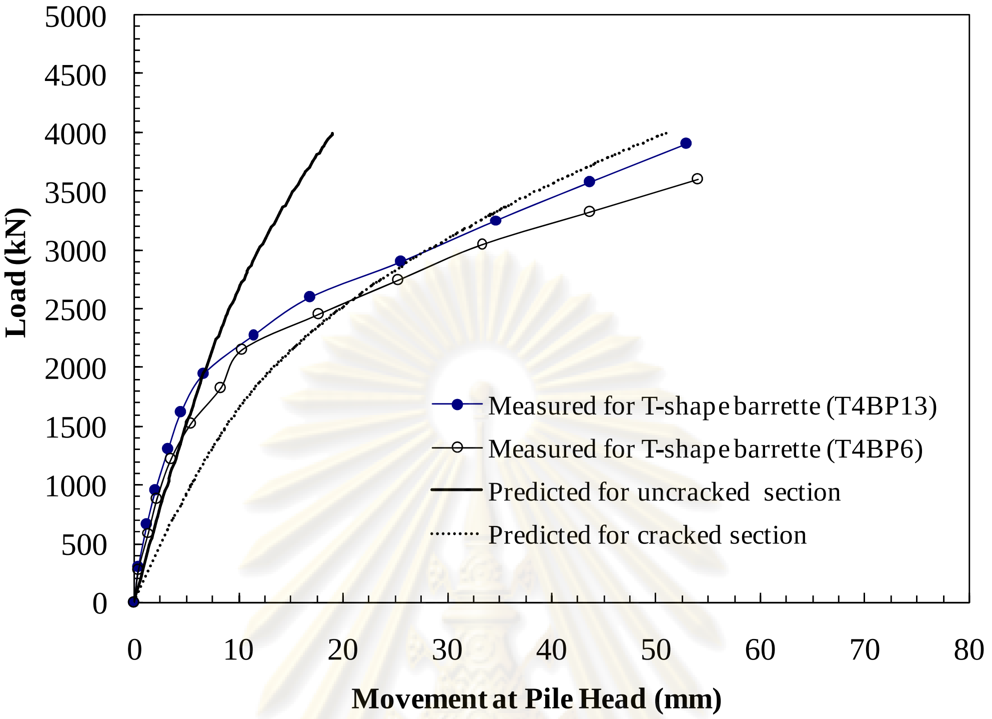

a) T-shape barrette

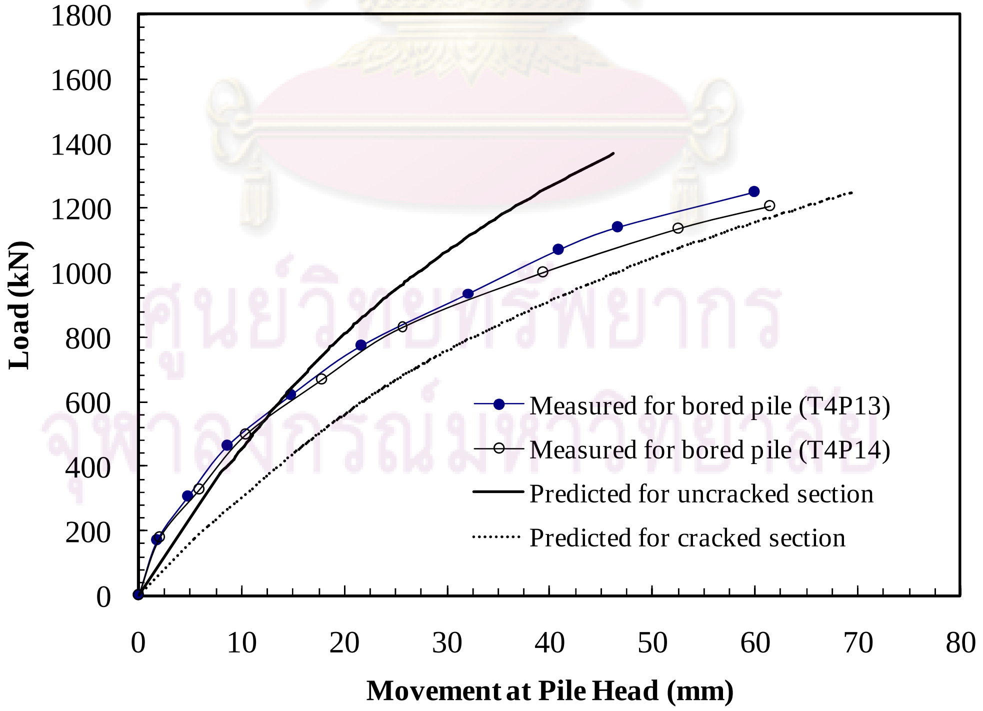

b) Bored pile

Figure 5.12 Movement at pile head under lateral load

5.2.2.1 INFLUENCE OF STRAIN LEVEL

Well understanding of stress-strain relationship is of importance for prediction of deformation in the design of foundation. From various published papers and back-analysis from large numbers of field test data, it is also well understood that under working conditions the strain in the ground surrounding the foundation element is relatively small. Therefore, it is important to measure stiffness at small strain level since stress-strain relationships are non-linear (Burland, 1989, Atkinson, 2000).

Figure 5.13 illustrates the variations of the soil stiffness for service deformation levels of different foundation elements from the work of Mair (1993).

In this study, based on the results of instrumented static lateral load tests, attempt was made to determine the strain level under lateral loading in relation to shear stiffness. According to the back-calculated results, T-shape barrette having lower strain level had higher shear stiffness than that of bored pile having lower shear stiffness. Table 5.2 summarized the range of shear strain for un-cracked and cracked section of T-shape barrette and bored pile. It is to be noted that upper bound values for cracked sections shown in Table 4 are of the trains at maximum applied loads.

From the back-analysis results for un-cracked section, for T-shape barrette, at G/Su ratio of 430, low strain level of 0.09% is estimated whereas relatively higher strain level of 0.40% is estimated at lower G/Su ratio of 150 for bored pile. These estimated values are plotted on the graph (Figure 5.14) showing variation in stiffness ratios with shear strain for Bangkok soft clay, first stiff clay and sand layers reported by Prinzl and Davies (2006). Though it is not advisable to apply these values from limited test results, they will be used as guideline for initial estimation of strains at applied lateral loads in the design.

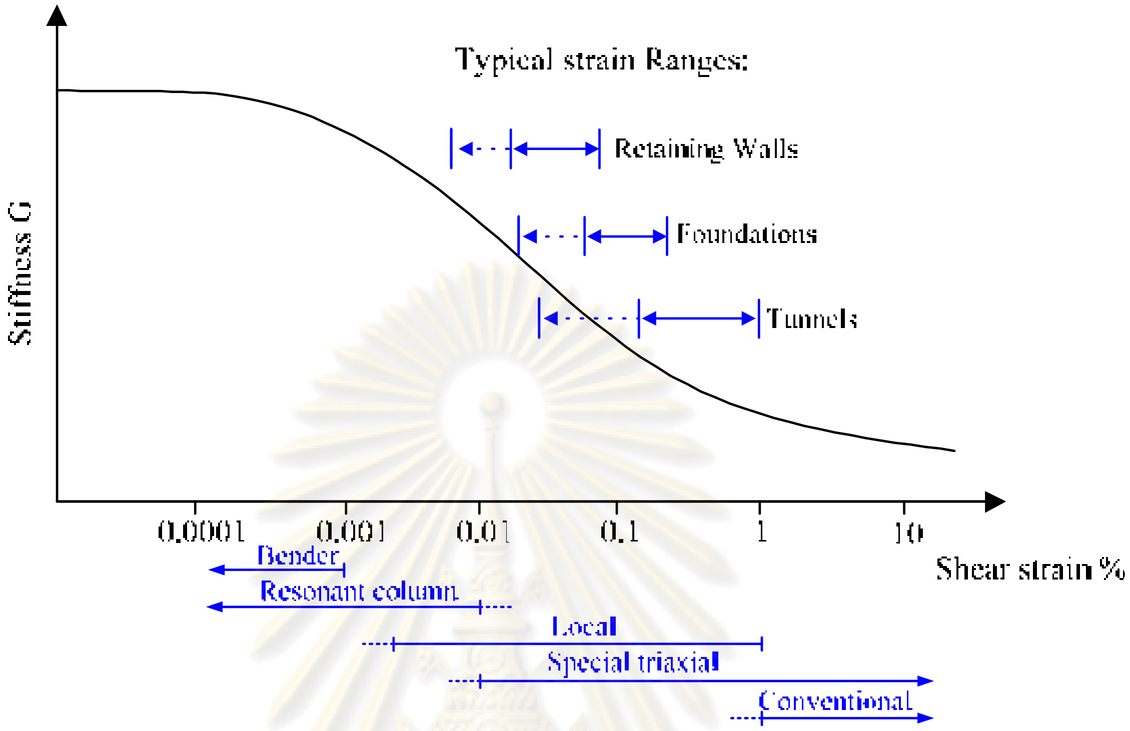

Figure 5.13 Variations of the soil stiffness for service deformation levels of different foundation elements (Mair, 1993)

Table 5.2 Range of shear strain from lateral load test results

Condition	Shear strain (%)	
	T-shape barrette	Bored pile
Un-cracked section	0.00-**0.09**	0.00-**0.40**
Crack section	0.09-**0.62**	0.40-**0.76**

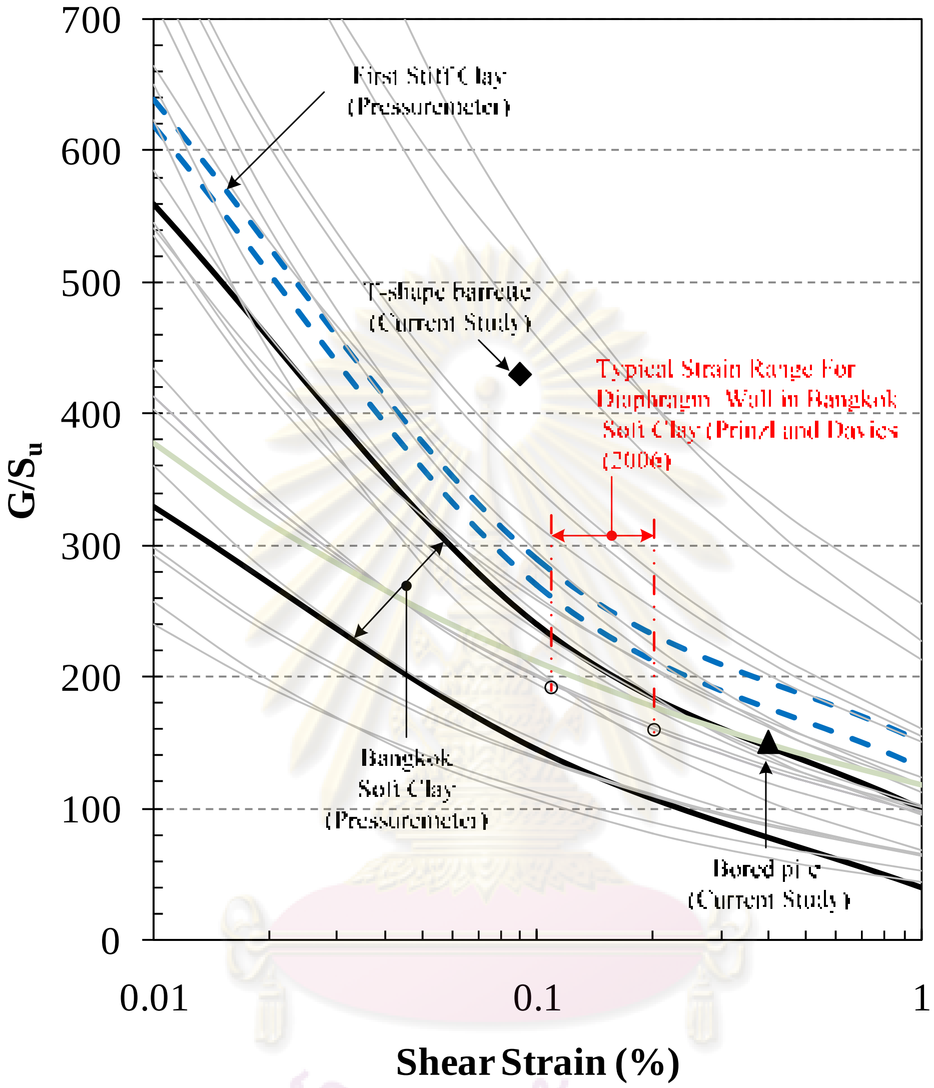

Figure 5.14 Strain level of T-barrette and bored pile plotted on stiffness ratio vs shear strain for Bangkok Soft Clay reported by Prinzl and Davies (2006)

5.2.2.2 UN-CRACKED SECTION ANALYSES

T-shape barrette and bored pile materials consist of concrete and reinforcement are taken to be linear elastic with the constant flexural stiffness. The predicted load-displacement curve under lateral loading with a constant flexible stiffness are plotted in Figure 5.12. At a virgin loading point up to the load of 2000 kN and 600 kN for T-shape barrette and bored pile, respectively, the predicted displacement agree very well with the measured movement. This may be because of no concrete cracking of pile. This characteristic can observe with the value of reinforcement strain installed in T-shape barrette and bored pile as shown in Figure 5.15. The measured reinforcement strain with the applied lateral load lower than 2000 kN for T-shape barrette and 460 kN for bored pile are in elastic condition. For predicted T-shape barrette head movement, the results from this analysis indicate that increasing about 3 times of soil stiffness of bored pile corresponding with the influence of strain level effect give the result in similar movement as measurement until an applied load is up to 2000 kN.

Table 5.3 summarized the assigned soil parameters used for T-shape barrette simulation in total stress analysis.

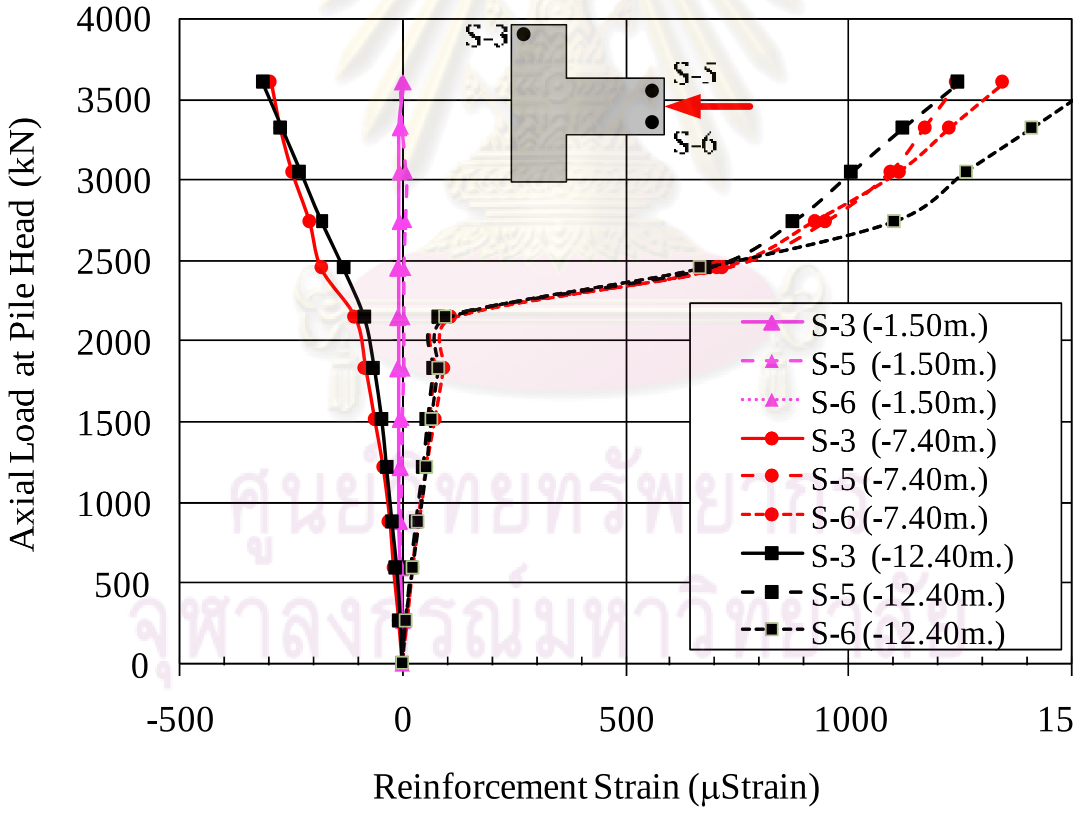

a) T-shape barrette

Figure 5.15 Measured reinforcement strain under lateral load

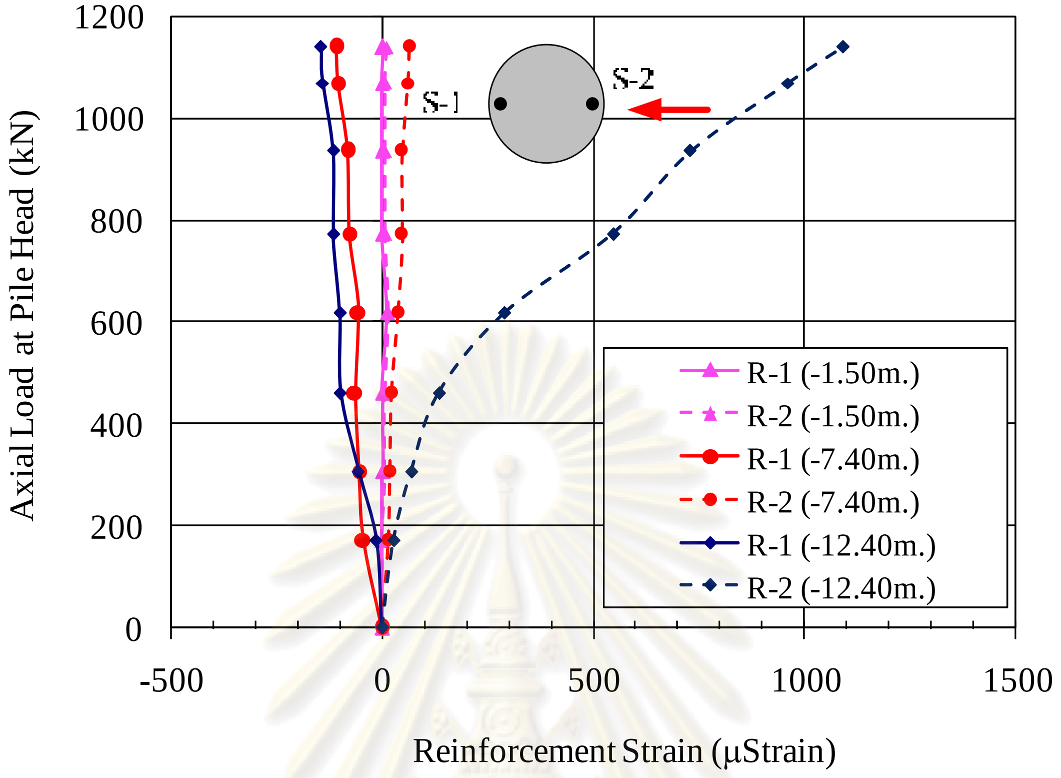

b) Bored pile

Figure 5.15 (Con't) Measured reinforcement strain under lateral load

Table 5.3 Soil parameters for defining the Mohr-Coulomb model in numerical analysis of T-shape barrette

Layer	Soil	From	to	γ	Su	E	Ko
				kN/m^3	kN/m^2	kN/m^2	
1	Crust	0.0	1.0	18.00	35	60000	0.70
2	Very soft clay	1.0	6.0	16.00	18	27700	0.60
3	Soft clay	6.0	13.0	16.50	22	35000	0.60
4	Medium stiff clay	13.0	15.0	18.00	35	60000	0.65
5	Stiff clay	15.0	20.5	17.50	100	310000	0.70
6	Medium dense sand	20.5	23.5	18.00	-	150000	0.80
7	Very stiff clay	23.5	40.0	18.00	110	350000	0.80
8	Hard clay	40.0	53.0	19.00	200	590000	0.80
9	Very dense sand	53.0	70.0	19.50	-	360000	0.80

5.2.2.3 CRACKED SECTION ANALYSES

The cracking moments of the T-shape barrette given in Figure 5.16 may be computed as 3900 kN-m, as shown in Figure 5.15. When lateral load increases to 2,000 kN, the reinforcement strain of the T-shape barrette at depth -7.20 m (Figure 5.15) apparently exceed their cracking moment, resulting in concrete cracking in the pile. Apparently, possible concrete cracking of the shaft significantly affects the calculated results of both T-shape barrette and bored pile. If concrete cracking effect is neglected in the numerical analysis, the results tend to overestimate the pile capacity. Figure 5.17 shows that for the calculated flexural stiffness by using effective moment of inertia of a cracked section proposed by Branson (1963) and incorporated into the ACI code, 2005. When the pile section cracks under large bending moment, the flexural stiffness of the section decreased to about 26% of its original value. For predicted pile head movement after concrete cracking, the results indicate that using the 70% reduction in the flexural stiffness would be required to obtain a lateral movement of the pile head similar to the measured movement.

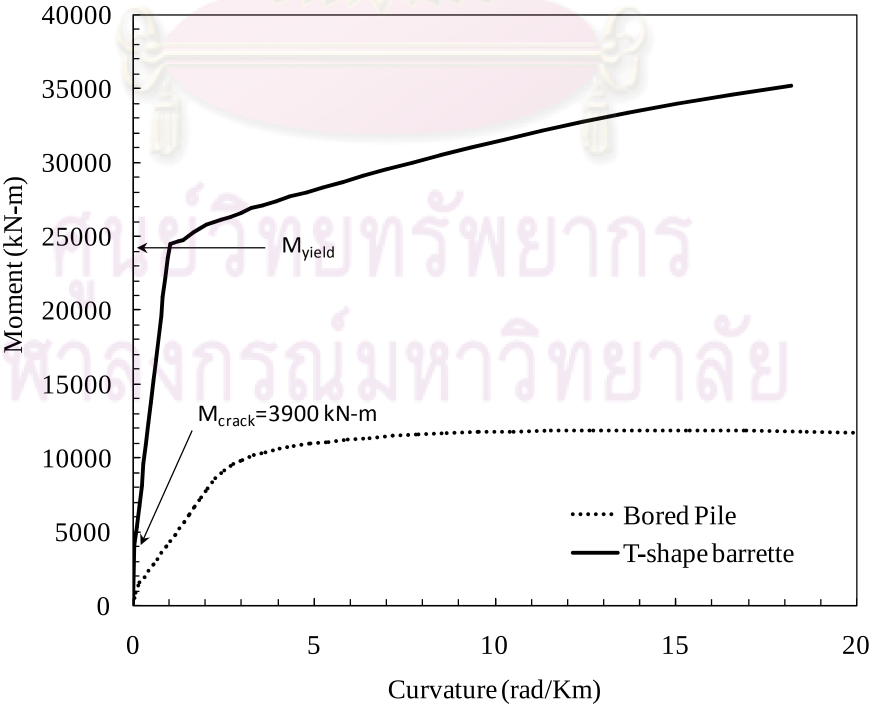

Figure 5.16 Moment curvature of T-shape barrette and bored pile

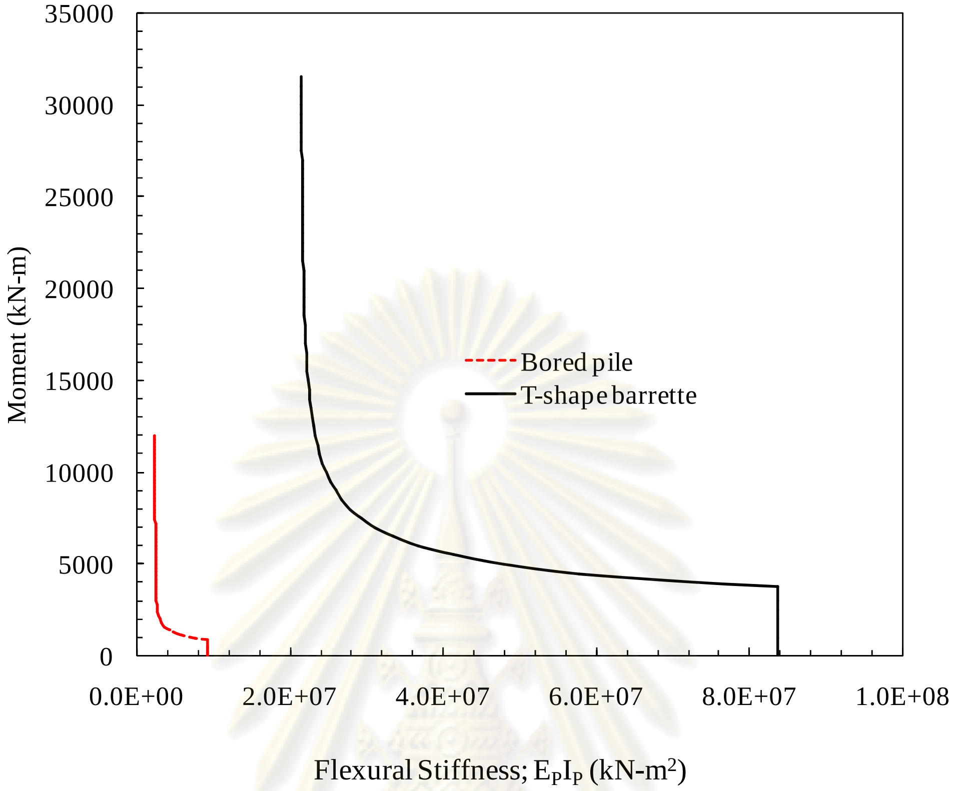

Figure 5.17 Relationship between flexural stiffness and bending moment

5.2.2.4 EFFECT OF VERTICAL GROUND MOVEMENT

The calculated results on ground movement around the T-shape barrette under different loading levels are shown in Figure 5.18. The ground soil in front of and behind T-shape barrette in the loading direction tends to move upward.

The maximum vertical movement in front of T-shape barrette at maximum test loading of 3600 kN is 23.5 mm. and the calculation from FEM agree reasonably well.

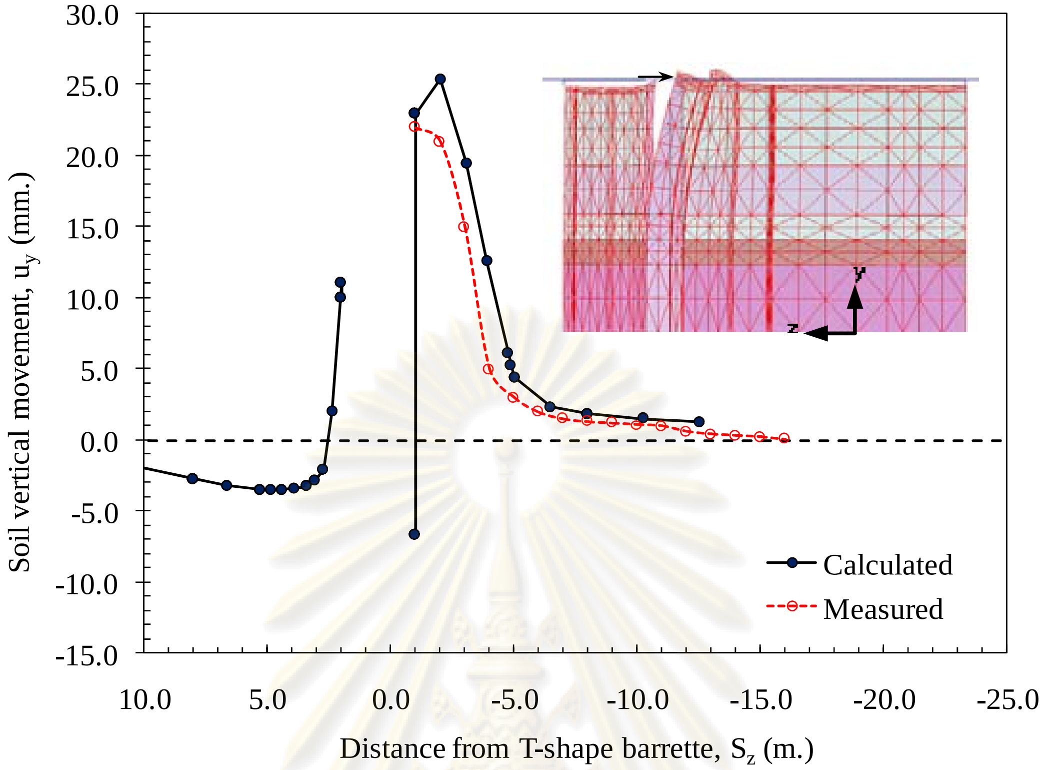

Figure 5.18 Vertical ground movement around T-shape barrette

5.2.2.5 EFFECT OF HORIZONTAL GROUND MOVEMENT

The horizontal ground movement perpendicular to the loading direction at maximum test load of 3600 and 1150 kN for T-shape barrette and bored pile, respectively are shown in Figure 5.19. As shown in the figure, the ratio of soil movement; u_z to the movement of pile head; u_{pile} trend to decreases along the distance away from the centered axis of pile. The results show that under the maximum loading, the affected distance in the loading direction is mainly within about 15m (10 times of centroid or center of gravity (c.g) of stem for T-shape barrette) from T-shape barrette and 10m (6 times of bored pile diameter) from bored pile.

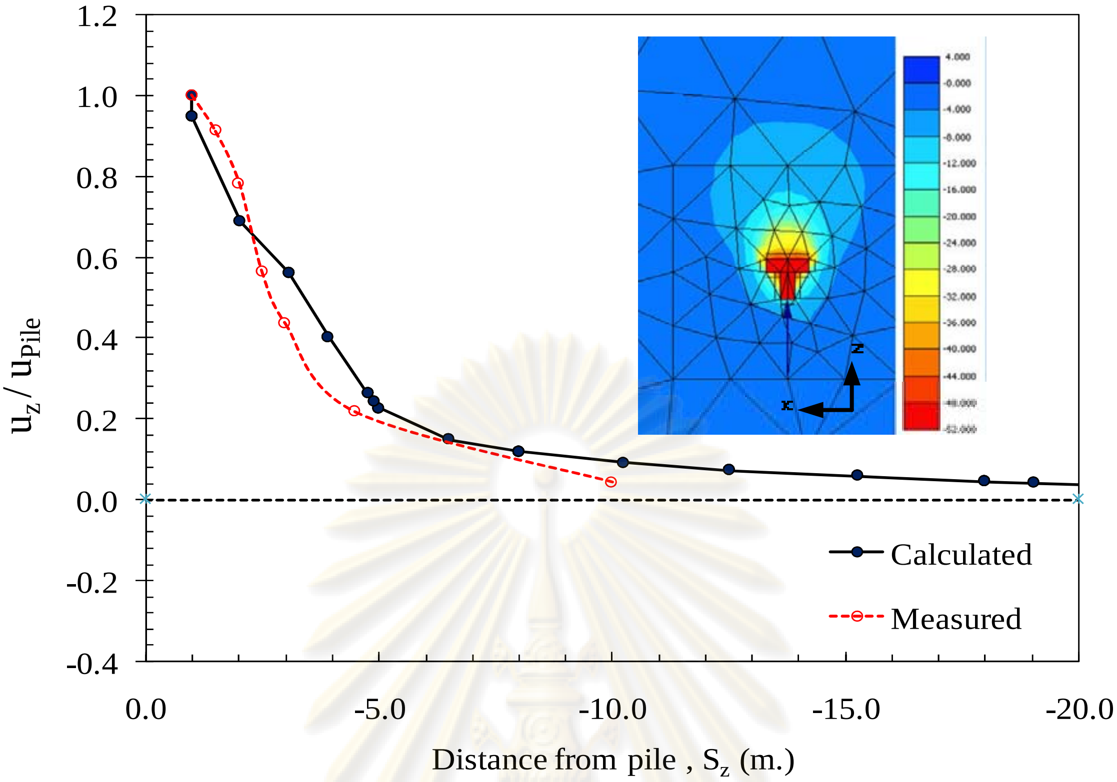

a) T-shape barrette

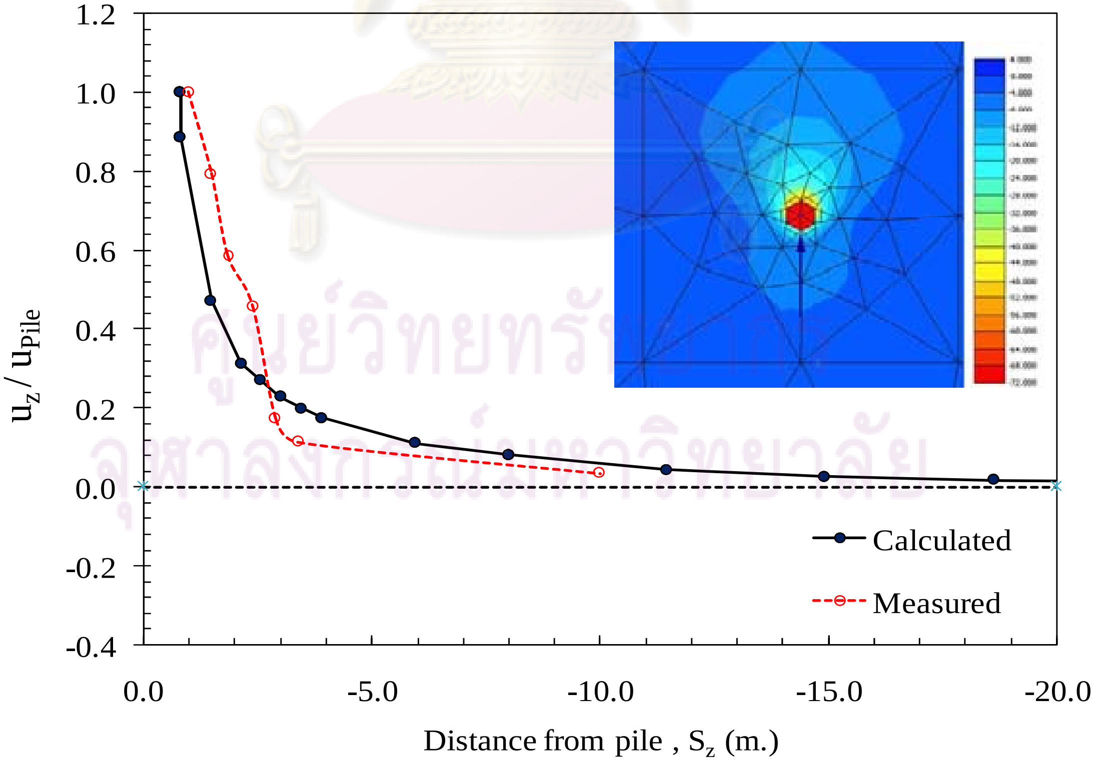

b) Bored pile

Figure 5.19 Horizontal ground movement perpendicular to the loading direction

CHAPTER VI

CONCLUSIONS AND RECOMMENDATION

6.1 CONCLUSIONS

This research aim to study the behavior of vertical and lateral load on T-shape barrette compare with bore pile. The static compression test were performed on 2.00 m diameter bored pile and 5.00 m^2 T-shape barrette with approximately 55 m length in both types of pile. To compare the behavior between both pile under test loading, Vibration wire stain gauges (VWSG) were installed in both piles to measure the strain in each layer. The friction and end bearing resistant were derived to compare with numerical method with PLAXIS 3D Foundations, the 3D FEM Program.

The static lateral load test was preformed to compare between 1.65 diameter bored pile and 5 m^2 T-shape barrette with 55 m length which have different pile geometry. Two sets of both types of pile were installed with inclinometer and VWSG.

6.1.1 VERTICAL LOAD

Load distribution along the pile length from the test results for T-shape barrette and bored pile showed that almost load is carried by friction along the pile. The end bearing load at the failure load for T-shape barrette and bored pile is about 5% of failure load

Based on the 3D FEM analysis, the results show that the shear plane of T-shape barrette under the compression load must consider the effect of pile plug. Thus, the shear plane of T-shape barrette will consist of 2 parts. Almost shear plane is a boundary interface between pile shaft and soil around the shaft. Another plane is in the soil mass. The calculation method to determine the shaft perimeter and sectional area of T-shape barrette without considering soil plug, tend to underestimate the pile capacity.

6.1.2 LATERAL LOAD

In the numerical analysis for lateral load on piles, the analysis results will deal as the following:

1. T-shape barrette having lower strain level had higher shear stiffness than that of bored pile having lower shear stiffness. From the back-analysis results for un-cracked section, for T-shape barrette, at G/Su ratio of 430, low strain level of 0.09% is estimated whereas relatively higher strain level of 0.40% is estimated at lower G/Su ratio of 150 for bored pile.

2. For predicted T-shape barrette head movement in un-cracked section condition, the results from this research indicate that increasing about 3 times of soil stiffness of bored pile corresponding with the influence of strain level effect.

3. When the pile section cracks under large bending moment, the flexural stiffness of the T-shape barrette section decreased to about 26% of its original value. For predicted pile head movement after concrete cracking, the results indicate that using the 70% reduction in the flexural stiffness would be required to obtain a lateral movement of the pile head similar to the measured movement.

4. The ground soil in front of and behind T-shape barrette in the loading direction tends to move upward under the lateral load. For the horizontal movement under the maximum loading, the affected distance in the loading direction is mainly within about 10 times of centroid or center of gravity (c.g) of stem for T-shape barrette and 6 times of bored pile diameter.

6.2 RECOMMENDATION

In order to improve the quality of geotechnical works in terms of academic research, which is the major sources for updating the knowledge of geotechnical engineers, the following recommendations are beneficial to future research:

a) To get a realistic data from instrumentation, the locations of strain gauges should be confirmed with the exact soil data at the test area.

b) Although the output might slightly vary from one to another, the different kind of soil models can be used and the analysis results have to be compared among them and with the real monitored data obtained from the field performance.

c) Due to the lack more data and limited test results, it is not advisable to apply all suggest values. They will be used as guideline for initial estimation of strains at applied lateral loads in the design.

REFERENCES

Abbas, J. M., Chik, Z. H. and Taha, M. R. 2008. Single Pile Simulation and Analysis Subjected to Lateral Load. The Electronic Journal of Geotechnical Engineering 3E: 1-15.

American Society for Testing and Materials (ASTM) 1992. Method of testing piles under lateral loads. USA: ASTM International.

American Concrete Institute (ACI) 2005. ACI Building code requirements for structural concrete and Commentary (ACI 318R-2005). USA: Farmington Hills.

Atkinson J. H. 2000. Non-linear soil stiffness in routine design. Geotechnique 50: 487-508.

Bentley, K. J. and Naggar, M. H. El. 2000. Numerical analysis of kinematic response of single piles. Canadian Geotechnical Journal 37:1368–1382.

Branson, D.E. 1963. Instantaneous and time dependent deflection of simple and continuous reinforced concrete beams. Alabama Highway Research Report No. 7, pp. 78. USA: Bureau of Public Roads.

Brinkgreve, R.B.J. & Broere, W. 2004. PLAXIS 3D Foundation-version 1. Netherlands: A.A. Balkema.

Broms, B. 1964. The lateral resistance of piles in cohesive soils. Journal of the Soil Mechanics Division 90: 27-63.

Burland J. 1989. Small is beautiful: the stiffness of soils at small strains. Canadian Geotechnical Journal 26: 499-516.

Butler, H.D. and Hoy, H. E. 1977. Users manual for the Texas quick-load for foundation load testing. Report Number FHWA–IPO–77-8, pp. 59. Washington: Federal Highway Administration.

Coulomb, C. A. 1776. Essai sur une application des regles des maximis et minimis a quelquels problemesde statique relatifs, a la architecture. Memoires de l'Academie Royale pres Divers Savants 7: 343–387.

Hsueh, C. K., Lin, S. S. and Chern S. G. 2004. Lateral performance of drilled shaft considering Nonlinear soil and structure material behavior. Journal of Marine Science and Technology 12: 62-71.

Davisson, M.T. and Gill, H. L. 1963. Laterally-loaded piles in a layers soil system. Journal of the Soil Mechanics Division 89: 93-94.

Fellenius , B. H. 2001. From strain measurements to load in an instrumented pile. Geotechnical News Magazine 19: 35-38.

Intraratchaiyakit, C. 2001. Prediction of horizontal movement due to lateral load acting on vertical pile using beam on elastic foundation theory. Master ‘s Thesis. Department of Civil Engineering Faculty of Engineering Chulalongkorn University.

Mair, R.J. 1993. Development in geotechnical engineering research, application to tunnels and deep excavations. Unwin Memorial Lecture 1992. Proceedings of the Institution of Civil Engineers, pp. 27-41. London: ICE.

Matlock, H. and Reese, L. C.1960. Generalize solution for lateral load pile. Journal of the Soil Mechanics Division 86: 63-91.

Ooi, P. S. K., and Ramsey, T. L. 2003. Curvature and bending moments from inclinometer data. International Journal of Geomechanics 3: 64 -74.

Phienwej, N. 1996. Geotechnical experiences from previous tunnel project in Bangkok soils. Proceedings of the International Symposium on Geotechnical Aspects of Underground Construction in Soft Ground, pp. 311-316. London.

Phienwej, N. 1997. Ground movements in shield tunneling in Bangkok soils. Proceedings of the 14th International Conference on Soil Mechanics and Foundation Engineering, pp. 1469-1472. Germany.

Pimpasugdi, S. 1989. Performance of bored, driven and auger press piles in Bangkok Subsoils. Master 's Thesis. Asian Institute of Technology Bangkok.

Plumbridge, G. D., Sze, J. W. C. and Tram, T. T. F. 2000. Full Scale Lateral Load Tests on Bored Piles and a Barrette. Proceedings of 19th Annual Seminar of the Geotechnical Division, pp. 211-220. Hong Kong: Hong Kong Institution of Engineers.

Poulos, H. G. 1971, Behavior of Laterally Loaded Piles: I – Single Piles. Journal of Soil Mechanics and Foundations 97: 711-731.

Prinzl, F. and Davies, J.A. 2006. Some Aspects of the Design of Tunnel Linings in Anisotropic Ground Conditions. International Symposium on Underground Excavation and Tunnelling, pp. 231-238. Bangkok: EIT.

Raymond J. C. and Ke Fan (2002). Lateral Load Test Results on Drill Shafts in Marl at Jacksonville, Florida. Proceedings of the International Deep Foundations Congress, pp. 825-835. Florida:

Reese. L. C. 1997. Analysis of Laterally Loaded Piles in Weak Rock. Journal of Geotechnical and Geoenvironmental Engineering 123: 1010-1017.

Reese, L. C., and Van Impe, W. F. 2001. Single piles and pile groups under lateral loading. Netherlands: Balkema.

Shibuya, S. and Tamrakar, S. B. 2003. Engineering properties of Bangkok clay. Proceedings of International Symposium on Characterization and Engineering properties of Natural Soils, pp. 645-692. Singapore.

Submaneewong, C. 1999. Behavior of Instrumented Barrette and Bored pile in Bangkok subsoils. Master 's Thesis. Department of Civil Engineering Faculty of Engineering Chulalongkorn University.

Teparaksa, W. 1999. Principal and application of instrumentation for the first MRTA subway project in Bangkok. Proceedings of the 5th International Conference on Field Measurement in Geomechanics, pp. 411-416. Singapore.

Teparaksa, W. and Heidengren, C. R. 1999. Geotechnical aspects of the design and construction of the MRTA initial system project - The Bangkok Subway. Journal of the Society of Professional Engineers 24: 21-34.

Tomlinson, M. J. 1995. Foundation Design and practice, 6th ed. Singapore: Longman.

Zhang L. M. 2003. Behavior of Laterally Loaded Large-Section Barrettes. Journal of Geotechnical and Geoenvironmental Engineering 135: 639-648.

APPENDICES

APPENDIX A:
COMPRESSION LOAD TEST RESULTS

STATIC COMPRESSION LOAD TEST RESULT

PILE TYPE : T-shape Barrette

TEST PILE : T4BP6

SIZE : 1.00x3.00 + 1.00x2.00

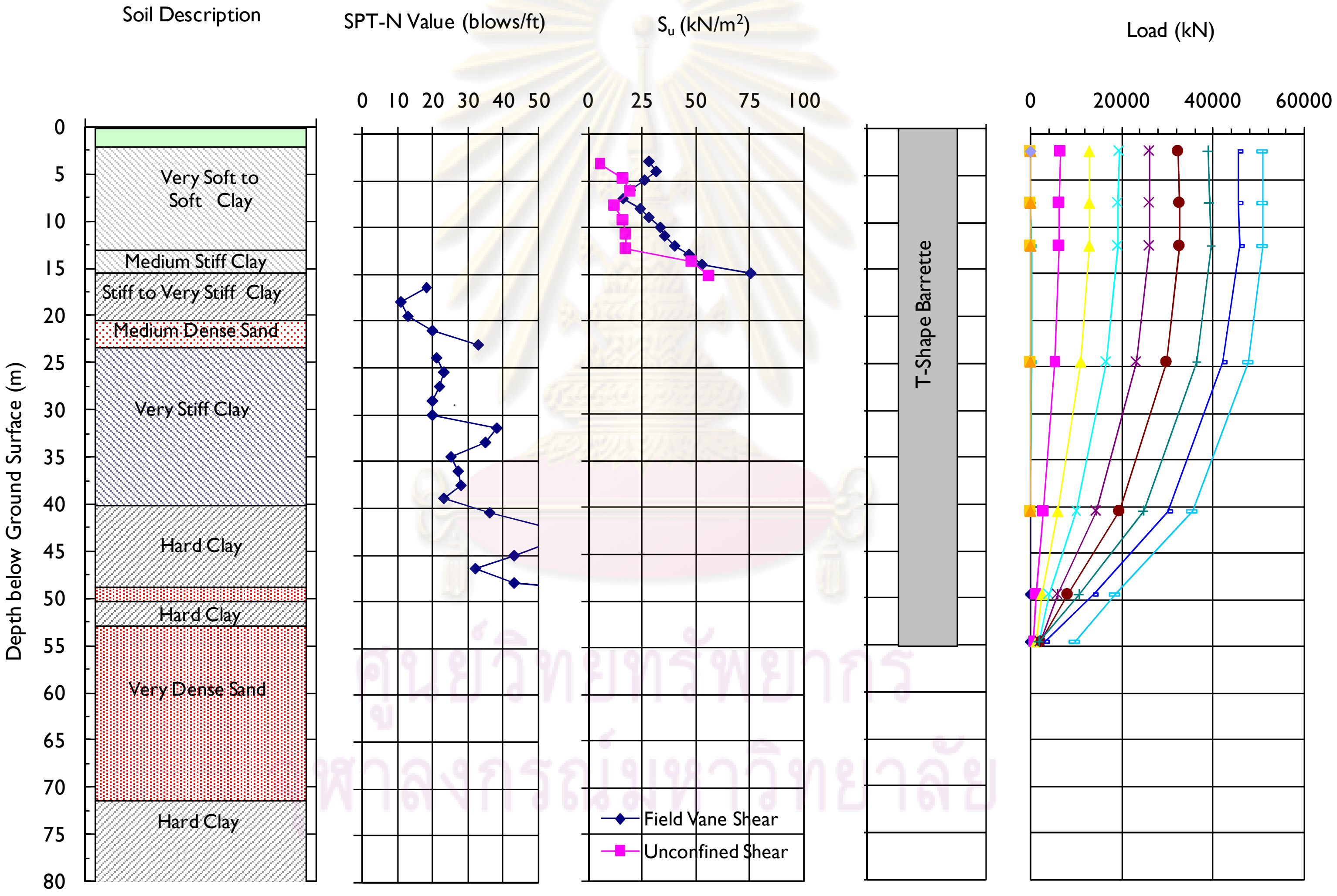

STATIC COMPRESSION LOAD TEST RESULT

PILE TYPE : T-shape Barrette

TEST PILE : T4BP6

SIZE : 1.00x3.00 + 1.00x2.00

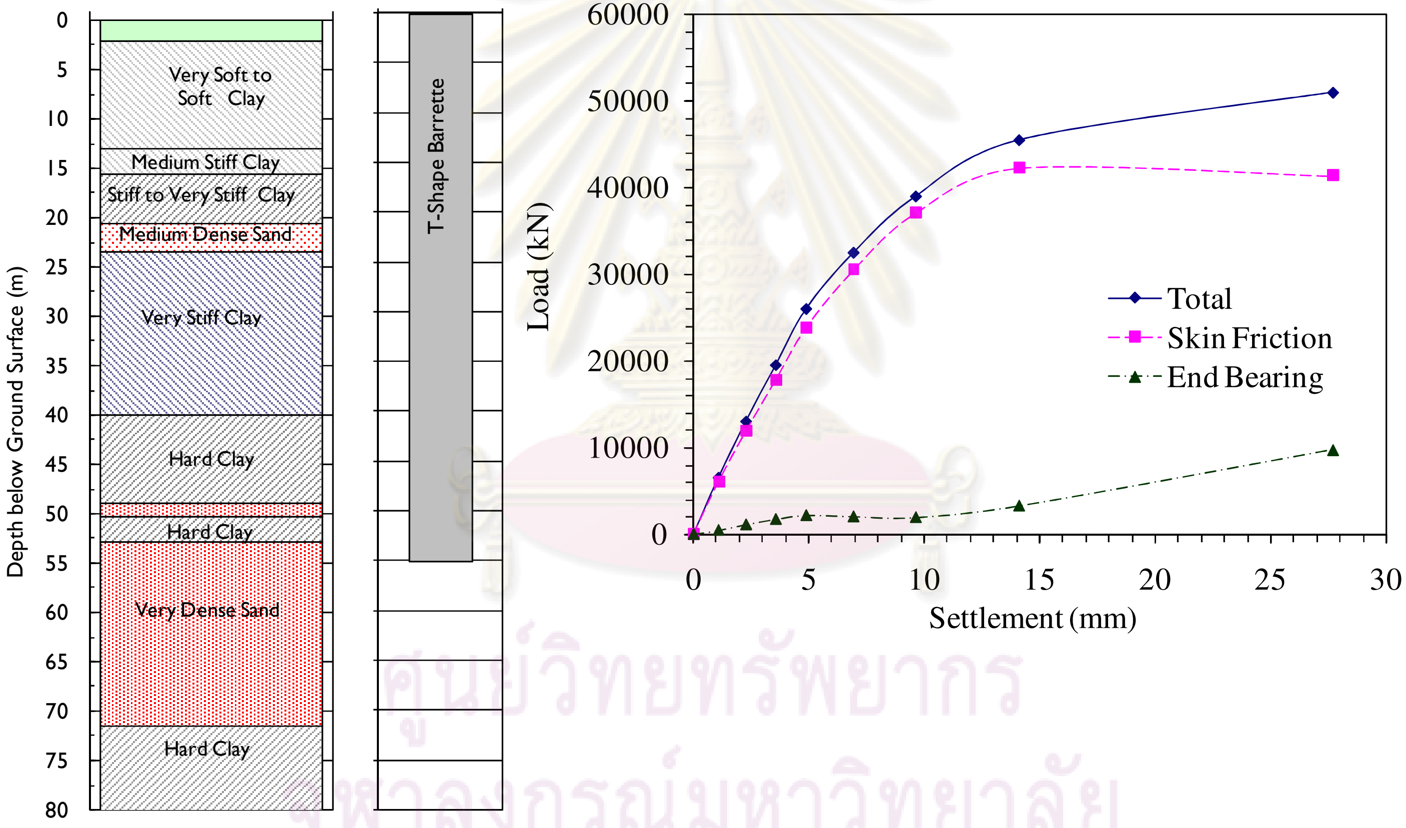

STATIC COMPRESSION LOAD TEST RESULT

PILE TYPE : Bored Pile

TEST PILE : T4P17

SIZE : 2.0 m diameter

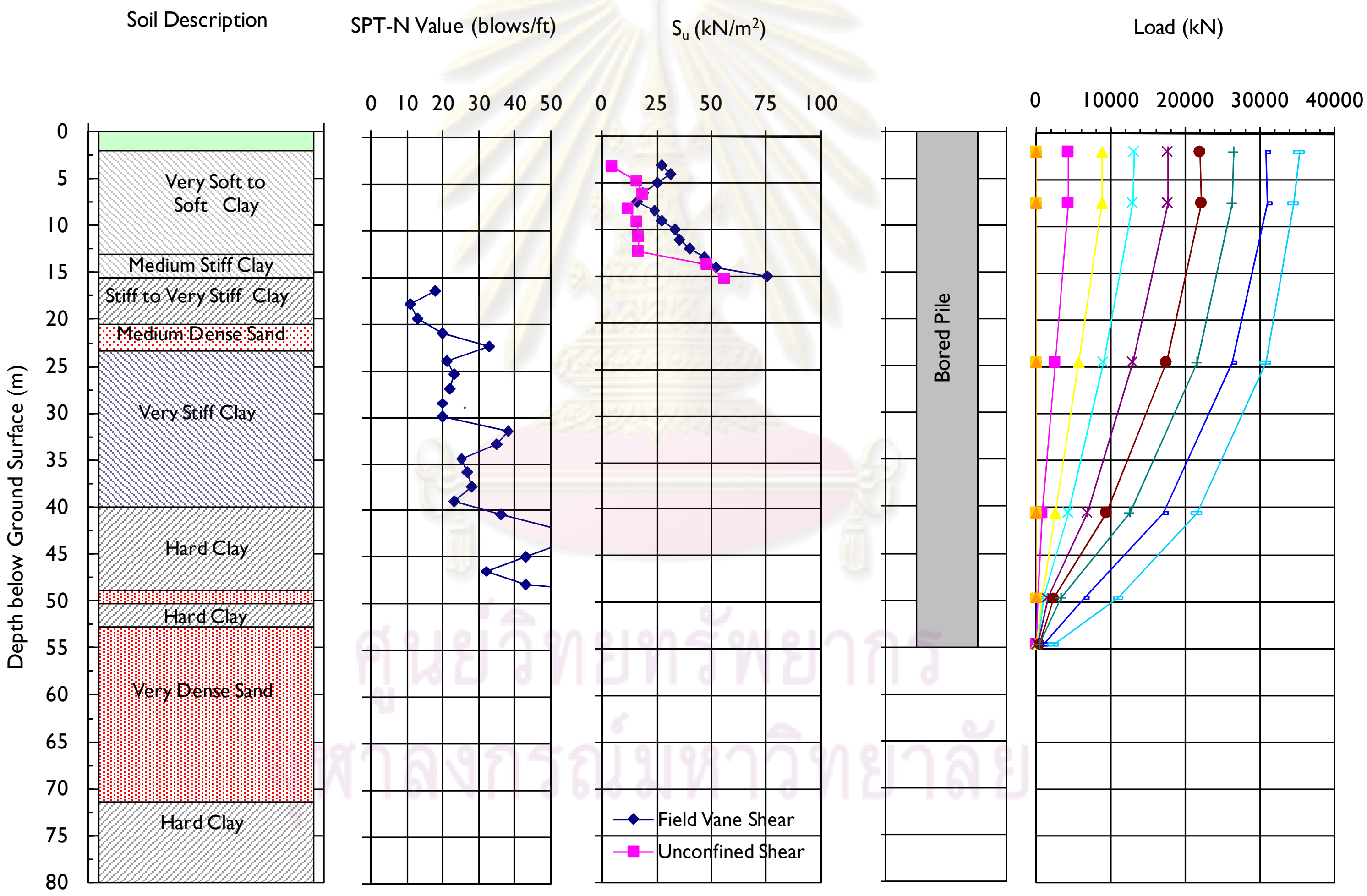

STATIC COMPRESSION LOAD TEST RESULT

PILE TYPE : Bored Pile

TEST PILE : T4P17

SIZE : 2.0 m diameter

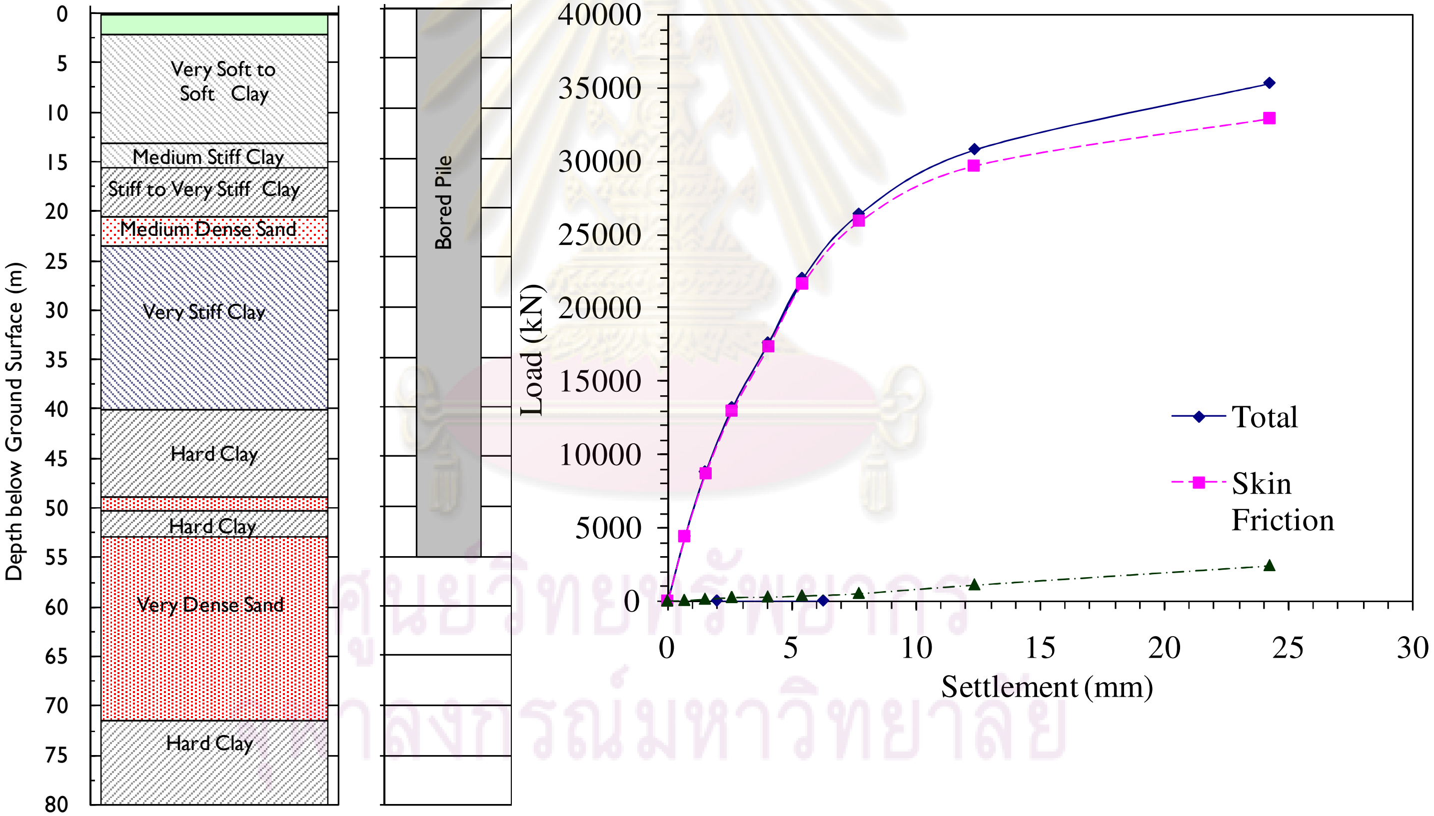

APPENDIX B:
LATERAL LOAD TEST RESULTS

STATIC LATERAL LOAD TEST RESULT

TEST PILE : T4BP13 & T4BP6

PILE TYPE : T-shape Barrette

SIZE : 1.00x3.00 + 1.00x2.00

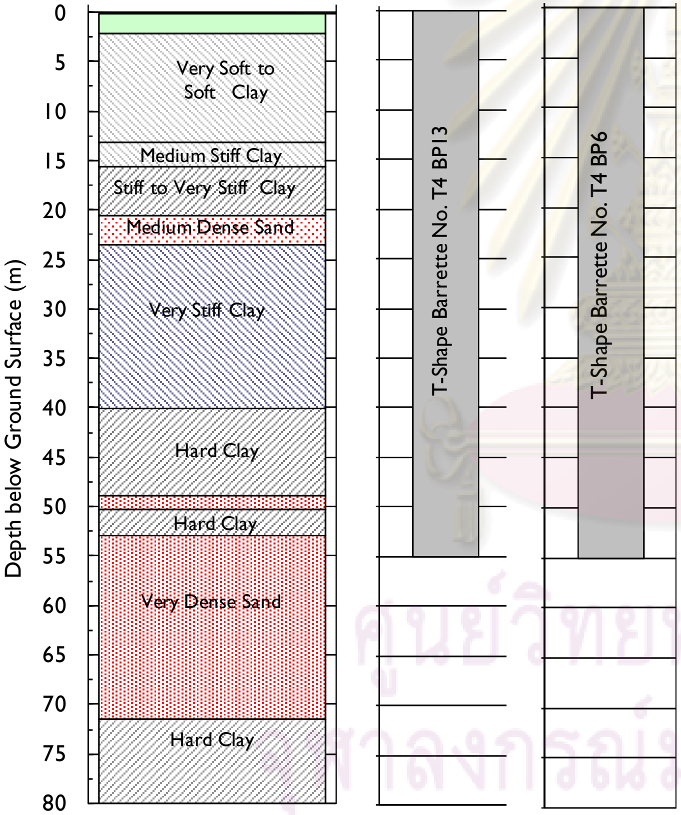

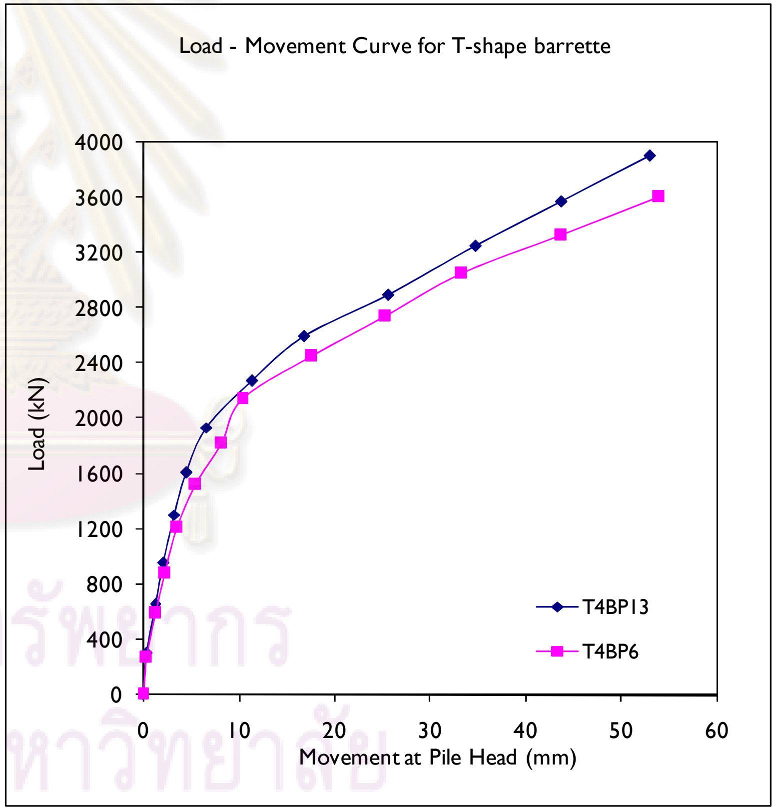

STATIC LATERAL LOAD TEST RESULT

PILE TYPE : Bored Pile

TEST PILE : T4 P13 & T4 P14

SIZE : 1.65m Diameter

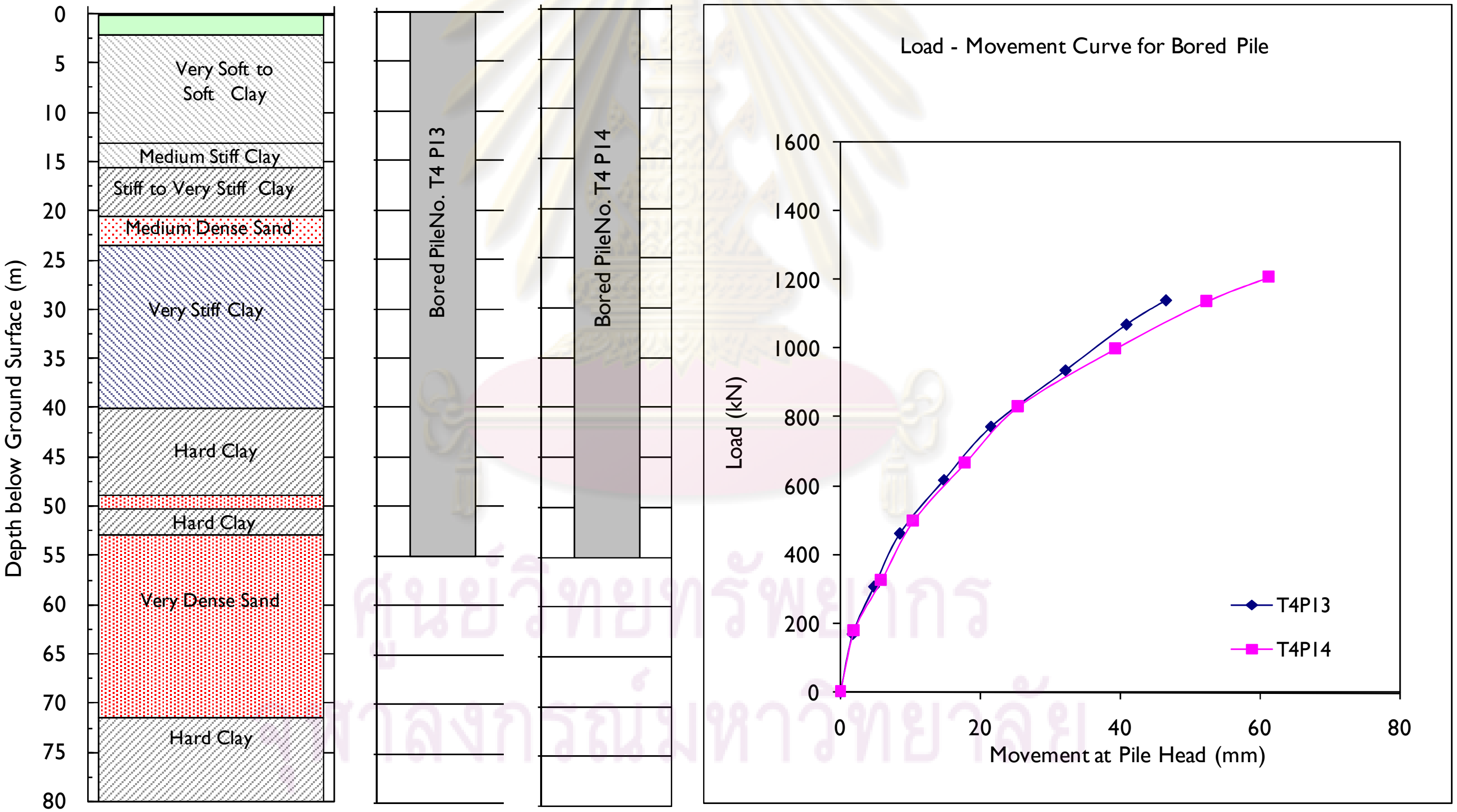

APPENDIX C:
TEST PILE SHOP DRAWING

Test T-Shape Barrette Shop Drawing
For Compression Load Test
(1.00x3.00 + 1.00x2.00)

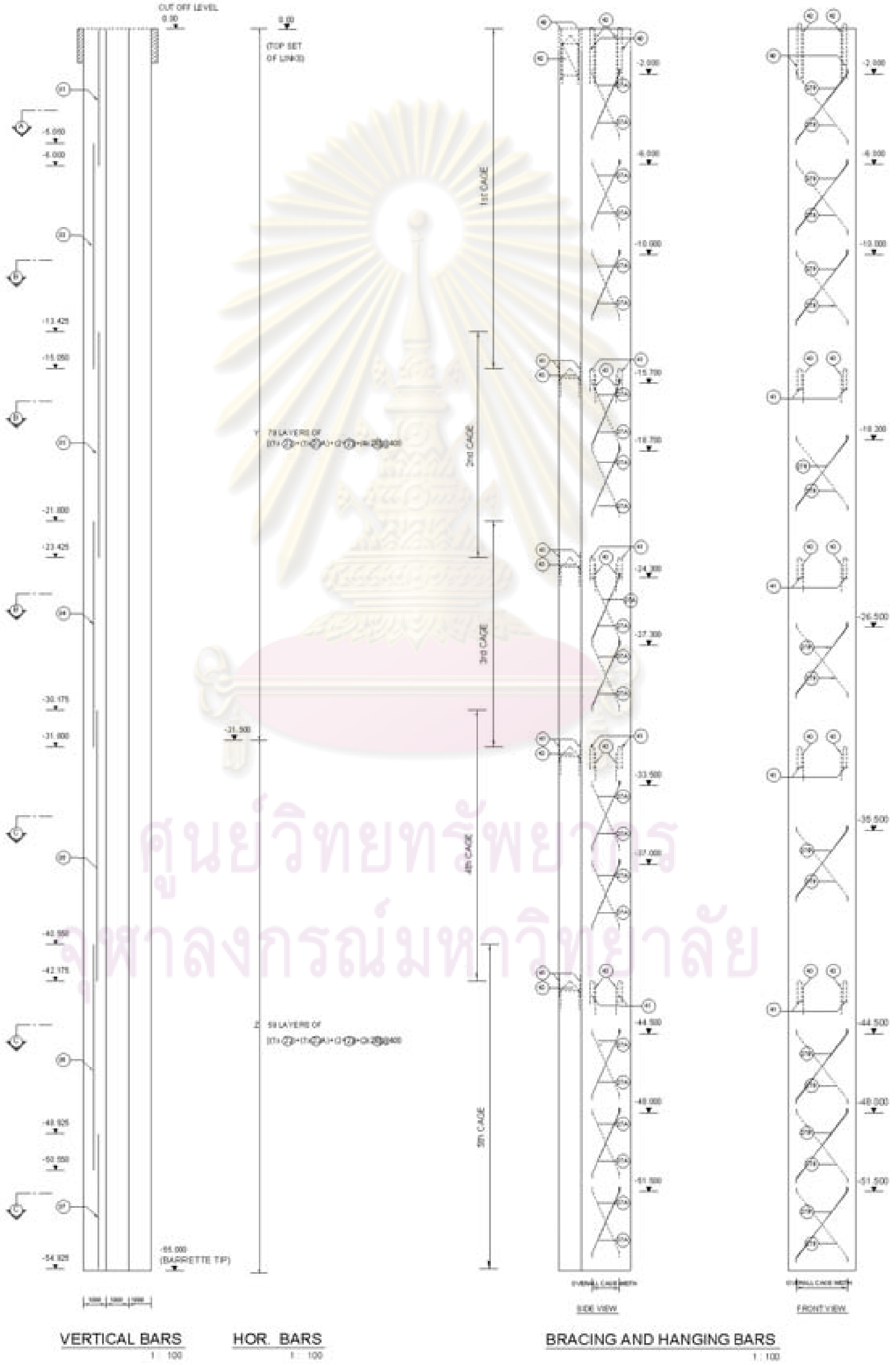

Test T-Shape Barrette Shop Drawing For Compression Load Test (1.00x3.00 + 1.00x2.00)

SECTION A
1 : 50

SECTION B
1 : 50

SECTION C
1 : 50

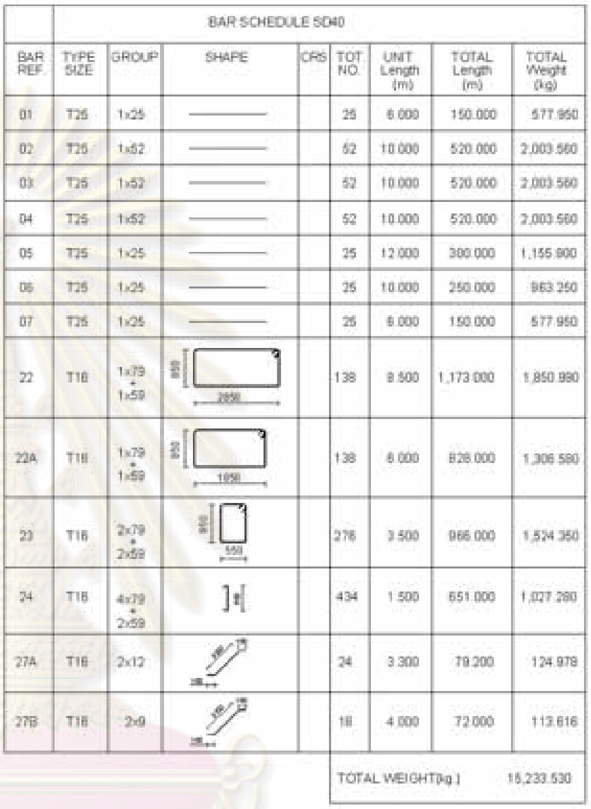

BAR SCHEDULE SD40

BAR REF.	TYPE SIZE	GROUP	SHAPE	CRS	TOT. NO.	UNIT Length (m)	TOTAL Length (m)	TOTAL Weight (kg)
01	T25	1x25			25	6.000	150.000	577.950
02	T25	1x52			52	10.000	520.000	2,003.560
03	T25	1x52			52	10.000	520.000	2,003.560
04	T25	1x52			52	10.000	520.000	2,003.560
05	T25	1x25			25	12.000	300.000	1,155.900
06	T25	1x25			25	10.000	250.000	963.250
07	T25	1x25			25	6.000	150.000	577.950
22	T16	1x79 + 1x59	850 2850		138	8.500	1,173.000	1,850.990
22A	T16	1x79 + 1x59	850 1850		138	6.000	828.000	1,306.580
23	T16	2x79 + 2x59	850 550		276	3.500	966.000	1,524.350
24	T16	4x79 + 2x59			434	1.500	651.000	1,027.280
27A	T16	2x12			24	3.300	79.200	124.978
27B	T16	2x9			18	4.000	72.000	113.616
					TOTAL WEIGHT(kg.)			15,233.530

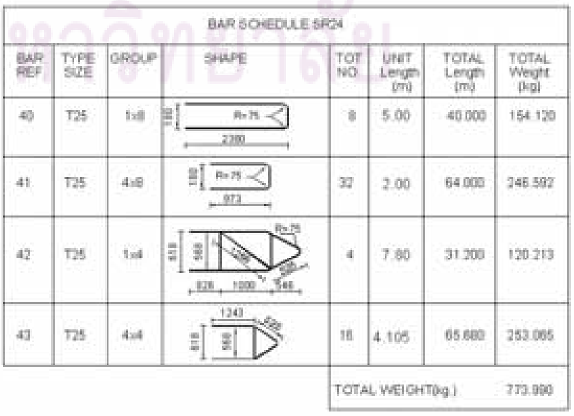

BAR SCHEDULE SR24

BAR REF	TYPE SIZE	GROUP	SHAPE	TOT NO	UNIT Length (m)	TOTAL Length (m)	TOTAL Weight (kg)
40	T25	1x8	180 R=75 2380	8	5.00	40.000	154.120
41	T25	4x8	180 R=75 973	32	2.00	64.000	246.592
42	T25	1x4	618 568 R=75 826 1000 546	4	7.80	31.200	120.213
43	T25	4x4	1243 618 568	16	4.105	65.680	253.065
				TOTAL WEIGHT(kg.)			773.990

Test Bored Pile ϕ 2.00m. Shop Drawing
For Compression Load Test

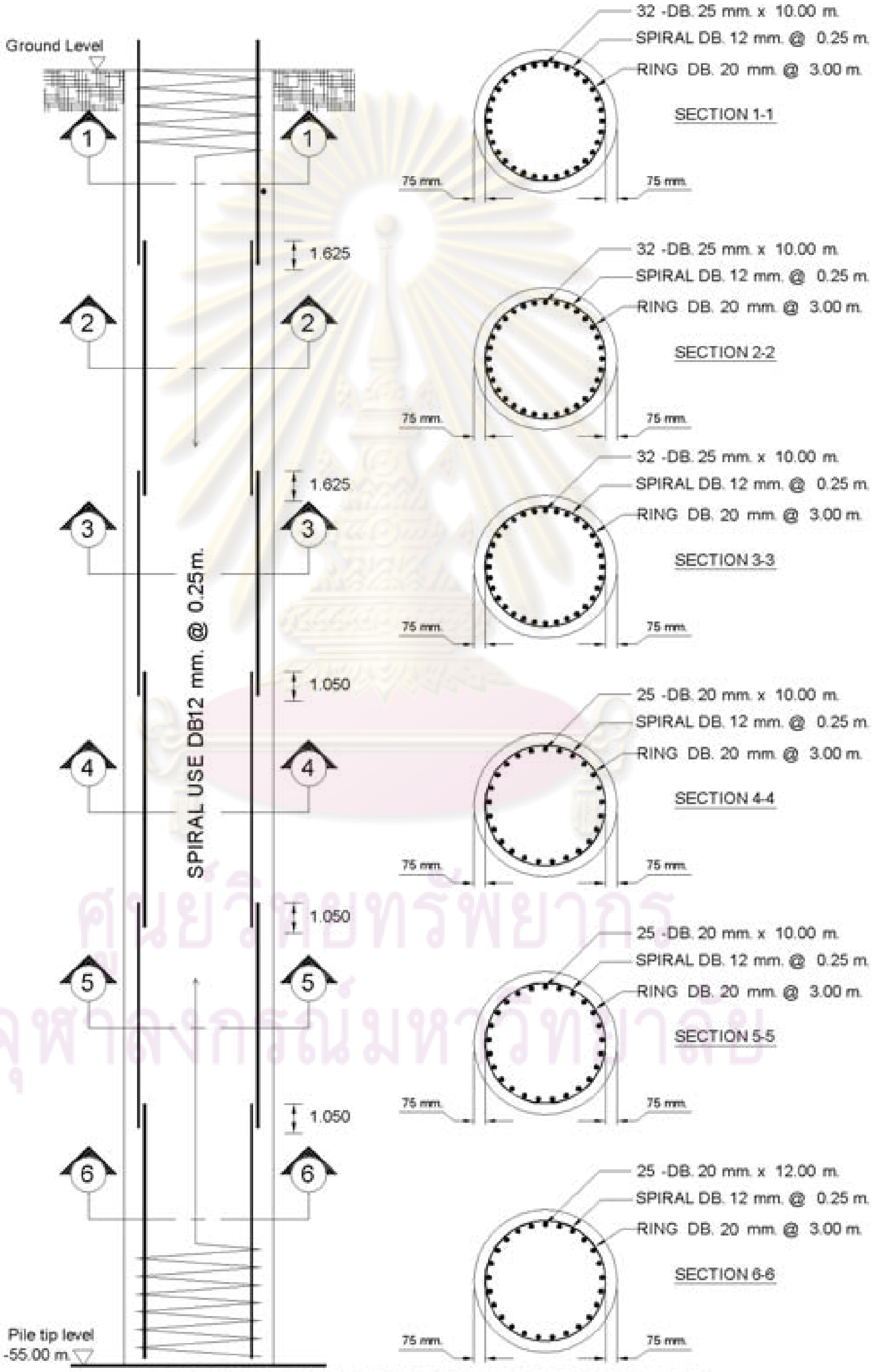

NOT: CONCRETE COMPRESSIVE STRENGTH, fc' (CYLINDER,28 DAY)>240 ksc.
REBAR GRADE SHALL BE SD40

Test T-Shape Barrette Shop Drawing
For Lateral Load Test
(1.00x3.00 + 1.00x2.00)

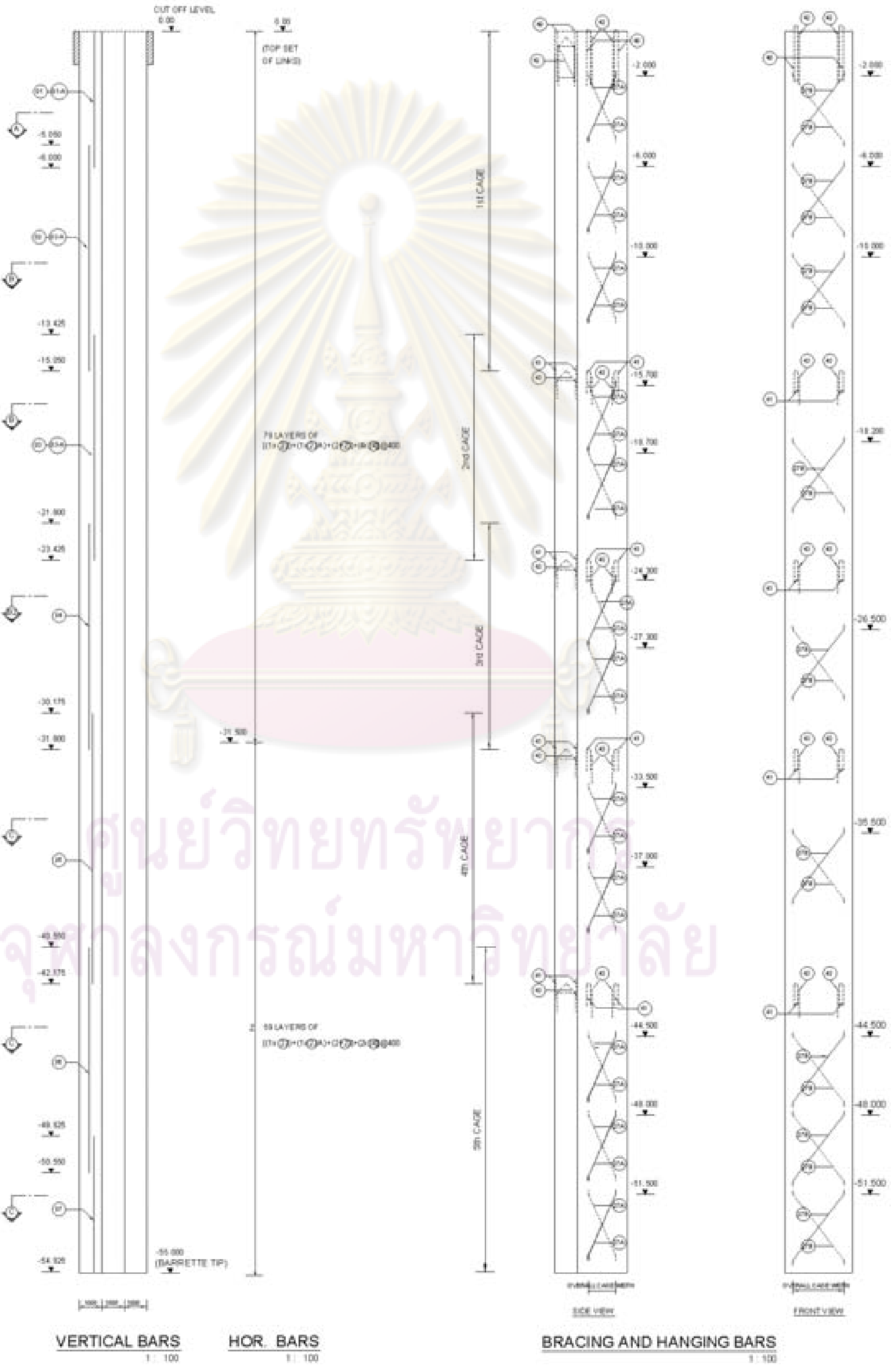

Test T-Shape Barrette Shop Drawing
For Lateral Load Test
(1.00x3.00 + 1.00x2.00)

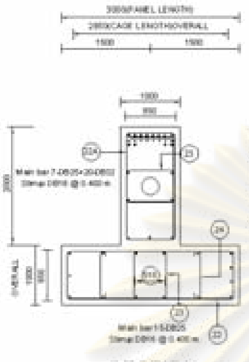

SECTION A
1 : 50

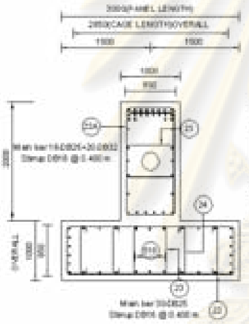

SECTION B
1 : 50

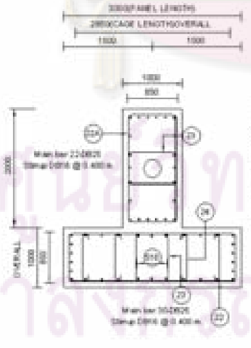

SECTION B2
1 : 50

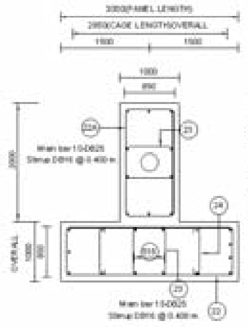

SECTION C
1 : 50

NOTES

BAR SCHEDULE SD40

BAR REF	TYPE SIZE	GROUP	SHAPE	CRS	TOT NO.	UNIT Length (m)	TOTAL Length (m)	TOTAL Weight (kg)
01	T25	1x22	—		22	6.000	132.000	508.596
02	T25	1x46	—		46	10.000	460.000	1,772.380
03	T25	1x46	—		46	10.000	460.000	1,772.380
04	T25	1x52	—		52	10.000	520.000	2,003.560
05	T25	1x25	—		25	12.000	300.000	1,155.900
06	T25	1x25	—		25	10.000	250.000	963.250
07	T25	1x25	—		25	6.000	150.000	577.950
22	T16	1x79 + 1x59	650 2950		138	8.500	1,173.000	1,850.990
22A	T16	1x79 + 1x59	650 1850		138	6.000	828.000	1,306.580
23	T16	2x79 + 2x59	650 552		276	3.500	966.000	1,524.350
24	T16	4x79 + 2x59			434	1.500	651.000	1,027.280
27A	T16	2x12			24	3.300	79.200	124.978
27B	T16	2x9			18	4.000	72.000	113.616
					TOTAL WEIGHT(kg)			14,701.820

BAR SCHEDULE SR24

BAR REF	TYPE SIZE	GROUP	SHAPE	TOT NO.	UNIT Length (m)	TOTAL Length (m)	TOTAL Weight (kg)
40	T25	1x8	150 R=75 2388	8	5.00	40.000	154.120
41	T25	4x8	150 R=75 872	32	2.00	64.000	246.592
42	T25	1x4	918 568 R=75 826 1000 546	4	7.80	31.200	120.213
43	T25	4x4	1240 918 568	16	4.105	65.680	253.065
				TOTAL WEIGHT(kg)			773.990

BAR SCHEDULE SD50

BAR REF	TYPE SIZE	GROUP	SHAPE	CRS	TOT NO.	UNIT Length (m)	TOTAL Length (m)	TOTAL Weight (kg)
01-A	T32	1x20	—		20	6.000	120.000	757.560
02-B	T32	1x20	—		20	10.000	200.000	1,262.600
03-C	T32	1x20	—		20	10.000	200.000	1,262.600
					TOTAL WEIGHT(kg)			3,282.760

Test Bored Pile ϕ 1.65m. Shop Drawing
For Lateral Load Test

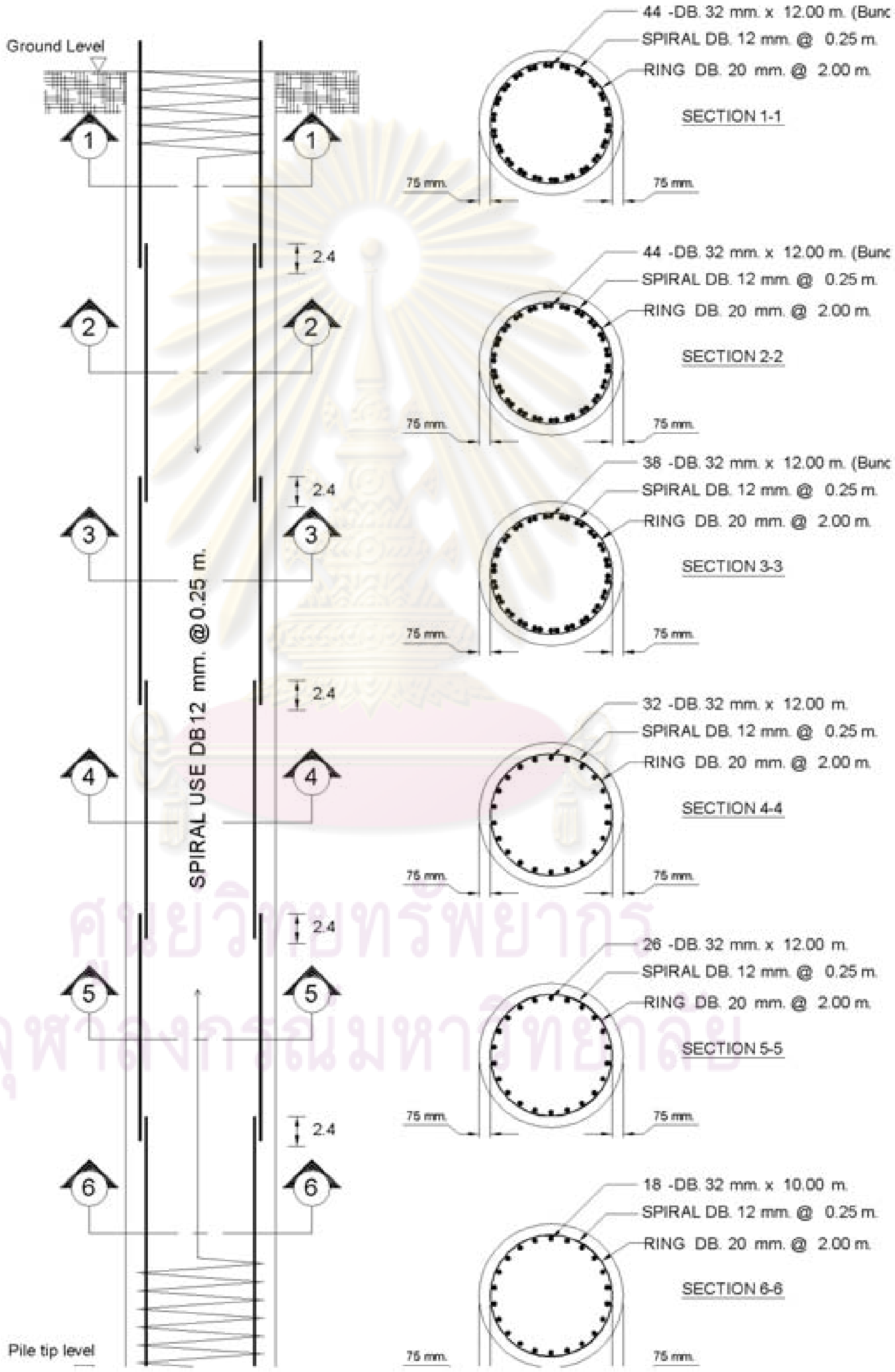

APPENDIX D:
SOIL PROPERTIES

STS INSTRUMENTS COMPANY LIMITED
SUMMARY OF TEST RESULTS

PROJECT Sukhumvit Soi 18 Bangkok Towers

LOCATION Sukhumvit Soi 18 , Bangkok

DATE 10/4/2005

BORING No. BH-6

JOB No. 10352

BY PT

OBSERVED W.L. -0.55 M.

SAMPLE No.	DEPTH M.		WATER CONTENT %	ATTERBERG LIMIT %			WET UNIT WEIGHT t/m^3	SIEVE ANALYSIS % FINER					CLASSIFICATION	UNDRAINED SHEAR STRENGTH t/m^2						STANDARD PENETRATION(N) (blow/ft)	
														UNCONFINED SHEAR		FIELD VANE SHEAR		UU TEST	POCKET PENETRATION		
	FROM	TO		LL.	PL.	PI.		No. 3/8"	No. 4	No. 10	No. 40	No. 200		Qu/2	Qu'/2	Qv	Qv'	Su	1/2Qp		
SS-01	1.50	1.95	31.70										SM/CH							3	
ST-02	3.00	3.50	67.00				1.54						CH	0.50							
ST-03	4.50	5.00	57.50				1.63						CH	1.60							
ST-04	6.00	6.50	55.30				1.67						CH	1.90							
ST-05	7.50	8.00	85.80				1.52						CH	1.20							
ST-06	9.00	9.50	82.20				1.49						CH	1.60							
ST-07	10.50	11.00	62.40				1.62						CH	1.70							
ST-08	12.00	12.50	58.70				1.60						CH	1.70					1.3		
ST-09	13.50	14.00	44.90				1.74						CH	4.80					2.5		
ST-10	15.00	15.50	88.50				1.79						CH	5.60					8.8		
SS-11	16.50	16.95	36.40	78.80	31.80	47.00	1.87						CH						11.3	18	
SS-12	18.00	18.45	30.90				1.92				100	98	CH	12.18					10.0	1	
SS-13	19.50	19.95	21.40						100	99	98	58	CL							13	
SS-14	21.00	21.45	22.10						100	99	97	42	SC							20	
SS-15	22.50	22.95	20.60						100	99	99	48	SC							33	
SS-16	24.00	24.45	22.60				2.01						CH						15.0	21	
SS-17	25.50	25.95	28.40				1.98						CH	11.80					16.3	23	
SS-18	27.00	27.45	27.80				1.91						CH						16.3	22	
SS-19	28.50	28.95	27.20				2.01						CH						11.3	20	
SS-20	30.00	30.45	26.50				1.97						CH	14.60					17.5	20	
SS-21	31.50	31.95	21.90				2.08						CH						22.5+	38	

STS INSTRUMENTS COMPANY LIMITED
SUMMARY OF TEST RESULTS

PROJECT Sukhumvit Soi 18 Bangkok Towers **LOCATION** Sukhumvit Soi 18 , Bangkok

DATE 10/4/2005 **BORING No.** BH-6 **JOB No.** 10352 **BY** PT **OBSERVED W.L.** -0.55 M.

SAMPLE No.	DEPTH M.		WATER CONTENT %	ATTERBERG LIMIT %			WET UNIT WEIGHT t/m^3	SIEVE ANALYSIS % FINER					CLASSIFICATION	UNDRAINED SHEAR STRENGTH t/m^2						STANDARD PENETRATION(N) (blow/ft)	
														UNCONFINED SHEAR		FIELD VANE SHEAR		UU TEST	POCKET PENETRATION		
	FROM	TO		LL.	PL.	PI.		No. 3/8"	No. 4	No. 10	No. 40	No. 200		Qu/2	Qu'/2	Qv	Qv'	Su	1/2Qp		
SS-22	33.00	33.45	26.50				1.98						CH						22.5+	35	
SS-23	34.50	34.95	30.20										CH						12.5	25	
SS-24	36.00	36.45	30.70				1.96						CH	12.97					15.0	27	
SS-25	37.50	37.95	24.90										CH						15.0	28	
SS-26	39.00	39.45	25.30				2.00						CH						20.0	23	
SS-27	40.50	40.95	24.90				1.99						CH	17.70					22.5+	36	
SS-28	42.00	42.45	22.00				2.03						CH						22.5+	52	
SS-29	43.50	43.95	19.90				2.15						CH						22.5+	54	
SS-30	45.00	45.45	18.10				2.09						CH						22.5+	43	
SS-31	46.50	46.95	19.20				2.09						CH						20.0	32	
SS-32	48.00	48.45	18.50				2.16						CH						22.5+	43	
SS-33	49.50	49.95	14.70							100	96	27	SM							89	
SS-34	51.00	51.45	16.60				2.12						CH						22.5+	75	
SS-35	52.50	52.95	20.60							100	94	48	CH/SM						22.5+	51	
SS-36	54.00	54.28	15.80						100	98	77	16	SM							50/3"	
SS-37	55.50	55.80	16.40										SM							50/6"	
SS-38	57.00	57.45	13.40					99	98	98	73	19	SM							67	
SS-39	58.50	58.80	14.70										SM							50/6"	
SS-40	60.00	60.45	15.60					100	99	99	87	20	SM							85	
SS-41	62.00	62.45	13.40										SM							81	
SS-42	64.00	64.30	12.50										SM							50/6"	

STS INSTRUMENTS COMPANY LIMITED
SUMMARY OF TEST RESULTS

PROJECT Sukhumvit Soi 18 Bangkok Towers | **LOCATION** Sukhumvit Soi 18 , Bangkok

DATE 10/4/2005 | **BORING No.** BH-6 | **JOB No.** 10352 | **BY** PT | **OBSERVED W.L.** -0.55 M.

SAMPLE No.	DEPTH M.		WATER CONTENT %	ATTERBERG LIMIT %			WET UNIT WEIGHT t/m^3	SIEVE ANALYSIS % FINER					CLASSIFICATION	UNDRAINED SHEAR STRENGTH t/m^2						STANDARD PENETRATION(N) (blow/ft)	
	FROM	TO		LL.	PL.	PI.		No. 3/8"	No. 4	No. 10	No. 40	No. 200		UNCONFINED SHEAR		FIELD VANE SHEAR		UU TEST	POCKET PENETRATION		
														Qu/2	Qu'/2	Qv	Qv'	Su	1/2Qp		
SS-43	66.00	66.45	11.50					100	99	94	53	18	SM							98	
SS-44	68.00	68.45	13.30										SM							67	
SS-45	70.00	70.45	12.50					99	96	89	60	35	SM							74	
SS-46	72.00	72.45	19.70				2.12						CH						22.5+	68	
SS-47	74.00	74.45	14.60				1.95						CH						22.5+	74	
SS-48	76.00	76.45	19.30				2.12						CH							65	
SS-49	78.00	78.45	21.30				2.06						CH							64	
SS-50	80.00	80.45	19.50				2.01						CH						22.5+	69	

STS INSTRUMENTS COMPANY LIMITED

SUMMARY OF FIELD VANE SHEAR TEST

PROJECT : Millenium Residence **JOB No.** 11142 **DATE :** 26/10/06

LOCATION : Bangkok **BY :** BK. **VANE BLADE :** 55x110mm

TEST No. FV-1

DEPTH (m.)	Undisturbed Vane Shear Strength t/m²	Remolded Vane Shear Strength t/m²	Sensitivity
3.00	2.77	0.57	4.82
4.00	3.15	0.57	5.48
5.00	2.58	0.57	4.49
6.00	1.91	0.38	4.98
7.00	1.62	0.29	5.63
8.00	2.39	0.38	6.22
9.00	2.77	0.57	4.82
10.00	3.34	0.67	4.99
11.00	3.53	0.57	6.15
12.00	4.01	0.86	4.66
13.00	4.68	1.34	3.50
14.00	5.25	1.53	3.43
15.00	7.54	1.81	4.15

TEST No.

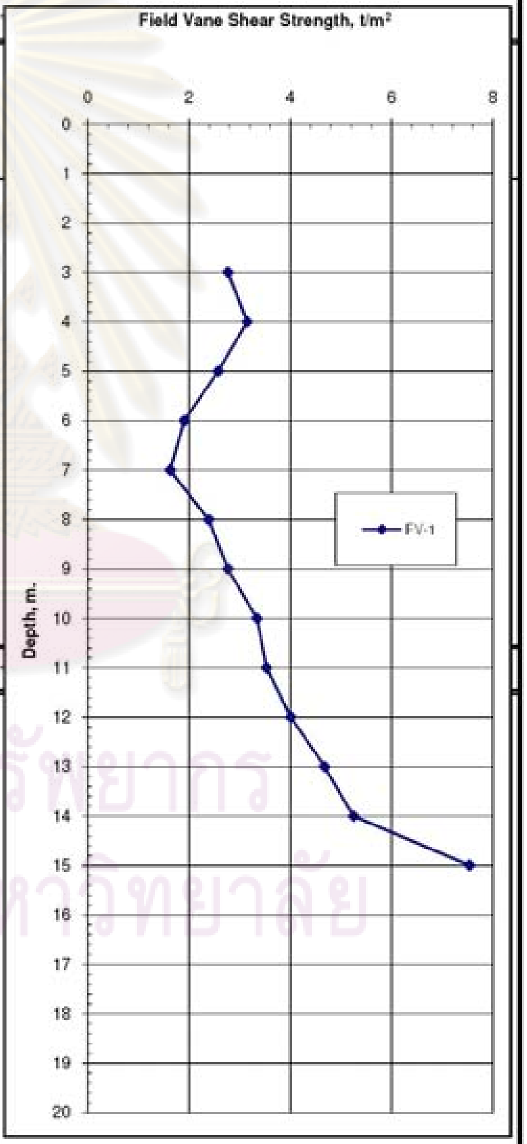

LOG OF BORING No. BH-6

PROJECT : **Sukhumvit Soi 18 Bangkok Towers**

LOCATION : **Sukhumvit Soi 18, Bangkok**

CLIENT :

DEPTH,m	SAMPLE No.	TYPE OF SAMPLE	SAMPLE DIST	RECOVERY	DESCRIPTION OF MATERIAL
0					Silty sand, brownish light grey. (SM,Fill)
	01	SS			1.80 m.
	02	ST			
5	03	ST			
	04	ST			
	05	ST			Clay, trace sand, dark grey, soft to medium. (CH)
10	06	ST			
	07	ST			
	08	ST			
	09	ST			
15	10	ST			15.50 m.
	11	SS			Silty clay, trace sand, light greyish brown, stiff to very stiff. (CH)
	12	SS			18.70 m.
20	13	SS			Fine sandy clay, yellowish light brown, stiff. (CL) 20.50 m.
	14	SS			Clayey fine sand, yellowish light brown, medium to dense. (SC)
	15	SS			23.40 m.
25	16	SS			Silty clay, trace sand, light greyish brown, very stiff. (CH)

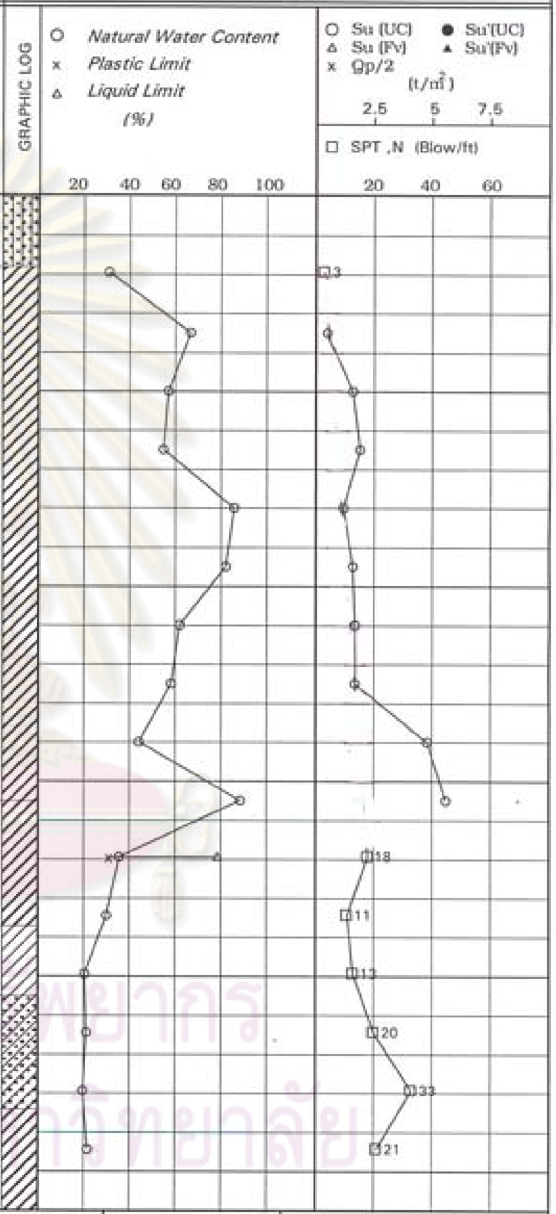

STS INSTRUMENTS COMPANY LIMITED	BORING STARTED. 22/09/05	RIG. ACKER	WL. -0.55 M. 24 HRS AFTER BORING.
	BORING FINISHED.26/09/05	FOREMANSS.	JOB No.10352

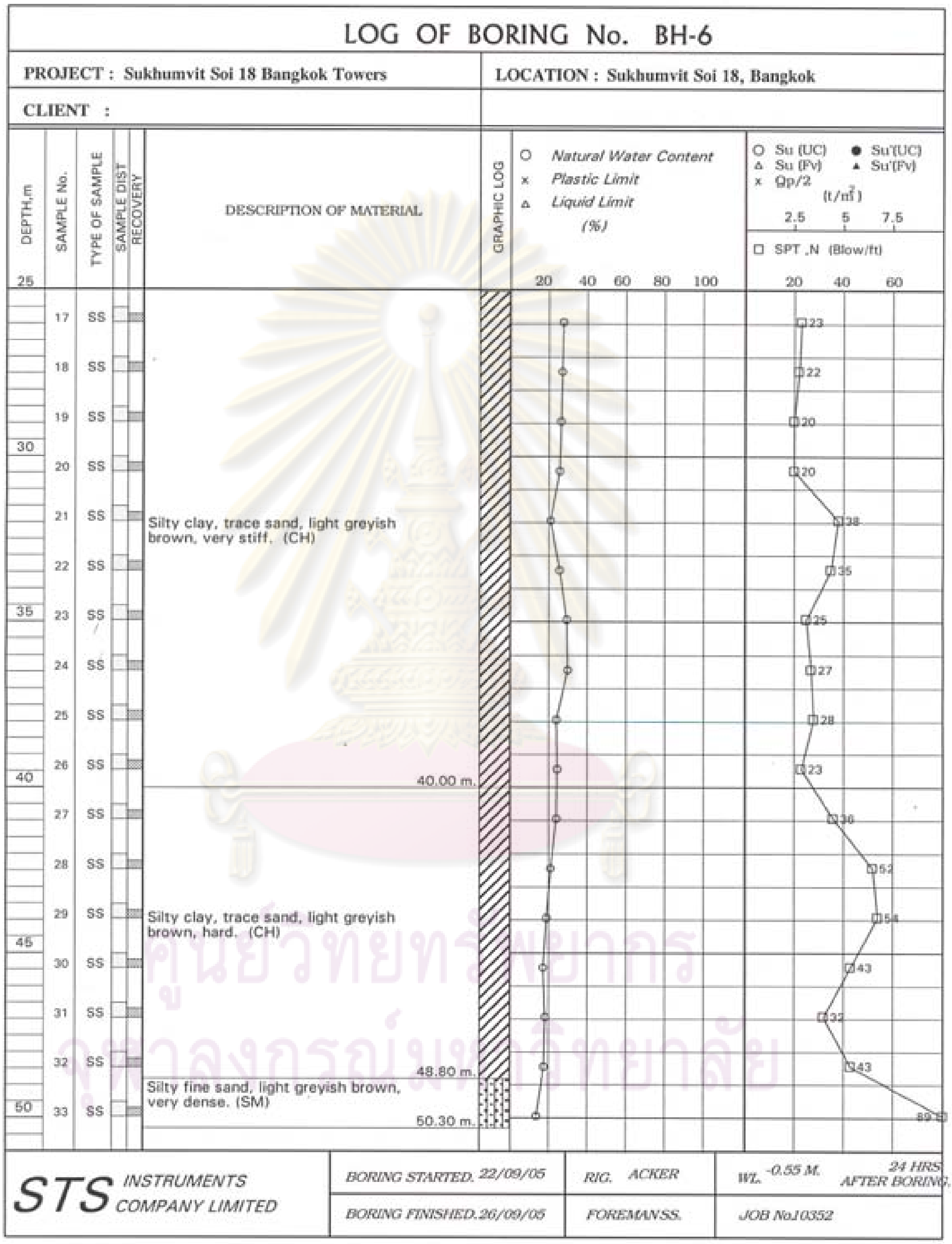

LOG OF BORING No. BH-6

PROJECT : Sukhumvit Soi 18 Bangkok Towers

LOCATION : Sukhumvit Soi 18, Bangkok

CLIENT :

SAMPLE No.	TYPE OF SAMPLE	SPT ,N (Blow/ft)
17	SS	23
18	SS	22
19	SS	20
20	SS	20
21	SS	38
22	SS	35
23	SS	25
24	SS	27
25	SS	28
26	SS	23
27	SS	36
28	SS	52
29	SS	54
30	SS	43
31	SS	32
32	SS	43
33	SS	89

Silty clay, trace sand, light greyish brown, very stiff. (CH)

40.00 m.

Silty clay, trace sand, light greyish brown, hard. (CH)

48.80 m.

Silty fine sand, light greyish brown, very dense. (SM)

50.30 m.

STS INSTRUMENTS COMPANY LIMITED

BORING STARTED. 22/09/05

BORING FINISHED.26/09/05

RIG. ACKER

FOREMANSS.

WL. -0.55 M. 24 HRS AFTER BORING.

JOB No10352

LOG OF BORING No. BH-6

PROJECT : Sukhumvit Soi 18 Bangkok Towers

LOCATION : Sukhumvit Soi 18, Bangkok

CLIENT :

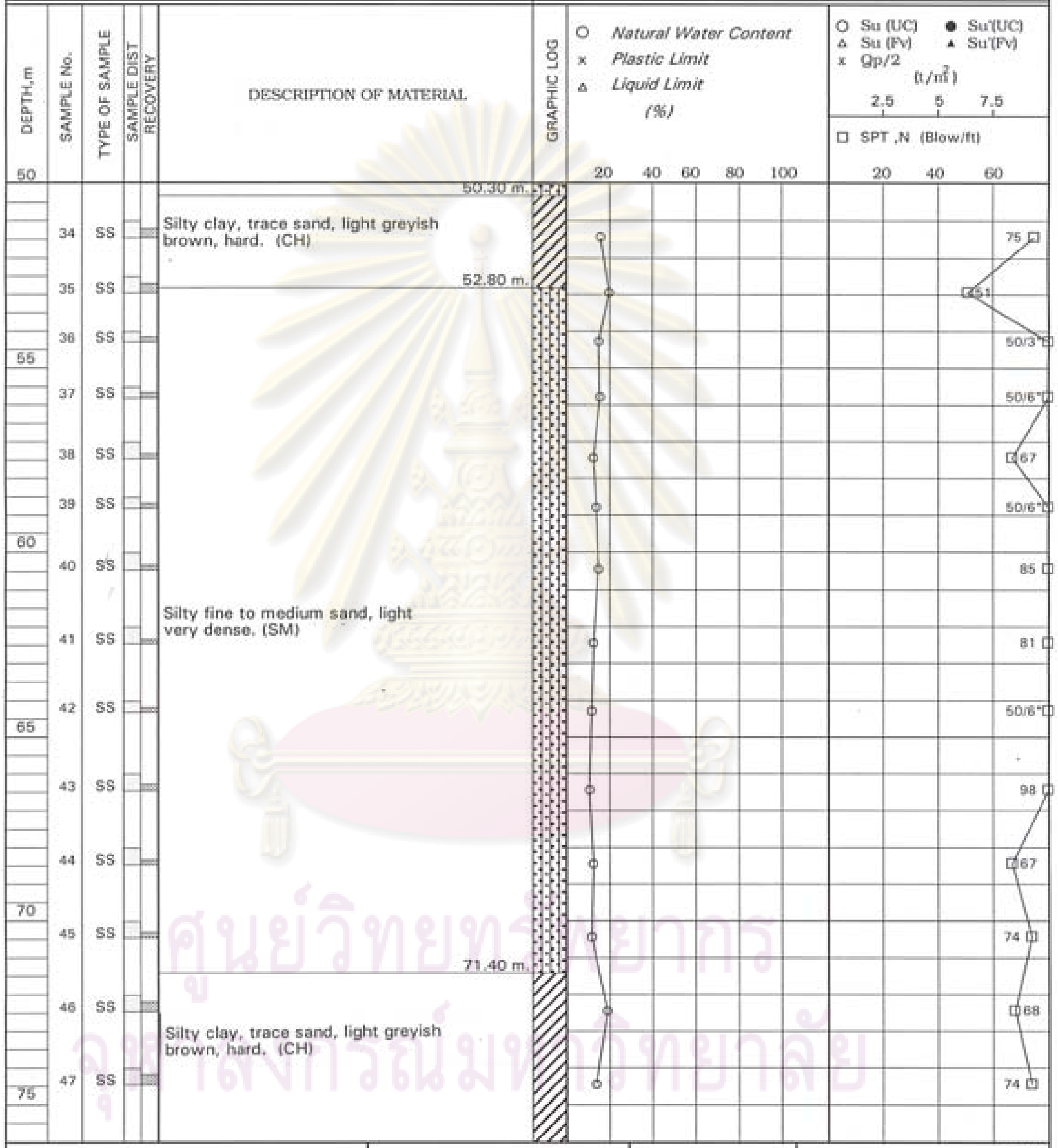

34	SS	Silty clay, trace sand, light greyish brown, hard. (CH)	75
35	SS		51
36	SS	Silty fine to medium sand, light very dense. (SM)	50/3"
37	SS		50/6"
38	SS		67
39	SS		50/6"
40	SS		85
41	SS		81
42	SS		50/6"
43	SS		98
44	SS		67
45	SS		74
46	SS	Silty clay, trace sand, light greyish brown, hard. (CH)	68
47	SS		74

STS INSTRUMENTS COMPANY LIMITED	BORING STARTED. 22/09/05	RIG. ACKER	WL. -0.55 M. 24 HRS AFTER BORING.
	BORING FINISHED. 26/09/05	FOREMAN SS.	JOB No.10352

LOG OF BORING No. BH-6

PROJECT : Sukhumvit Soi 18 Bangkok Towers

LOCATION : Sukhumvit Soi 18, Bangkok

CLIENT :

DEPTH,m	SAMPLE No.	TYPE OF SAMPLE	DESCRIPTION OF MATERIAL
75			
	48	SS	Silty clay, trace sand, light greyish brown, hard. (CH)
	49	SS	
80			
	50	SS	80.45 m.
			END OF BORING
85			
90			
95			
100			

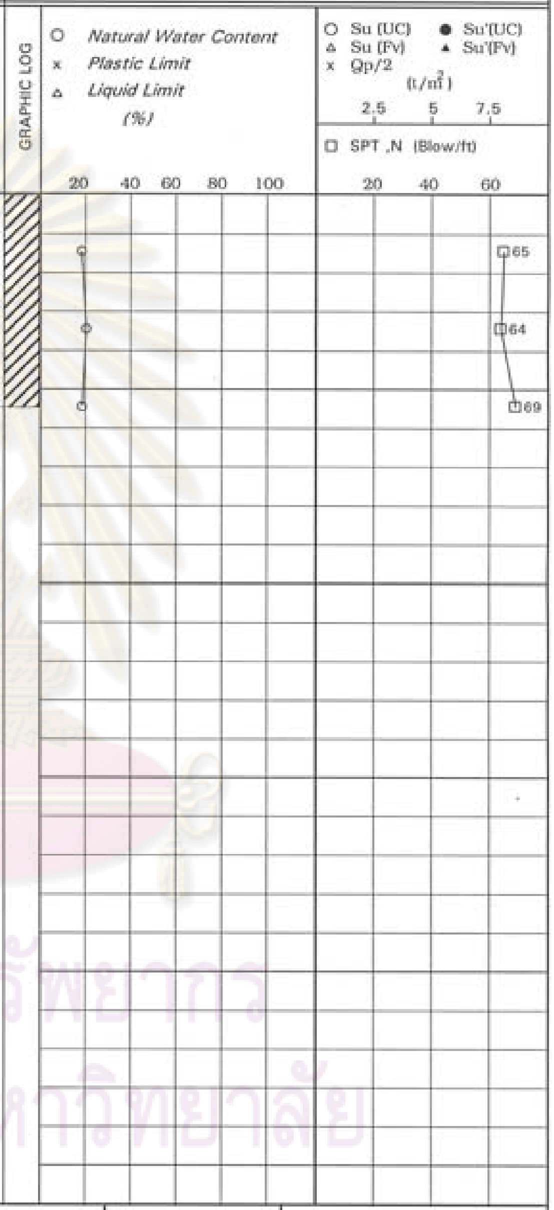

STS INSTRUMENTS COMPANY LIMITED

BORING STARTED. 22/09/05	RIG. ACKER	WL. -0.55 M. 24 HRS AFTER BORING.
BORING FINISHED. 26/09/05	FOREMAN SS.	JOB No.10352

BIOGRAPHY

Mr. Chanchai Submaneewong was born on February 23, 1974 in Bangkok, Thailand. He received his Bachelor’s Degree in Engineering, Civil Engineering (Second Class Honours) from King Mongkut's University of Technology Thonburi in 1996 and Master’s Degree in Engineering, Geotechnical Engineering from Chulalongkorn University in 1999. After graduation, he has been employed under the position of senior geotechnical engineer by SEAFCO Public Co., Ltd. In 2005, he continued with Ph.D. studies in the Geotechnical Engineering Program, Department of Civil Engineering, Faculty of Engineering, Chulalongkorn University.